UNIVERSITÀ
DEGLI STUDI
DI PADOVA

Università Degli Studi Di Padova

SEDE AMMINISTRATIVA: UNIVERSITÀ DEGLI STUDI DI PADOVA

DIPARTIMENTO DI SCIENZE CHIMICHE

SCUOLA DI DOTTORATO DI RICERCA IN SCIENZE MOLECOLARI
INDIRIZZO: SCIENZE CHIMICHE
CICLO XXVI

Fe(III) AND V(V) AMINO TRIPHENOLATE COMPLEXES AS CATALYSTS FOR THE CONVERSION OF RENEWABLE CARBON FEEDSTOCKS

Direttore della Scuola: Ch.mo Prof. Antonino Polimeno

Supervisore: Ch.mo Prof. Cristiano Zonta

Dottoranda: Blerina Gjoka

31 Gennaio 2014

Contents

Chapter 1 General Introduction

Chapter 2 Synthesis of *ortho*-Substituted Trithiophenol Amines by Miyazaki–Newman–Kwart Rearrangement

Chapter 3 Vanadium (V) Amino Triphenolate Complex as Catalyst for Aerobic Oxidation of Diols and β-idrossi Ether Compounds

Chapter 4 Fe(III) Amino Triphenolates as Catalysts for CO_2 Activation

Chapter 1

General Introduction

1.1 Introduction

The design and study of metal catalysts able to mimic the activity of biological systems is of considerable interest nowadays. This can be achieved through the modulation of the electronic properties and the steric volume around the metal modes using synthetic ligands. This translates in the control of the catalytic behaviour and coordination chemistry of the resulting system. Among the different strategies, the use of multi-dentate ligands is emerging as the leading route for the synthesis of stable and active metal catalysts.[1] The nearly complete filling of all vacant coordination sites around the metal by a single ligand results in intrinsic thermodynamic stability and it allows the use of low catalyst concentrations to prevent the formation of multi-meric species during catalyst turnover. In addition, the presence of single mononuclear species greatly facilitates mechanistic studies and catalyst optimization, particularly in stereoselective processes.

While C_2 symmetric bi-dentate ligands have been extensively studied, ligands with a C_3 symmetric axis have attracted attention only recently.[2] These systems have attracted the interest to a substantial number of research groups concerning their synthesis, complexation behaviour and catalysis.

In this context, triphenolamines Figure 1, have proven to be excellent ligands due to the particular stability, and catalytic abilities of their corresponding metal complexes.[3] The tripodal ligand system bearing a central amino and three phenoxide donors (NO_3 donor ligand) has attracted great interest (triphenolamines, Figure 1).

In view of this thesis work, different approaches used for their synthesis will be reported, followed by some examples of their coordination chemistry and subsequently their use in catalysis.

[1] a) A. J. Chmura, C. J. Chuck, M. G. Davidson, M. D. Jones, M. D. Lunn, S. D Bull, M. F. Mahon. *Angew. Chem. Int. Ed.* **2007**, *46*, 2280. b) A. J. Chmura, M. G. Davidson, C. J. Frankis, M. D Jones, M. D. Lunn. *Chem. Commun.* **2008**, *11*, 1293. c) A. J. Chmura, D. M. Cousins, M. G. Davidson, M. D. Jones, M. D. Lunn, M. F. Mahon, *Dalton. Trans.* **2008**, *11*, 1437. d) S. D. Bull, M. G. Davidson, A. L. Johnson, D. Robinson, E. J. E. M. F. Mahon. *Chem. Commun.* **2003**, 1750. e) P. Axe, S. D. Bull, M. G. Davidson, J. E. Jones, M. D. Robinson, W. L. Mitchell, J. E. Warren. *Dalton Trans.* **2009**, *46*, 10169.

[2] a) C. Moberg. *Angew. Chem. Int. Ed.* **1998**, 37, 248. b) S. E. Gibson, M. P. Castaldi. *Chem. Commun.* **2006**, 29. b) K. Jyothish, W. Zhang. *Angew. Chem. Int. Ed.* **2011**, 50, 8478.

[3] a) G. Licini, M. Mba, C. Zonta. *Dalton Trans.* **2009**, 5265. b) M. Mba, L. J. Prins, G. Licini. *Org. Lett.* **2007**, *9*, 15. c) C. Zonta, E. Cazzola, M. Mba, G. Licini. *Adv. Synth. Catal.* **2008**, *350*, 2503. d) F. Romano, A. Linden, M. Mba, C. Zonta. *Adv. Synth. Catal.* **2010**, *352*, 2937.

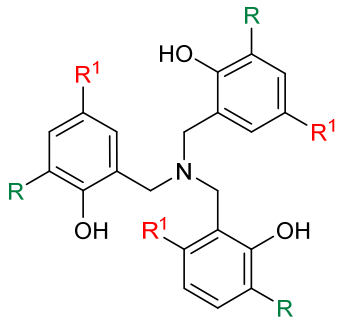

Figure 1. Triphenolamines

1.1.1 Synthesis of Triphenolamines

Triphenolamines molecules have traditionally been synthesized by reaction of *ortho/para*-disubstituted phenols with hexamethylenetetramine Scheme 1.[4] This synthetic pathway (Mannich reaction) involves only one-step from the phenol to the ligand. This procedure however, requires long reaction times (2-7 days), harsh reaction conditions and high temperatures. In addition, this strategy allows the formation of corresponding ligand only when the phenol moiety is substituted in either the *ortho*- and *para*-positions.

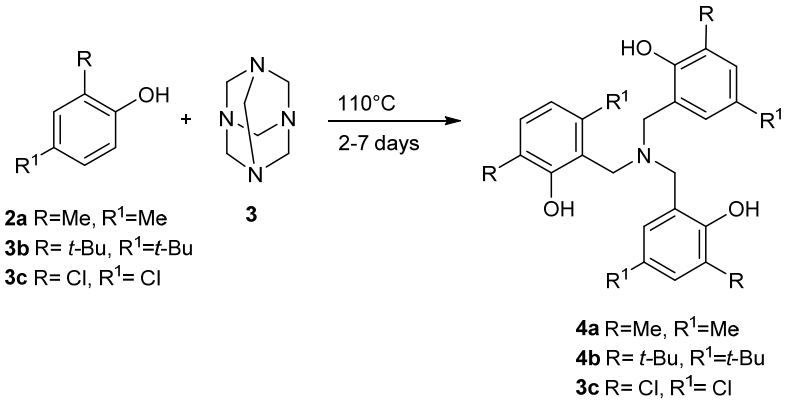

Scheme 1 Synthesis of Triphenolamines *via* Mannich reaction

An alternative route has been reported based on the nucleophilic substitution (S_N2) of a 2-methoxybenzylamine with two equivalents of 2-methoxybenzylbromide Scheme 2.[5] This strategy has the advantage of giving access to asymmetric triphenolamine **13** Scheme 3.

[4] A. Chandrasekaran, R. O. Day, R. R. Holmes. *J. Am. Chem. Soc.* **2000**, 122, 1066.
[5] J. Hwang, K. Govindaswamy, S. A. Koch. *Chem. Commun.* 1998, 1667.

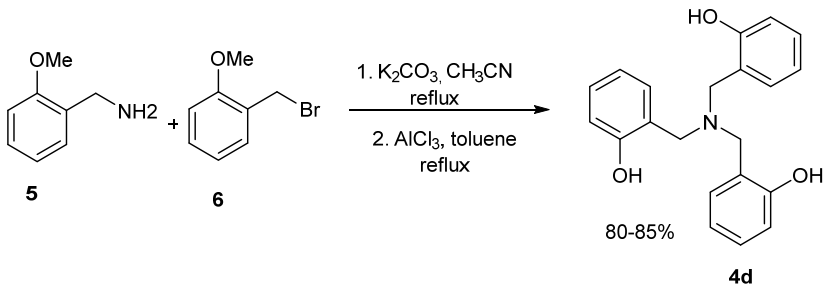

Scheme 2.

This strategy allows also access to enantiopure triphenolamines. The key step is the stereoselective reduction of a chiral imine **9**. Subsequently, this is converted to the primary amine by oxidation in the presence of $Pb(OAc)_4$, followed by hydrolysis.[6] Finally, the enantiopure triphenolamine **4d** is obtained by reacting the amine with two equivalents of 2-benzyloxy-3-bromomethyl-biphenyl, followed by the hydrogenolysis of the benzyl group Scheme 3.

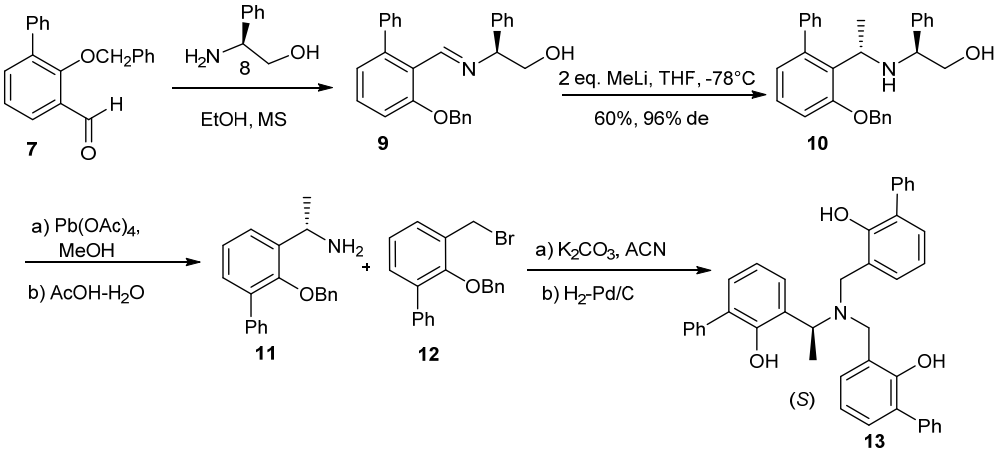

Scheme 3.

A third synthetic approach has been developed to synthesize C_3 symmetric *ortho*-substituted triphenolamine ligands as depicted in Scheme 4. This synthesis is based on a three-fold reductive amination starting from *ortho*-substituted salicyl aldehydes using a nitrogen source such as NH_4OAc and a reducing agent $NaBH(OAc)_3$.[7] Most of the salicylaldehyde derivatives are commercially available but they can also be easily prepared from their corresponding phenols. The phenoxy group is usually protected with an ether moiety, typically a benzyl group, during the reductive amination step. Finally, the ligand is obtained in good yield by removing the ether group *via* hydrogenolysis. The easy availability of the starting materials and the possibility to have direct access to this important class of ligands, make this strategy an efficient route for the preparation of *ortho*-substituted triphenolamines.

[6] G. Bernardinelli, D. Fernandez, R. Gosmini, P. Meier, P.A. Ripa, B. Treptov, E. P. Kunding. *Chirality* **2000**, 12, 529.
[7] L. J. Prins, M. Blázquez. Mba, A. Kolarovic, G. Licini. *Tetrahedron Lett.* **2006**, 47, 2735.

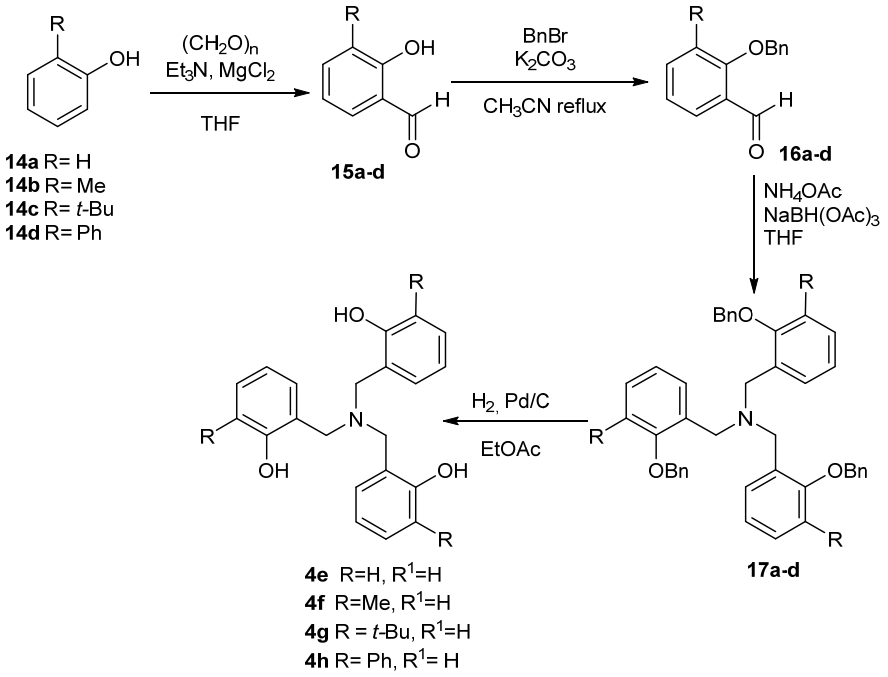

Scheme 4. Synthesis of triphenolamines *via* reductive amination

1.2 Coordination chemistry of amine triphenolate complex

Amino triphenolate ligands are able to form metal complexes with early transition metals and main group elements in high oxidation states. The coordination of these ligands to metal ions affords highly robust complexes. In these complexes, the ligand usually binds to the metal as a tetradentate ligand with the three anionic oxygen atoms in the equatorial positions and the tertiary amine in one of the axial positions. Generally, upon complexation with metal ions, mononuclear complexes with a ratio of 1:1 ligand–metal are obtained. As reported previously, a crucial role for their stability is given by the substituents in *ortho* and *para* positions to the phenoxy moiety of the ligand. For instance *ortho* groups, which are in close proximity to the metal center, can affect directly their stability and therefore the reactivity of the corresponding metal complexes. As examples, complexes bearing bulky substituents such as *t*-Bu groups are highly stable to hydrolysis in comparison to complexes having small groups such as Me or H. [3b,3c,8,9] Such complexes have the tendency to form di-nuclear complexes or aggregates after exposure to moisture.[10] *Para* substituents

[8] M. Kol, M. Shamis, I. Goldberg, Z. Goldschmidt, S. Alfiand, E. Hayut- Salant. *Inorg. Chem. Commun.* **2001**, 4, 177.
[9] V. Ugrinova, G. A. Ellis, S. N. Brown. *Chem. Commun.* **2004**, 468.
[10] A. J. Nielson, C. Shen, J. M. Waters. *Polyhedron*, **2006**, 25, 2039.

to the phenoxy groups are able to modify the electronic properties of the ligand and therefore can directly affect the catalytic properties of the corresponding complex.

In the majority of the reported examples the usual geometry assumed by the complexes are trigonal bipyramidal (TBP) and octahedral (OCT), whereas tetra-coordinate complexes with trigonal monopyramidal (TMP) geometry are less observed as depicted in Figure 2.

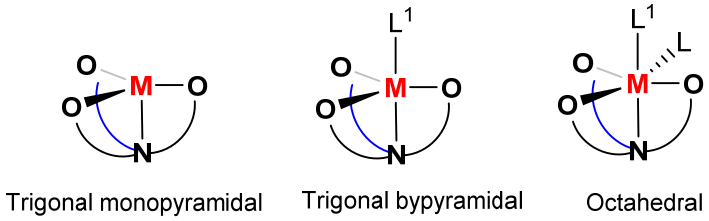

Figure 2. Common geometries of the complexes

Moreover, amino triphenolate ligands can form stable metal complexes with a wide range of metal ions and main group elements such as Ti, Zr, Hf, V, Nb, Ta, Mo, W, Al, Ga, In, and Fe. However, in view of this thesis work, the attention will be focused on the coordination chemistry and the reactivity of vanadium and iron amino triphenolate complexes in order to compare and identify new opportunities in catalysis.

1.3 Vanadium amino triphenolate complexes and their reactivity in catalysis

Vanadium complexes belong to the group V in which usually the octahedral geometry predominates, except for the vanadium species. Generally vanadium (V) complexes assume a trigonal bypyramidal (TBP) geometry, however different binding behaviour was found upon complexation with very electron-poor ligands such as dichloro-substituted *ortho*/*para* amino triphenolate (R_1=R_2=Cl).[11] In this example, a hexa-coordinate octahedral crystal structure was obtained with the oxo moiety present in the *trans*- position to the amine group and a molecule of water as ligand in the apical position of the complex Figure 3.

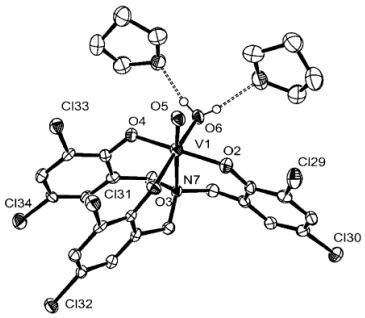

[11] S. Groysman, I. Goldberg, Z. Goldschmidt, M. Kol. *Inorg. Chem*. **2005**, 44, 5073.

Figure 3. Crystal structure of V(V) *ortho*/*para* Cl amino triphenolate [11]

The first synthesis of vanadium amino triphenolate complexes was reported by Kol *et al.*[11] The synthesis was carried out mixing equimolar amounts of *ortho*/*para* di-substituted amino triphenolate ligand with VCl_3-THF affording, vanadium complexes with C_3-TBP in which in the apical position is occupied with a labile ligand such as THF.

Also when other metal precursors are used in the synthesis of vanadium complexes, such as $V(O)(OR)_3$, the same geometry was obtained with an oxo moiety in the trans position to the nitrogen of the amino triphenolate ligand.[12] Vanadium oxo complexes have a much longer distance between the amino donor group (N) and the metal centre (V), in comparison to the distance found for the V(III) species.

The catalytic behaviour of V(V) amino triphenolate complexes was also investigated in the oxidation of styrene to styrene oxide, in the presence of *t*-butyl hydrogen peroxide (*t*-BuOOH) as oxidant. In these catalytic studies reported by Kol, Goldschmidt and others, [11] the oxidation reaction was carried out using 5% mol of V(V) catalysts in a solution of benzene and *t*-BuOOH. Under these conditions, the catalysts showed poor reactivity and the evolution of side products were observed.

More recently, the catalytic studies of V(V) amino triphenolate complexes, were focused on sulfoxidation and halogenation reactions.[13] In these studies, vanadium complexes were obtained by the reaction of ligands with an equimolar amount of vanadium precursor VO(O*i*-Pr) in dry THF in an inert atmosphere affording mononuclear complexes in high yield (92-94%) as deep red crystalline solids Scheme 5. All (V) amino triphenolate complexes where characterized by ^{1}H-NMR, ^{51}V-NMR spectroscopy and *X*-ray diffractometric analysis, the results are reported in Table 1 and Figure 4.

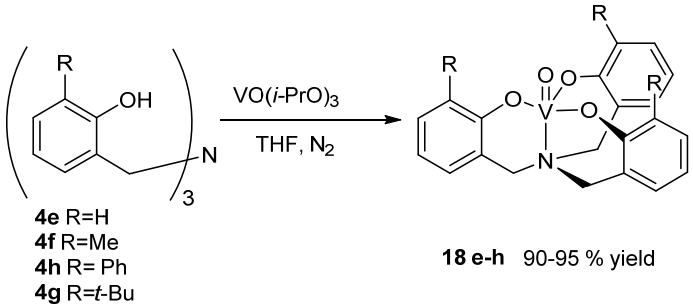

Scheme 5. Synthesis of V(V) complexes **18e-h**

Table 1. ^{51}V NMR chemical shift (ppm) of **18e-h** in $CDCl_3$ solvent.

[12] M. Mba, M. Pontini, S. Lovat, C. Zonta, G. Bernardinelli, E. P. Kundig, G. Licini. *Inorg. Chem*. **2008**, 47, 8616.

COMPLEX	^{51}V NMR - δ (ppm), $CDCl_3$
18e	-396.83, -428.78
18f	-381.90
18g	-389.07

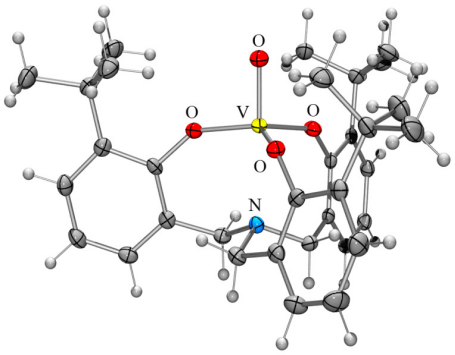

Figure 4. *X*-Ray complex **18 g**

Complexes bearing Me and *t*-Bu groups in the *ortho* position have shown highly symmetric ^{1}H-NMR proton spectra in accordance with the presence of a mononuclear species having C_3 symmetry and singlet signals in the ^{51}V-NMR spectrum were detected (-381,90 ppm and -389 ppm respectively recorded in $CDCl_3$). Whereas for the complex **18e**, a non-symmetric ^{1}H-NMR spectra with different signals in ^{51}V-NMR spectrum was observed, suggesting the formation of aggregates or the presence of a mixture of species. This confirms the strong importance of bulky *ortho* substituents for the formation of stable metal complexes.

As mentioned previously, the catalytic activity of amino triphenolate complexes was studied in the sulfoxidation reaction. The complexes firstly were tested in sulfoxidation of thioanisol, using hydrogen peroxide as oxidant at room temperature. V(V) catalysts were found to efficiently catalyze the reaction in fast and highly selective manner to the corresponding sulfoxide, reaching quantitative yields in the case of the complex **18g** (R= *t*-Bu). Further optimization of the reaction conditions was obtained by decreasing the catalyst loading to 0.01 mol%. In this case, high selectivity of methyl phenyl sulfoxide with respect to methyl phenyl sulfone was obtained reaching high TONs and TOFs (up to 8000h^{-1}). The optimized procedure was then extended to other sulphides Table 2. In this case, the catalytic systems based on vanadium complexes were found to be extremely active with high selectivity, confirming the efficiency of these catalysts in oxygen transfer reactions. The results obtained employing complex **18g** as catalysts are reported in Table 2.

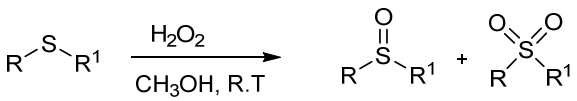

Table 2. Oxidation of sulphides catalysed by **18g**.

Entry	R	R^1	Yield (%)	SO/SO_2	Time
1	Ph	Me	98	99:1	120
2	*p*-Tol	Me	> 99	> 99:1	120
3	*p*-Tol	*n*-Bu	96	99:1	120

4	Ph	Bn	> 99	> 99:1	90
5	*n*-Bu	*n*-Bu	99	>99:1	60
6	*p*-MeO-C_6H_4	Me	98	99:1	100

[a] Reaction conditions: Reactions carried out at 28 °C with a 1:1 molar ratio of substrate aq H_2O_2 ; 0,1 catalyst.
[b] conversion determined by ^{1}H-NMR (CD_3OD), 300MHz). [c] yield determined by GC analysis on the crude reaction mixture after total oxidant consumption.

In general, the mechanism is believed to proceed through the addition of hydrogen peroxide to the metal centre affording a metal peroxide species, which is the active species in the sulfoxidation reaction. The sulfide acts as nucleophile and can attack the electrophilic oxygen of the peroxo moiety to subsequently give cleavage of the O-O bond leading the oxidized product and the formation of the di-oxo species. Finally, this complex, in the presence of H^+, can form again the initial species.

Vanadium-based complexes have also attracted recently the interest as biomimetic systems, as some of these catalytic systems are able to mimic vanadium haloperoxidases.[13] These enzymes, which catalyse the oxidation of halides to the corresponding "X^+" halonium species in the presence of hydrogen peroxides, can generate halogenated compounds. These vanadium-dependent enzymes, have shown a five coordinate V(V) centre with a trigonal bipyramidal geometry.[14] [15] The most reported vanadium dependent enzymes are bromoperoxidases VBrPO, which are able to catalyse the oxidation of bromide by hydrogen peroxides. Generally, the catalytic cycle, proceeds towards the formation of a peroxovanadium species, which represents the active oxidant in the cycle. The peroxo derivatives are able to oxidize the bromide ion to a brominating intermediate, which subsequently reacts with the substrate, generally a nucleophile, affording the brominated product.

V(V) amino triphenolate complexes can be considered to be good candidates for structural and functional models of vanadium haloperoxidase enzymes and for these reasons they have been studied in halide oxidations, for example; bromination reactions. In these catalytic systems, the ligands play an important role in order to stabilize the monomeric vanadium complex preventing the formation of oligomeric species under acidic conditions. The catalytic performance of vanadium (V) amino triphenolate complexes were tested in the bromination of 1,3,5-trimethoxybenzene using tetrabutyl ammonium bromide (TBAB) as a halogen source, in the presence of an oxidant, hydrogen peroxide (1 eq.) and in acidic conditions (1 eq.), according to the stoichiometry of the reaction. The

[13] a) M. A. Andersson, A. Willetts, S.G. Allenmark, *J. Org. Chem*. **1997**, 8455. b) A. G .J. Ligtenbarg, R. Hage, B. L. Feringa, *Coord. Chem. Rev*. **2003**, 98.
[14] a) A. Messerschmidt, R. Wever. *Proc. Natl. Acad. Sci. U.S.A*. **1996**, 93, 392. b) A. Messerschmidt, R. Wever. *Biol. Chem*. **1997**, 378, 309.
[15] R. A. Tschirret, A. Butler. *J. Am. Chem. Soc*. **1994**, 116, 411.

brominated product 2,4,6-trimethoxybromobenzene was afforded in high yield, up to 92%, reaching TONs up to 1260 Scheme 6.

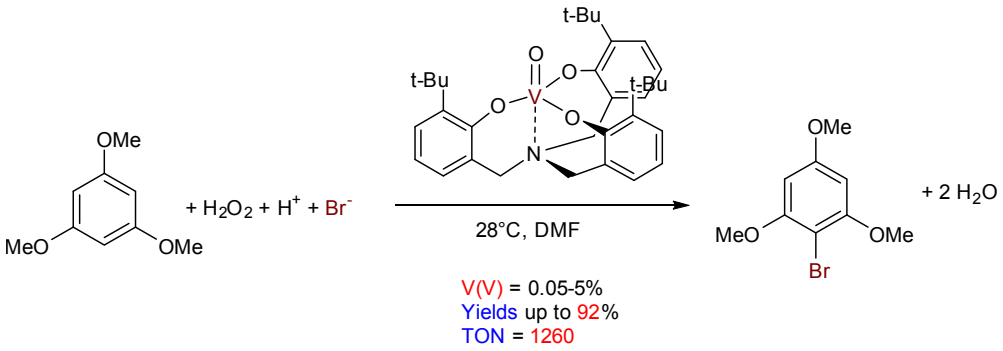

Scheme 6. Bromination of 1,3,5-trimethoxybenzene using **18g** as catalyst

1.4 Iron amino triphenolate complexes and their use in catalysis

Iron (III) complexes bearing amino triphenolate ligands were originally reported by Koch and co-workers more than 10 years ago.[5] The ligand was synthesized by the reaction of two equivalents of 2-methoxybenzyl bromide with commercially available 2-methoxybenzylamine in refluxing CH_3CN and K_2CO_3 affording tris (2-methoxybenzyl) amine in 80–85% yield. The protecting groups were removed by refluxing the compound in toluene with five equivalents of $AlCl_3$ yielding triphenolamine which was reacted with $FeCl_3$ leading to a penta-coordinate TBP structure having 1-methylimidazole in apical position. Crystal structures demonstrated that Fe (III) is able to bind an extra ligand which confers an octahedral geometry Figure 5. The catalytic activity of these complexes was not exploited at that time.

Figure 5. Structure and crystal structure of Fe(III) amino triphenolate having 1-methylimidazole in apical position.[5]

More recently, Kleij and co-workers reported an iron(III) amino triphenolate complex to be an efficient catalyst for the cycloaddition of carbon dioxide to a wide variety of oxiranes and oxetanes to yield the corresponding cyclic carbonate products under mild reaction conditions.[16] The

[16] C. J. Whiteoak, E. Martin, M. Martínez Belmonte, J. Benet-Buchholz, A. W. Kleij. *Adv. Synth. Catal*. **2011**, 354, 469.

ligand was synthesized following the Scheme 1 (Mannich reaction) starting from *ortho/para* dimethyl substituted phenol.

The Fe (III) amino triphenolate complex was prepared by mixing a solution of the ligand with three equivalents of NaH and $FeCl_3$ as the metallic precursor. The corresponding complex was characterized by *X*-ray crystallographic analysis showing a di-meric form Figure 6. The synthesis of the complex and the crystal structures obtained are reported in Scheme 7.

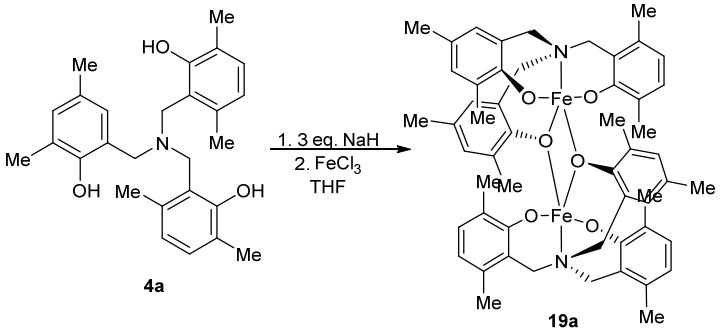

Scheme 7. Synthesis complex **19a**

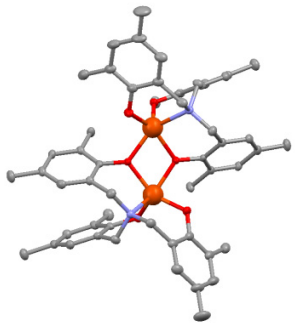

Figure 6. *X*-Ray complex **19a**[16]

As mentioned above, the complex was employed as catalyst in cycloaddition of carbon dioxide to oxirane and oxetanes to yield the corresponding cyclic carbonate. The synthesis of these compounds from epoxides and CO_2 catalysed by metal complexes has been widely investigated[17] and nowadays represents a successful example of carbon dioxide utilization. In these metal-based complexes, catalysis is made possible by the combination of a binary system, which consists commonly of quaternary ammonium halide salt[18,19] (tetrabutyl ammonium chloride, bromide TBAB and iodide TBAI) or phosphonium halide salts and a metal complex. In this context, Fe(III) amino triphenolate complexes together with a presence of a co- catalyst (TBAI or TBAB), have shown good performance for the synthesis of cyclic carbonates. The reactions were carried out employing 0.5 mol% of Fe (III) catalyst, 5 mol% of co-catalyst using methylethyl ketone as solvent at 10 bar of CO_2. Some of the results are summarized in Table 3.

[17] a) A. Berkessel, M. Brandenburg. *Org. Lett*. **2006**, 8, 4401. b) W. Clegg, R. W. Harrington, M. North, R. Pasquale. *Chem. Eur. J*. **2010**, 16, 6828. c) R. L. Paddock, S. T. Nguyen. *Chem. Commun*. **2004**, 1622. d) A. Decortes, A. W. Kleij. *ChemCatChem*. **2011**, 3, 831.

[18] S. Fukuoka, M. Kawamura, K. Komiya, M. Tojo, H. Hachiya, K. Hasegawa, M. Aminaka, H. Okamoto, I. Fukawa, S. Konno. *Green Chem*. **2003**, 5, 497.

[19] a) M. Yoshida. M. Ihara. *Chem. Eur. J*., **2004**, 10, 2886. b) J. Sun, S. I. Fujita, M. Arai. *J. Organomet. Chem*. **2005**, 690, 3490. c) W. L. Dai, S. L. Luo, S. F. Yin, C. T. Au. *Appl. Catal*., **2009**, 366, 2. d) T. Sakakura. K. Kohno. *Chem. Commun*. **2009**, 1312.

Table 3. Cycloaddition of CO_2 to terminal epoxides.

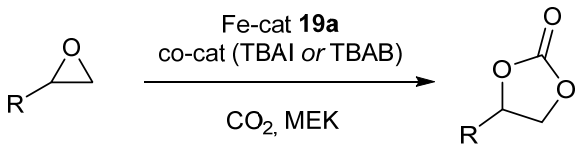

Substrate	Product	Co-cat	Yield (%)
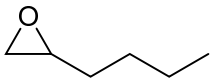	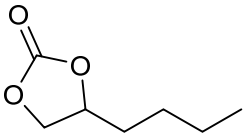	TBAI	96
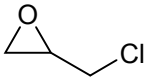	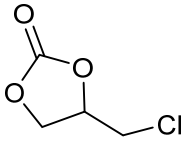	TBAB	*83*
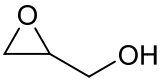	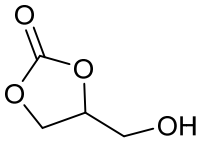	TBAI	91
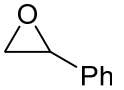	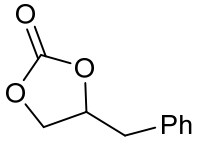	TBAB	56
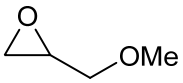	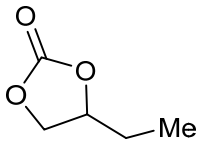	TBAI	90
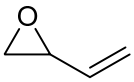	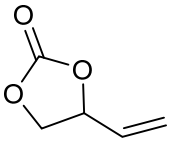	TBAI	70

Reaction conditions: substrate (2.0×10^{-3} mol), catalyst (1.0×10^{-5} mol, 0.5 mol%), co-catalyst (1.0×10^{-4} mol, 5 mol%) methyl ethyl ketone (5 mL), pCO_2=0.2 MPa, 25 °C, 18 h. Conversions based on ^{1}H NMR analysis of reaction mixture aliquots using mesitylene as an internal standard. [c] The selectivity toward the cyclic carbonates was>99% as determined by ^{1}H NMR.

All the cyclic carbonate products were obtained in good yields using either an iodide or a bromide salt as co-catalyst. In general, the iron complex acts as Lewis Acid which has the role of activating the epoxide towards ring opening by the nucleophile, followed by the insertion of CO_2 into the activated intermediate. The carbonate intermediate can either undergo a ring-closure reaction leading to formation of the cyclic carbonate or react further through the alternating insertion of epoxide and CO_2 molecules, yielding a polycarbonate.

More recently, three different *ortho/para* substituted Fe(III) amino triphenolate complexes were reported and their catalytic activity in the synthesis of cyclic and polymeric cyclohexane carbonates were described.[20,21] In this work, it has been shown that the selectivity towards formation of either the cyclic carbonate or the polycarbonate can be controlled by using Fe(III) catalysts and a carefully combination of the reactions conditions, such as temperature and pressure.

1.5 Aim of the thesis work

This thesis has the aim to search for and develop catalytic systems based on metal complexes for different uses in catalysis. In particular, catalysts based on amino triphenolate complexes, which have shown to be highly stable and reactive, will be reported. Furthermore, an extension toward the synthesis of their analogues will be described.

In this respect, Chapter 2 will report a new strategy for the synthesis of the analogues *tris*-thiophenol amine.

In Chapter 3 and 4 the results obtained with Fe(III) amino triphenolate and V(V) amino triphenolate for the synthesis of small molecules from a renewable carbon feedstock such as carbon dioxide will be discussed.

In particular, Chapter 3 will describe novel reactivity of V(V) amino triphenolate complexes as catalysts for the aerobic oxidation of diols and ether compounds in order to investigate their use for the transformation of lignin into valuable chemicals.

In Chapter 4 the reactivity of Fe(III) amino triphenolate complexes as a catalyst for the synthesis of cyclic organic carbonates, starting from epoxides and CO_2, is reported.

[20] M. Taherimehr, S. M. Al-Amsyar, C. J. Whiteoak, A. W. Kleij, P. P. Pescarmona. *Catal. Sci. Technol.,* **2012**, 2, 2231.
[21] M. Taherimehr, S. M. Al-Amsyar, C. J. Whiteoak, A. W. Kleij, P. P. Pescarmona. *Green Chem.,* **2013**, 15, 3083.

Chapter 2

Synthesis of *ortho*-Substituted Trithiophenol Amines by Miyazaki–Newman–Kwart Rearrangement

Abstract

In this chapter, the synthesis of ligands analogous of triphenolamines is described. An efficient synthetic pathway of *ortho*-substituted trithiophenol amines *via* Miyazaki–Newman–Kwart rearrangement followed by reductive amination is reported. This project has the aim to affect directly a modification of the binding and electronic properties of the parent ligand in order to have access to different metal complexes and consequently different catalysis.

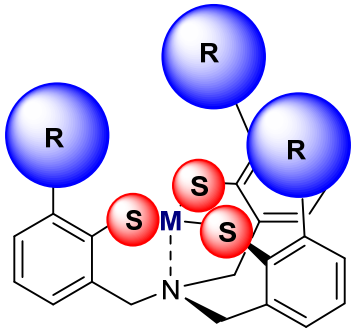

This chapter has been published.[1]

2.1 Introduction

Owing to the numerous publications on the topic, it is clear that the use of polydentate ligands, and in particular C_3 symmetric complexes, is emerging as one of the leading strategies for the formation of catalytically stable complexes.[2] As discussed in the first chapter, these ligands are used to control the environment of the metal, modulate the electronic and steric properties around the metal centre and therefore control their catalytic properties. In the last decade, many studies have been carried out for the synthesis of triphenolamines, their complexation with a wide variety of transition metals and main group elements[3] and catalytic activity[4] (triphenolamine Figure 1 right).

[1] B. Gjoka, F. Romano, C. Zonta, G. Licini. *Eur. J. Org. Chem.* **2011**, 5636.
[2] a) C. Moberg. *Angew. Chem. Int. Ed.* **1998**, 37, 248. b) S. E. Gibson, M. P. Castaldi. *Chem. Commun.* **2006**, 29. c) G. Licini, M. Mba, C. Zonta. *Dalton Trans*. **2009**, 5265. d) K. Jyothish, W. Zhang. *Angew. Chem. Int. Ed*. **2011**, 50, 8478.
[3] a) M. Mba, L. J. Prins, G. Licini. *Org. Lett.* **2007**, 9, 15. b) G. Bernardinelli, T. M. Seidel, E. P. Kündig, L. J. Prins, A. Kolarovic, M. Mba, M. Pontini, G. Licini. *Dalton Trans*. **2007**, 1573. c) C. Zonta, E. Cazzola, M. Mba, G. Licini. *Adv. Synth. Catal.* **2008**, 350, 2503. d) M. Mba, M. Pontini, S. Lovat, C. Zonta, G. Bernardinelli, E. P. Kündig, G. Licini. *Inorg. Chem*. **2008**, 47, 8616. e) F. Romano, A. Linden, M. Mba, C. Zonta. *Adv. Synth. Catal*. **2010**, 352, 2937. f) M. Mba, L. J. Prins, C. Zonta, M. Cametti, A. Valkonen, K. Rissanen, G. Licini. *Dalton Trans.* **2010**, 39, 7384.
[4] S. D. Bull, M. G. Davidson, A. L. Johnson, D. E. Robinson, M. F. Mahon. *Chem. Commun.* **2003**, 1750. b) A. J. Chmura, C. J. Chuck, M. G. Davidson, M. D. Jones, M. D. Lunn, S. D. Bull, M. F. Mahon. *Angew. Chem. Int. Ed*. **2007**, 46, 2280. c) A. J. Chmura, M. G. Davidson, C. J. Frankis, M. D. Jones, M. D. Lunn. *Chem. Commun.* **2008**, 11, 1293. d) A. J. Chmura, D. M. Cousins, M. G. Davidson, M. D. Jones, M. D. Lunn, M. F. Mahon. *Dalton Trans*. **2008**, 11, 1437. e) P. Axe, S. D. Bull, M. G. Davidson, M. D. Jones, D. E. J. E. Robinson, W. L. Mitchell, J. E. Warren. *Dalton Trans*. **2009**, 46, 10169. f) S. D. Bull, M. G. Davidson, A. L. Johnson, M. F. Mahon, D. E. J. E. Robinson. *Chem. Asian J*. **2010**, 5, 612.

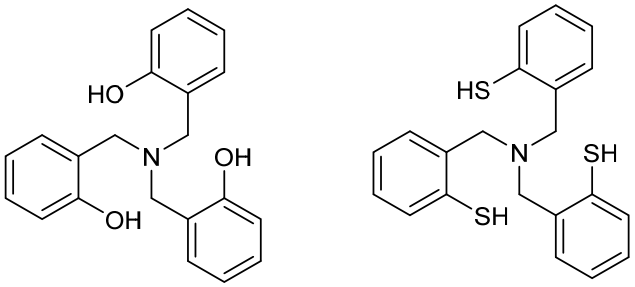

Figure 1. Triphenolamine (left) and trithiophenol amine (right).

Usually the synthesis of triphenolamines is performed *via* a one-step Mannich reaction of *ortho*/*para* disubstituted phenols with HMTA (hexamethylenetetramine) but this synthetic pathway requires long reaction times and harsh conditions. As previously reported, an effective synthesis based on a three-fold reductive amination starting from protected salicyl aldehydes was employed to achieve *ortho*-substituted triphenolamines.[5] This synthesis has been shown to be a successful methodology to build a large family of complexes with various functionalities in a multi-gram scale.

Taking advantage of this synthetic approach work proceeded in the study of the analogous trithiophenol amines (Figure 1, left). Ligands based on thiophenolate systems coordinated to transition metals can be efficiently employed in homogeneous catalysis and bioinorganic chemistry, although they are still rare and unexplored compared to their related phenolate derivatives.

In view of the results obtained with triphenolamines and inspired by the trigonal FeS_3 coordination sites present in the Fe Mo-cofactor of nitrogenase, the study was extended to trithiophenol amine in order to understand if the variation of the environment around the metal center would led to different reactivity and therefore different applications in catalysis and in coordination chemistry.

Very little has been reported on ligands-based on thiophenolate and the first synthesis of such ligand (R =H) was reported by Koch *et al*. nearly 20 years ago. It was employed for the preparation of the corresponding iron(II) and iron(III) complexes.[6] The catalytic behaviour of iron complexes was not explored at that time.

The ligand was synthesized starting from thiol-protected benzylamine, which was reacted with 2 equiv of the corresponding benzyl bromide using K_2CO_3 as base in acetonitrile (ACN), yielding the corresponding protected trithiophenol amine in 80% yield. After the removal of the protecting group, the ligand was obtained as a salt in 40% yield. The synthetic pathway is depicted in Scheme 1.

[5] L. J. Prins, M. Mba Blázquez, A. Kolarovic´, G. Licini. *Tetrahdron Lett.* **2006**, 47, 2735.
[6] N. Govindaswamy, D. A. Quarless Jr, S. A. Koch. *J. Am. Chem. Soc*. **1995**, 117, 8468.

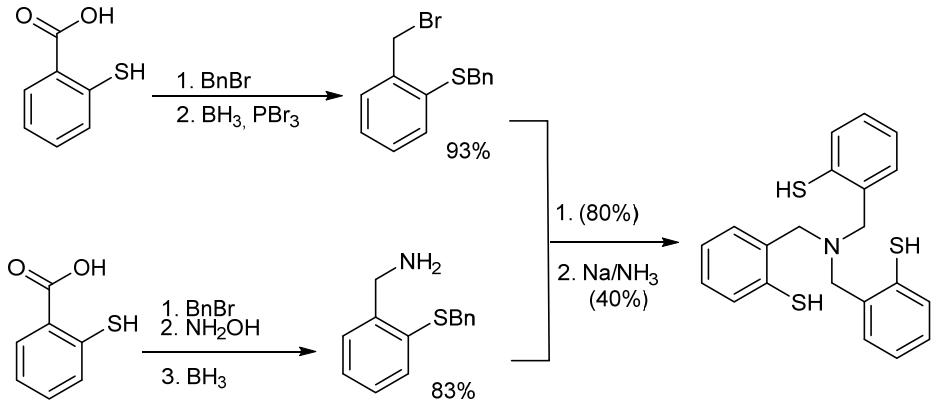

Scheme 1. Synthesis of trithiophenol amine

This synthetic route opened the way for the study of a new class of ligands however this strategy (Scheme 1), provided only non-substituted trithiophenol amine ligand in quite low yield involving the preparation of the two reagents separately.

In view of these results others have been investigated amino trithiophenolate when coordinated with Ga(III) and In(III).[7] In particular, Ga(III) amino trithiophenolate complexes have shown promising applications in the radiolabelling of large biomolecules such as peptides for use in receptor-based imaging. The tripodal ligand for Ga(III) was found to be stable to enzymatic hydrolysis, neutral and able to pass the BBB (blood-brain barrier). Although extensive theoretical studies have been carried out on amino trithiophenolate (R= H) complexes with iron,[8] *ortho*-substituted trithiophenol amine derivatives and their coordination chemistry with different metals have not been intensively investigated.

As consequence, the development of a general and efficient synthesis for this type of ligand is desirable and it will offer the opportunity to extend their application in catalysis. In light of our experience in the synthesis of triphenolamines and in their use as ligands for complexation and catalysis, we planned to prepare trithiophenol amine molecules *via* a similar methodology, i.e. the use of reductive amination as the key step for the preparation of the amino skeleton and Miyazaki–Newman–Kwart (MNK) rearrangement for the preparation of the thiophenol salicaldehyde monomers Scheme 2.

[7] a) R. J. Motekaitis, A. E. Martell, S. A. Koch, J. Hwang, D. A. Quarless Jr, M. J. Welch. *Inorg. Chem.* **1998**, 37, 5902. b) L. G. Luyt, J. A. Katzenellenbogen. *Bioconjugate Chem*. **2002**, 13, 1140. c) C. S. Cutler, M. C. Giron, D. E. Reichert, A. Z. Snyder, P. Herrero, C. J. Anderson, D. A. Quarless, S. A. Koch, M. J. Welch. *Nucl. Med. Biol*. **1999**, 26, 305.
[8] a) J. Conradie, D. A. Quarless, H.-F. Hsu, T. C. Harrop, S. J. Lippard, S. A. Koch, A. Ghosh. *J. Am. Chem. Soc*. **2007**, 129, 10446. b) J. Conradie, K. H. Hopmann, A. Ghosh. *J. Phys. Chem. B,* **2010**, 114, 8517.

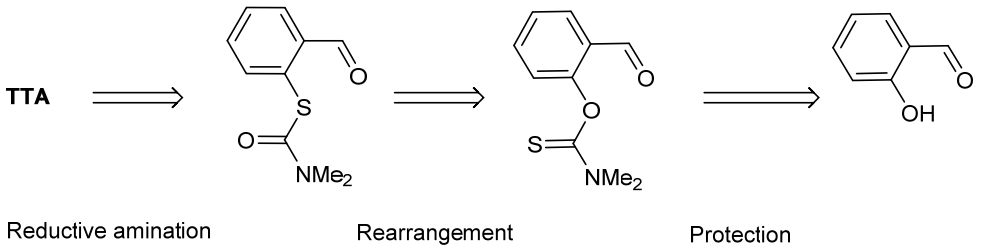

Scheme 2 Trithiophenol amine Retro-Synthesis

2.1.1 Miyazaki-Newman-Kwart Rearrangement

MNK rearrangement is a tautomeric rearrangement, which allows the migration of the aryl group of an *O*-aryl thiocarbamate from the oxygen to the sulfur atom through a four membered transition state, which forms an *S*-aryl thiocarbamate.[9] Because the sulphur atom has a stronger nucleophilicity compared to the oxygen atom, it becomes the driving force of the reaction toward the displacement of the oxygen as depicted in Scheme 3.

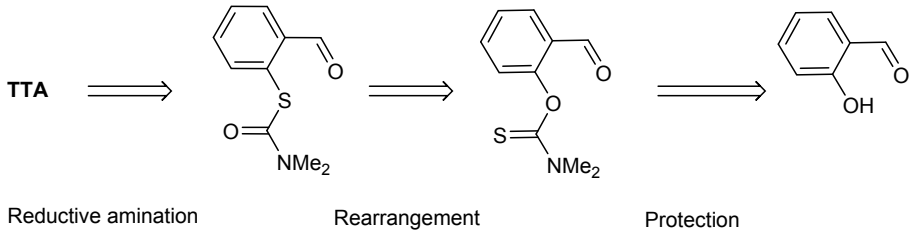

Scheme 3 Miyazaki -Newmann–Kwart rearrangement

The electronic and steric properties of substituents, in either the aromatic ring or *N*-substituent, are important in the rearrangement in order to stabilize both the negative and positive charge. For example, it was shown that electron withdrawing groups such as NO_2 in para position to the thiocarbamate have a positive effect in stabilizing the negative charge. On the other hand, *N*-alkyl substituents strongly affected the yield in rearranged product. Investigations also of the steric effects have been carried out, showing that hindered groups at the *ortho* position generally favoured the rearrangement except in the case of *t*-Bu groups.[10]

Taking account of these considerations, the work proceeded by planning the synthesis of a series of *ortho*-substituted trithiophenol amines, which can be easily and effectively prepared by reductive amination of the corresponding MNK rearranged *S*-thiocarbamoyl salicaldehydes. The key issue that makes this method successful is the use of the thiocarbamoyl group both as a rearranging agent and protecting group during the reductive amination carried out in the presence of $NaBH(OAc)_3$ and

[9] a) C. Zonta, O. De Lucchi, R. Volpicelli, L. Cotarca. *Topics Curr. Chem*. **2007**, 275, 131. b) G. C. Lloyd-Jones, J. D. Moseley, J. S. Renny. *Synthesis*, **2008**, 5, 661. c) M. Burns, G. C. Lloyd-Jones, J. D. Moseley, J. S. Renny. *J. Org. Chem*. **2010**, 75, 6347.
[10] H. M. Relles, G. Pizzoato. *J. Org. Chem*. **1968**, 33, 2249.

NH_4OAc. This strategy allows the effective construction of the ligand skeleton and differently substituted trithiophenol amines.

Initially a synthetic approach was examined, which proceeded toward the preliminary protection of the H group of substituted salicaldehydes **2a**–**d** (R = H, Me, Ph, *t*Bu, respectively), followed by MNK rearrangement of the resulting *O*-thiocarbamate esters **3a**–**d**, a threefold reductive amination of the thiosalicaldehyde *S*-thiocarbamates **4a**–**d**, and finally the reductive removal of the protecting carbamoyl groups, yielding **1a**–**c** (Scheme 4). The starting materials are commercially available (**2a**–**c**) or easily accessible from the corresponding phenol using paraformaldehyde and $MgCl_2$ (**2d**).[5]

2.2. Synthesis of S-thiocarbammate compounds

Treatment of **2a**–**d** with *N*,*N*-dimethylthiocarbamoyl chloride (DMTCl) in acetonitrile in the presence of potassium carbonate gave the desired *O*-thiocarbamates **3a**–**d** in good yields after purification (75–77%). The compounds were purified by either column chromatography or crystallization. Alternative procedures with different bases, such as 1,4-diazabicyclo[2.2.2] octane or NaH in *N*,*N*-dimethylformamide, did not furnish satisfactory yields for all of the products. Reaction conditions for the MNK rearrangement were optimized for **3a** (R = H, Table 1). The rearrangement was performed initially using the Lewis acid catalyst $BF_3{\cdot}OEt_2$ as reported by Brooker *et al*.[11] Although the reaction proceeded smoothly in high yield, it requires long reaction times **3d** and strictly anhydrous reaction conditions. To obtain a more reliable method the classical thermal rearrangement was attempted (Table 1, Entry 2).

Table 1. Optimisation of MNK rearrangement reaction conditions for **3a**.

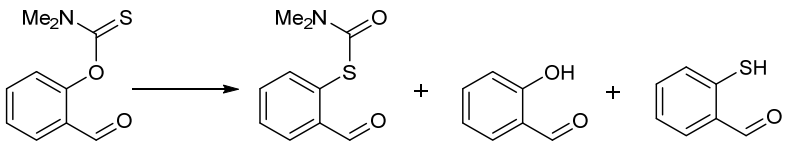

3a **4a** **2a** **6a**

#	Method[a]	Solvent[b]	Temp °C	Time (min)	Conversion[c] (%)	**4a**:**2a**:**6a**[c]
1	$BF_3{\cdot}OEt_2$	DCE	85	72 h	95	90:10:0
2	Thermal	Neat	300	5	80	30:70:0
3	MW	NMP	200	10	30	>99:1:0
4	MW	NMP	230	5	95	>99:1:0
5	MW	NMP	230	10	99	>99:1:0
6	MW	NMP	230	15	99	90:0:10

[11] S. Brooker, G. B. Caygill, P. D. Croucher, T. C. Davidson, D. L. J. Clive, S. R. Magnuson, S. P. Cramer, C. Y. Ralston. *J. Chem. Soc., Dalton Trans.* **2000**, 3113.

[a] $BF_3{\cdot}OEt_2$: Lewis acid rearrangement using the conditions described in ref. 9, Thermal: thermal rearrangement induced by heating, MW: microwave rearrangement. [b] DCE: dichloroethane, NMP *N*-methylpyrrolidone. [c] Data obtained using ^1H NMR of the crude mixture.

The reaction was performed at 300 °C and 25% of the desired product **4a** was obtained, in a very short time. However, under these conditions, extensive hydrolysis of the reagent to **2a** (56%) was observed. On the contrary, the reaction carried out using microwave (MW) induced heating, after dissolving the sample in *N*-methylpyrrolidone (NMP), enables the tuning and optimization of the reaction conditions and the maximization of conversion of **3a** into **4a** without reagent or product hydrolysis (Table 1, Entries 3–6). [12] The best reaction conditions were obtained, using anhydrous NMP at 230 °C for 10 min (Table 1, Entry 5). Shorter reaction times did not permit complete conversion of the reagent, and longer reaction times resulted in the partial hydrolysis of the *S*-thiocarbamoyl group yielding thiosalicaldehyde (**6a**, 10%, Table 1, Entry 6). The best reaction conditions obtained with **3a** were also applied to **3b–d** (Table 2). As mentioned previously, the presence of an *ortho* substituent to the thiols moiety is known to strongly influence the MNK rearrangement. [9a] Preliminary tests showed that, although a clean and quantitative rearrangement was obtained for the phenyl substituted aldehyde **4c**, the presence of an aliphatic group in the *ortho* position, as the methyl group **3b** or *tert*-butyl **3d** systems, resulted in extensive reagent and/or product hydrolysis, lowering the final yield of **4**. Therefore, irradiation times were decreased to 5 min and under this conditions a good yield of **3c** was obtained (95% conversion, Table 2, Entry 4), whereas **3b**, with 97% conversion, gave a rearrangement yield of 78% for *S*-thiocarbamate **4b** (54%) and the hydrolyzed **6b** (24%, Table 2, Entry 2 and 4). For **3d**, reagent and product hydrolysis were even more evident. The MNK rearrangement furnished 10% yield of **4d** and 50% of **6d**. It seems likely that the aliphatic substituent is not responsible for the reduced yield in the rearrangement reaction rather the starting material **3d** and the thiocarbamate product **4d** are more susceptible to hydrolysis. Further variation of the reaction times and reaction temperatures under MW induced heating conditions or the use of $BF_3{\cdot}OEt_2$ did not result in better yields.

Table 2. MNK rearrangement for **3a–d**.

[12] J. D. Moseley, R. F. Sankeya, O. N. Tanga, J. P. Gildaya. *Tetrahedron,* **2006**, 62, 4685.

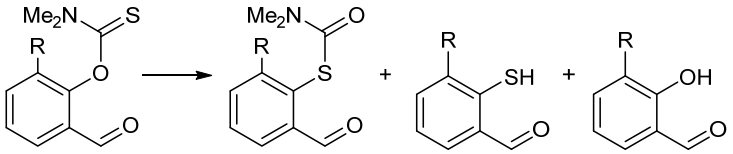

3a R = H
3b R = Me
3c R = Ph
3d R = *t*-Bu

4a R = H
4b R = Me
4c R = Ph
4d R = *t*-Bu

6a R = H
6b R = Me
6c R = Ph
6d R = *t*-Bu

2a R = H
2b R = Me
2c R = Ph
2d R = *t*-Bu

#	Aldehyde	Temp (°C)	Time (min)	Conversion[a] (%)	**4**:**6**:**2**[a]
1	**3a**	230	5	95	90:0:10
2	**3b**	230	5	97	54:24:22
4	**3c**	230	5	95	99:0:1
6	**3d**	230	5	99	10:50:40

[a] Data obtained using ^{1}H NMR of the crude mixture.

Compounds **3b** and **3d** were also irradiated without solvent and an increased yield of rearranged product was obtained for **3b** (90%, Table 2 Entry 3), whereas **3d** gave a higher yield of **4d** (25%) with an amount of **6d** (48 %). Because of the low yields of **4d**, the synthesis of trithiophenol amine **1d** was not further investigated. However, it must pointed out that the MNK rearrangement is effective (60% of rearranged product as **4d** and **6d**) and can still be synthetically useful. Moreover, **2b** and **2d** can be recycled. *S*-thiocarbamoyl aldehydes **4a**–**c** were purified by column chromatography after removal of the solvent by distillation at low pressure.

2.3 Synthesis of *ortho*-trithiophenol amines

The resulting *S*-thiocarbamoyl aldehydes **4a**–**c** were subsequently used for reductive amination in the presence of $NaBH(OAc)_3/NH_4OAc$. The yields of **5a**–**c** after purification were satisfactory (ca. 50%). The only by product of the reaction was the benzylic alcohol arising from the reduction of the corresponding aldehyde. The final step can be driven to completion under reductive conditions (lithium aluminium hydride), whereas hydrolytic methods (KOH/EtOH) gave only partial deprotection. The desired **1a**–**c** ligands were obtained in good yields after aqueous work up (60–65 %) Scheme 4. These compounds are known to have low stability under oxidative or basic

conditions (formation of disulfides and dibenzo[1,5] dithiocines) [13] and, for these reasons, they were usually used directly for the synthesis of the corresponding metal complexes without further purification. [14]

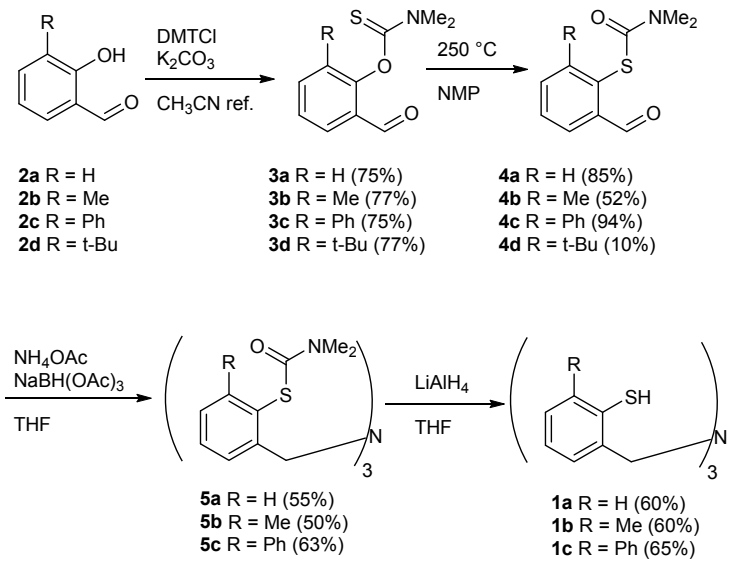

Scheme 4. Synthetic procedure for the synthesis of **1a-c**

The synthesis can be further optimized by carrying out the reductive amination and deprotection in a one-pot procedure. This strategy has been tested on **4c** affording the product in quite good yields. Therefore, only three steps are required to obtain the trithiophenol amines from the commercially available salicaldehydes.

Furthermore, in parallel with the synthetic pathway described above, another synthetic approach was attempted. To achieve directly the ligand, firstly it was prepared using a threefold reductive amination, as presented above, followed by the Miazaky-Newmann–Kwart rearrangement of the ligand itself. Although the threefold introduction of the thiocarbamoyl groups proceeded smoothly, the rearrangement did not take place and a mixture of either rearranged or non-rearranged products was observed. The synthesis is depicted in Scheme 5.

[13] K. Kanakarajan, H. Meier. *J. Org. Chem.* **1983**, 48, 881.

[14] a) R. Burth, A. Stange, M. Schäfer, *Eur. J. Inorg. Chem.* **1998**, 1, 1759. b) C. Belle, C. Bougault, M.-T. Averbuch, A. Du-Rif, J.-L. Pierre. J.-M. Latour, L. Le Pape. *J. Am. Chem. Soc.* **2001**, 123, 8053.

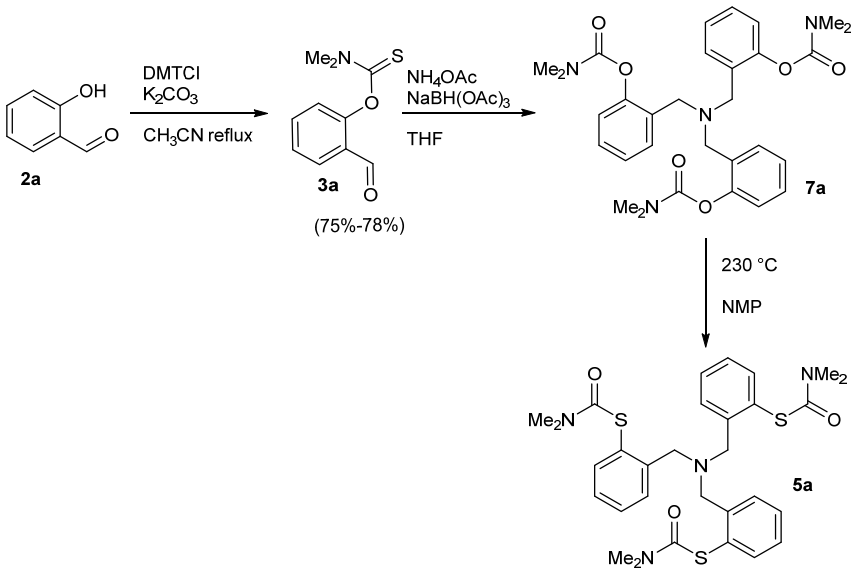

Scheme 5

2.4 Conclusions

In conclusion, the synthetic methodology reported allows the synthesis of *ortho*-substituted trithiophenolamines **1a-c** with very satisfactory yields *via* a three step procedure starting form commercially available aldehydes. This approach led us to the possibility, for the first time, to access this important class of ligands in a systematic way using either commercially or readily available building blocks. Moreover, the synthesis of thio-aldehydes could be important for the preparation of salan, salen and salalen ligands. This methodology will be employ for the synthesis of a large library of this class of ligands for applications in coordination chemistry and catalysis.

2.5 Experimental Section

General methods: Chemicals and solvents were purchased from commercial suppliers and used as supplied. Starting materials such as 3-substituted salycil aldehydes **2a-d** are commercially available or easily accessible from the corresponding phenols. ^{1}H-NMR spectra were recorded on a Bruker AC 250 (250.18 MHz) or Bruker Avance DRX 300 (300.13 MHz) spectrometer, using partially deuterated solvent or TMS as internal references (TMS = 0.00 ppm, $CHCl_3$= 7.26 ppm). ESI-MS and EA

Synthesis of substituted O-2-formylphenyl dimethylthiocarbamate (3a-d).

Substituted salicyl aldehydes **2a-d**, (0.05 mol) were dissolved in dry acetonitrile (20 ml) under nitrogen at room temperature. K_2CO_3 (26.25g, 0.2 mol) was added to the stirred solution. After 10

min solid dimethylthiocarbamoyl chloride (7.4 g, 0.06 mol) was added and the mixture heated at 80°C. After 24 hours the mixture was cooled at room temperature, the solid residue was filtered and washed with EtOAc (25 ml). The organic layer washed with water (3 x 15 ml), dried over Na_2SO_4 and concentrated under reduced pressure. The product was purified by flash chromatography (SiO_2, Petroleum Ether:EtOAc 8:2).

O-(2-formylphenyl)dimethylthiocarbamate (**3a**): white solid; yield: 75%; ^{1}H-NMR (250MHz, $CDCl_3$): δ= 10.07 (s, 1H), 7.91(d, *J* = 9.0 Hz, 1H), 7.89 (t, *J* = 9.0 Hz 1H), 7.4 (t, *J* = 13.0 Hz, 1H), 7.13 (d, *J*= 13.0 Hz 1H), 3.44 (d, *J* = 15.0 Hz, 6H) ppm; ^{13}C NMR (62.9 MHz, $CDCl_3$): δ= 187.92, 154.81, 134.43, 129.23, 128.69, 126.00, 123.96, 111.49, 43.40, 38.92 ppm.

O-(2-Formyl-6-methylphenyl) dimethylthiocarbamate (**3b**): orange oil; yield: 77%; ^{1}H-NMR (250MHz, $CDCl_3$): δ= 10.02 (s, 1H), 7.74 (d, *J* = 7.5 Hz, 1H), 7.49 (d, *J* = 7.2 Hz, 1H), 7.30 (t, *J* = 7.5, 1H), 3.46 (d, *J* = 10 Hz, 6H) 2.43 (s, 3H) ppm; ^{13}C NMR (62.9 MHz, $CDCl_3$): δ= 188.77, 153.45, 136.70, 132.38, 129.13, 127.55, 126.12, 111.84, 43.33, 38.69, 15.51 ppm.

O-(3-Formyl-biphenyl-2yl) dimethylthiocarbamate (**3c**): white solid ; yield: 75%; ^{1}H-NMR (250MHz, $CDCl_3$): δ= 10.09 (s, 1H), 7.94 (d, *J* =7.5, 1H), 7.62 (d, *J* = 7.5, 1H), 7.49 (s, 1H), 7.41 (m, 5H), 3.21 (d, *J* = 18Hz, 6H) ppm; ^{13}C NMR (62.9 MHz, $CDCl_3$): δ= 188.49, 152.45, 136.44, 130.19, 129.17, 128.39, 127.85, 126.47, 43.40, 38.63 ppm.

O-(2-Formyl-6-t-butylphenyl) dimethylthiocarbamate (**3d**); yellow solid; yield:75%, ^{1}H-NMR (250MHz, $CDCl_3$): δ= 9.92 (s, 1H), 7.75 (d, *J* =7.5 Hz, 1H), 7.67 (d, *J* =7.5 Hz, 1H), 7.30 (t, *J* = 7.5 Hz, 1H), 3.48 (s, 6H) 1.40 (s, 9H) ppm; ^{13}C NMR (62.9 MHz, $CDCl_3$): δ= 188.52, 153.30, 142.51, 133.20, 130.64, 128.53, 125.98, 126.47, 43.40, 39.10, 35.05, 30.83 ppm.

Synthesis of substituted S-2-formylphenyl dimethylthiocarbamate (4a-d).

Microwave reactions were performed in 10 ml sealed tubes in a regularly calibrated CEM Discover focused 300 W microwave reactor with IR temperature monitoring and non-invasive pressure transducer. In a typical procedure *O*-thiocarbamate **3a-d** (1 mmol) was dissolved in NMP (2.5 ml) and heated to the required temperature with stirring for a fixed time. The heating time to reach the set temperature was typically 60 s, depending on the scale, the maximum wattage supplied (100–300 W) and the temperature required. The heating time is not included in the quoted hold time for any given procedure. The *S*-thiocarbamate (**4a-c**) products were isolated either directly by aqueous drown-out from NMP solutions, or by extraction into EtOAc followed by flash silica gel chromatography.

S-(2-formylphenyl) dimethylthiocarbamate (**4a**): Irradiation time 230°C, 5 min. After extraction with EtOAc, the crude material was purified by flash (SiO_2, Petrolium Ether: Ethyl Acetate 8:2). Bright yellow oil; yield 85% ^{1}H-NMR (250MHz, $CDCl_3$): δ= 10.35 (s, 1H), 8.02 (d, *J* = 5.7 Hz,

1H), 7.55 (m, 3H), 3.07 (s, 6H) ppm; ^{13}C NMR (62.9 MHz, $CDCl_3$): δ= 191.82, 165.23, 148.24, 140.08, 138.58, 135.31, 129.58, 127.75, 37.09 ppm.

S-(2-Formyl-6-methylphenyl) dimethylthiocarbamate (**4b**): Irradiation time 230°C, 2 min. After extraction with EtOAc, the crude material was purified by flash (SiO_2, Petrolium Ether: Ethyl Ether 7:3). orange oil; yield: 52%; ^{1}H-NMR (250MHz, $CDCl_3$): δ= 10.42 (s, 1H), 7.80 (d, *J* =7.5 Hz, 1H), 7.40 (m, 2H), 3.04 (d, *J* =10 Hz, 6H), 2.43(s, 3H) ppm; ^{13}C NMR (62.9 MHz, $CDCl_3$): δ = 192.06, 164.61, 143.97, 138.39, 135.47, 131.60, 129.65, 126.20, 37.04, 20.84 ppm.

S-(3-Formyl-biphenyl-2yl) dimethylthiocarbamate (**4c**): Irradiation time 230°C, 5 min. After extraction with EtOAc, the crude material was purified by flash (SiO_2, Petrolium Ether: Ethyl Acetate 8:2). Bright yellow oil; yield 94%. ^{1}H-NMR (250MHz, $CDCl_3$): δ= 10.36 Hz (s, 1H), 8.0 (m, 1H), 7.52 (m, 2H), 7.34 (m, 3H), 7.2 (m, 2H), 2.97 (s, 6H) ppm; ^{13}C NMR (62.9 MHz, $CDCl_3$): δ= 191.69, 165.10, 148.26, 140.10, 138.59, 135.34, 130.75, 129.60, 127.77, 127.55, 36.96 ppm.

Synthesis of Tri-(2-N-dimethylthiocarbamoilbenzyl) amine (5a-c):

Rearranged aldehydes **4a-c** (3 mmol) were mixed with ammonium acetate (80 mg, 1 mmol) in THF (20 ml) under nitrogen atmosphere. After 2h sodium triacetoxy borohydride (920 mg, 4 mmol) was added. The mixture was stirred overnight at room temperature and evaporated to dryness. The residue was dissolved in EtOAc and washed twice in ammonium chloride and brine. The organic layer was dried over Na_2SO_4 and concentrated under reduced pressure. The product was purified by flash chromatography. (SiO_2, Petroleum Ether: EtOAc:TEA 8:2:0.01).

Tri-(2-N-dimethylthiocarbamoilbenzyl) amine (**5a**). 55%. Bright yellow oil; yield 55%. ^{1}H-NMR (250MHz, $CDCl_3$): δ = 7.53 Hz (d, *J* = 7.5, 3H), 7.42 (d, *J* = 5.0 Hz, 3H), 7.31 (t, *J*= 5.0 Hz, 3H), 7.21 (t, *J* = 7.5 Hz, 3H), 3.69 (s, 6H), 2.98 (s, 18H) ppm; ^{13}C NMR (62.9 MHz, $CDCl_3$): δ= 166.50, 142.82, 136.93, 130,96, 129.02, 128.74, 126.96, 56.95, 36.72 ppm. MS (ESI): calcd for $C_{30}H_{36}N_4O_3S_3$ $[M+H]^+$, 596.1, found 596.2.

Tri-(2-N-dimethylthiocarbamoil-3-metilbenzyl) amine (**5b**): 50%. Bright yellow oil; ^{1}H-NMR (250MHz, $CDCl_3$): δ= 7.80 (d, *J* =7.5 Hz, 3H), 7.40 (m, 6H), 3.73(s, 6H), 3.04 (s, 18H), 2.43 (s, 9H) ppm; ^{13}C NMR (62.9 MHz, $CDCl_3$): δ = 165.70, 147.97, 140.39, 138.30, 133.70, 131.44, 128.30, 37.04, 20.84 ppm. MS (ESI): calcd for $C_{33}H_{42}N_4O_3S_3$ $[M+H]^+$, 639.2, found 639.2.

Tri-(2-N-dimethylthiocarbamoil-3-phenylbenzyl) amine (**5c**): 53% Yellow oil; ^{1}H-NMR (250MHz, $CDCl_3$): δ= 7.80 Hz (d, *J* = 7.5 Hz, 3H), 7.30 (m, 3H), 7.27 (m, 15H), 7.20 (m, 3H), 3.96 (s, 6H), 2.85 (s, 18H) ppm; ^{13}C NMR (62.9 MHz, $CDCl_3$): δ = 166.29, 147.85, 144.74, 142,12, 129.53, 129.37, 129.04, 128.89, 127.32, 126.72, 57.65, 37.19 ppm. MS (ESI): calcd for $C_{48}H_{48}N_4O_3S_3$ $[M+H]^+$, 825.3, found 825.3.

Synthesis of Tris-(2-mercaptobenzyl) amine (1a-c): To a solution of compound **5a-c** (0.16 mmol) in dry THF (2 ml) was slowly added at -70°C $LiAlH_4$ (1.34 ml 1.0 M in THF, 1.34 mmmol). After 5 min the mixture was warmed to room temperature and refluxed for 3 hours. The excess of $LiAlH_4$ was quenched by careful addition of EtOAc (3 ml) at 0°C. This operation was followed by the addition of a solution of H_2SO_4 (10% water, 2 ml). The mixture was extracted with EtOAc (5 ml), washed with water and dried over Na_2SO_4. The resulting solution was concentrated under reduced pressure. Due to the instability of the ligands, the products were not purified.

Tris-(2-mercaptobenzyl) amine (**1a**). Bright yellow oil; yield 60%. ^{1}H-NMR (250MHz, $CDCl_3$): δ = 7.33 Hz (d, *J* = 7.5 Hz, 3H), 7.3 (d, *J* = 5.0 Hz, 3H), 7.17 (t, *J* = 5.0 Hz, 3H), 7.21 (t, *J* = 7.5 Hz, 3H), 3.69 (s, 6H) ppm; ^{13}C NMR (62.9 MHz, $CDCl_3$): δ = 142.82, 136.93, 130,76, 129.02, 128.74, 126.96, 56.95 ppm. MS (ESI): calcd for $C_{21}H_{21}NS_3$ $[M+H]^+$, 384.1, found 384.0.

Tris-(2-mercapto-3-methylbenzyl) amine (**2a)** Bright yellow oil; yield 60% ^{1}H-NMR (250MHz, $CDCl_3$): δ= 7.60 (d, *J* =7.5 Hz, 3H), 7.25 (m, 6H), 3.73(s, 6H), 2.41 (s, 9H) ppm; ^{13}C NMR (62.9 MHz, $CDCl_3$): δ =145.97, 140.39, 138.30, 133.70, 131.44, 128.30, 57.04, 21.84 ppm. MS (ESI): calcd for $C_{33}H_{42}N_4O_3S_3$ [M+H], 426.1, found 426.2.

Tris-(2-mercapto-3-phenylbenzyl) amine (**3a**): bright yellow oil 65%. ^{1}H-NMR (250MHz, $CDCl_3$): δ= 7.38 Hz (m, 3H), 7.35 (m, 3H), 7.30 (m, 15 H), 7.10 (m, 3H), 3.80 (s, 6H), ppm; 13C NMR (62.9 MHz, CDCl3): 147.85, 144.74, 142, 12, 129.53, 129.37, 129.04, 128.89, 127.32, 126.72, 57.65, ppm. MS (ESI): calcd for $C_{39}H_{33}NS_3$ $[M+H]^+$, 612.2, found 612.1.

Chapter 3

V(V) amino triphenolate as catalyst for C-C bond cleavage under aerobic conditions

Abstract

In this chapter, an exploration into new reactivity of V(V) amino triphenolate complexes will be described. In particular the activity in oxidative C-C bond cleavage of 1,2-diols and, in a preliminary way, β-hydroxy ethers has been investigated. These studies were carried out in order to develop catalysts capable of controlled oxidative degradation of more challenging substrates, such as lignin models to demonstrate the feasibility of producing fine chemicals from a renewable carbon feedstock.

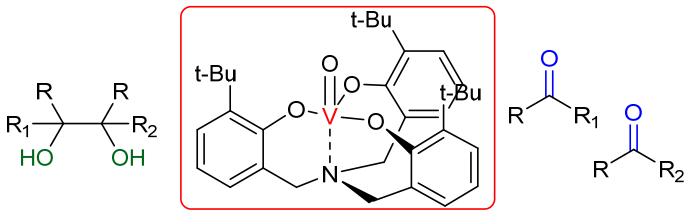

3.1 Introduction

The development of efficient catalytic systems able to transform biomass into useful chemicals is of great interest in the chemical world because biomass is considered to be the only renewable carbon feedstock available.[1] Both cellulose and lignin are constituents of non-food based biomass and therefore potential sources of complex organic building blocks. Several methods have been reported for the conversion of cellulose whereas little progresses have been made for the transformation of lignin into valuable compounds. This is related to its highly intricate structure; lignin is a polymer organized in irregular carbon-carbon and carbon-oxygen phenolic subunits and the abundance of these subunits linkages is different in each type of wood. Despite the diversity of lignin, the most common unit includes the β-O-aryl ether (β-O-4) linkages featured in Figure 1.

[1] a) A. Corma, S. Iborra, A. Velty. *Chem. Rev*. **2007**, 107, 2411. b) J. N. Chheda, G. W. Huber, J. A. Dumesic. *Angew. Chem.* **2007**, 119, 7298. c) G. W. Huber, S. Iborra, A. Corma, *Chem. Rev.* **2006**, 106, 4044.

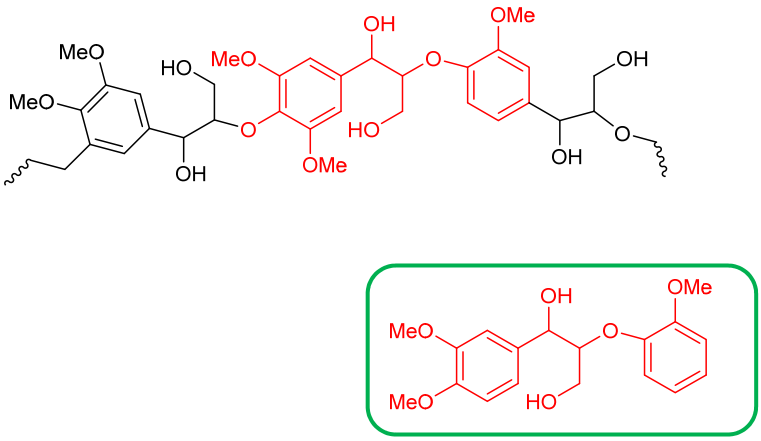

Figure 1. Representative structures of a fragment of lignin and the corresponding β−O−4-linked model compound 1.

This subunit represents a significant percentage of all the linkages, thus is a target of lignin de-polymerization. For this reason, the development of catalysts that can effectively cleave β-O-4′bonds under mild reaction conditions could provide the utilization of lignin for high-value applications. Aside from the difficulty related to its structural complexity, there are three main problems for the efficient use of lignin compounds: firstly the reaction conditions required for its degradation such as temperature, pressure[2] and solubility,[3] secondly the selectivity of the transformation in delivering valuable aromatic compounds[4] and finally the cost of the entire degradation process which has to be convenient in terms of both price and waste products.[5]

The primary pathway by which lignin is naturally depolymerized is oxidation using enzymes such as lignin peroxidases in the presence of oxidants such as hydrogen peroxide or oxygen. [6] Oxidation in aerobic conditions has shown to be advantageous since no added reagents are required. Furthermore, it could preserve a high degree of the functionalities present in the original lignin polymer.

A series of recent works report that homogeneous catalysis using non-toxic, abundant and cheap metals could provide a selective cleavage of lignin linkages, which as mentioned above, is highly desirable under mild and inexpensive conditions.[5]

In general, the homogeneous catalysts employed for lignin oxidation can be summarized into five classes of compounds: Schiff base catalysts,[7,8] metalloporphyrins,[9] tetraamidomacrocyclic iron

[2] a) V. M. Roberts, V. Stein, T. Reiner, A. Lemonidou, X. Li, J. A. Lercher, *Chem.-Eur. J.* **2011**, 17, 5939. b) C. Zhao, J. A. Lercher. *ChemCatChem.* **2012**, 4, 64.
[i3] a) A. G. Sergeev, J. F. Hartwig. *Science*, **2011**, 332, 439. b) A. Wu, B. O. Patrick, E. Chung, B. R. James. *Dalton Trans*. **2012**, 41, 11093. c) J. M. Nichols, L. M. Bishop, R. G. Bergman, J. A. Ellman. *J. Am. Chem. Soc*. **2010**, 132, 12554.
[4] a) C. Crestini, A. Pastorini, P. Tagliatesta. *J. Mol. Catal. A: Chem*. **2004**, 208, 195. b) A. R. Gaspar, J. A. F. Gamelas, D. V. Evtuguin, C. P. Neto. *Green Chem*. **2007**, 9, 717.
[5] a) P. Zakzeski, C. A. Bruijnincx, A. L. Jongerius, B. M. Weckhuysen. *Chem. Rev*. **2010**, 110, 3552. b) F. G Calvo-Flores, J. A. Dobado. *ChemSusChem*.**2010**, 3, 1227. c) J. C. Hicks, J. Phys. *Chem. Lett.* **2011**, 2, 2280. d) M. P. Panday, C. S. Kim. *Chem. Eng. Technol.* **2011**, 34, 29. e) P. Azadi, O. R. Inderwildi, R. Farnood, D. A. King. *Renew. Sust. Energy Rev*. **2013**, 21, 506.
[6] a) T. K. Kirk, R. L Farrell. *Annu. Rev. Microbiol*. **1987**, 41, 465. b) M. Tien, T. K Kirk. *Science,* **1983**, 221, 661.
[7] K. C. Gupta, A. K. Sutar, C.-C. Lin. *Coord. Chem. Rev*. **2009**, 253, 1926.
[8] C. Canevali, M. Orlandi, L. Pardi, B. Rindone, R. Scotti, J. Sipila, F. J. Morazzoni. *Chem. Soc., Dalton Trans*. **2002**, 3007.

catalysts,[10,11] polyoxometalates[12] and Co(III)[13] and Mn(III)[14] salts. For each system reported stoichiometric amounts of oxidants, *e.g.* hydrogen peroxide or oxygen, were employed.

3.1.1 Vanadium(V) as catalysts for lignin degradation

Among these catalytic systems developed in the last few years and in view of this thesis work, attention will be focused on homogeneous catalysis based on vanadium complexes, that have been shown to be able to degradate lignin model compounds under aerobic oxidation conditions. Son and Toste reported the V(V) tridentate Schiff-base catalyst **1** that effectively and selectively cleaves β-O-4′bonds in lignin substructures as depicted in Scheme 1.[15,16]

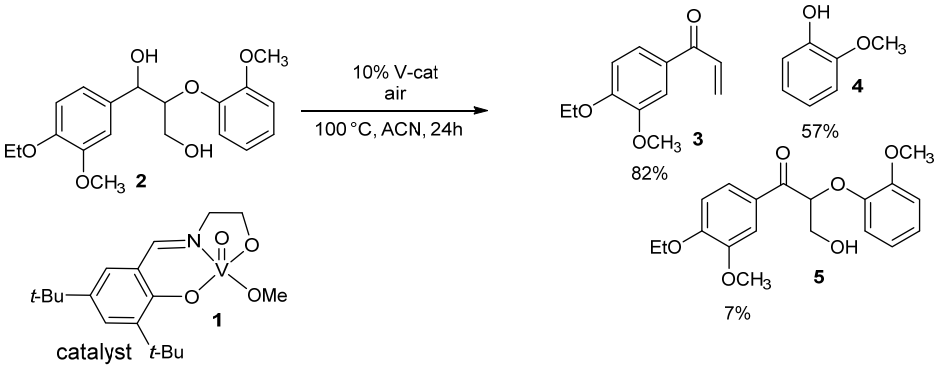

Scheme 1. Lignin model degradation by 1

The reaction was carried out using 10% catalyst **1** loading, at 80°C in MeCN and after 24 h it was possible to obtain almost complete conversion of lignin model compound (95%), yielding the products **3**, **4** and **5**. It was found that after 24 h under anaerobic conditions the same products were obtained, albeit in reduced yield. This demonstrates that the V(V) is reduced to V(IV) species during the reaction, but oxygen is not fundamental for catalyst turnover. For this catalytic system, a non-oxidative C-O bond cleavage was proposed which proceeds through one-electron process as depicted in Scheme 2.

[9] a) G. Labat, B. Meunier. *J. Org. Chem*. **1989**, 54, 5008. b) W. Zhu, W. T. Ford. *J. Mol. Catal.* **1993**, 78, 367. c) I. Artaud, K. Ben-Aziza, D. Mansuy. *J. Org. Chem.* **1993**, 58, 3373.
[10] T. J Collins. *Acc. Chem. Res*. **2002**, 35, 78.
[11] D.-L. Popescu, A. Chanda, M. J. Stadler, S. Mondal, J. Tehranchi, A. D. Ryabov, T. J. Collins. *J. Am. Chem. Soc.* **2008**, 130, 12260.
[12] J. A. F. Gamelas, A. R. Gaspar, D. V. Evtuguin, C. P. Neto. *Appl. Catal.,* **2005**, 295, 134. b) J. A. F. Gamelas, A. R. Gaspar, D. V. Evtuguin, C. P. Neto. *Chem. Eng. Commun*. **2009**, 196, 801. c) Y. S. Kim, H.-M. Chang, J. F. J Kadla. *Wood Chem. Technol*. **2007**, 27, 225.
[13] R. Di Cosimo, H. C. Szabo. *J. Org. Chem*. **1988**, 53, 1673. b) G. A. A. Labat, A. R. Goncalves. *Appl. Biochem. Biotechnol*. **2008**, 148, 151.
[14] S. Hwang, Y.-W. Lee, C.-H. Lee, I.-S. J. Ahn. Polym. Sci., Part A: *Polym. Chem*., 46, 6009.
[15] S. Son, F. D. Toste. *Angew. Chem. Int. Ed*. **2010**, 49, 3791.
[16] J. M. W. Chan, S. Bauer, H. Sorek, S. Sreekumar, K. Wang, F. D. Toste. *ACS Catal*. **2013**, 3, 1369.

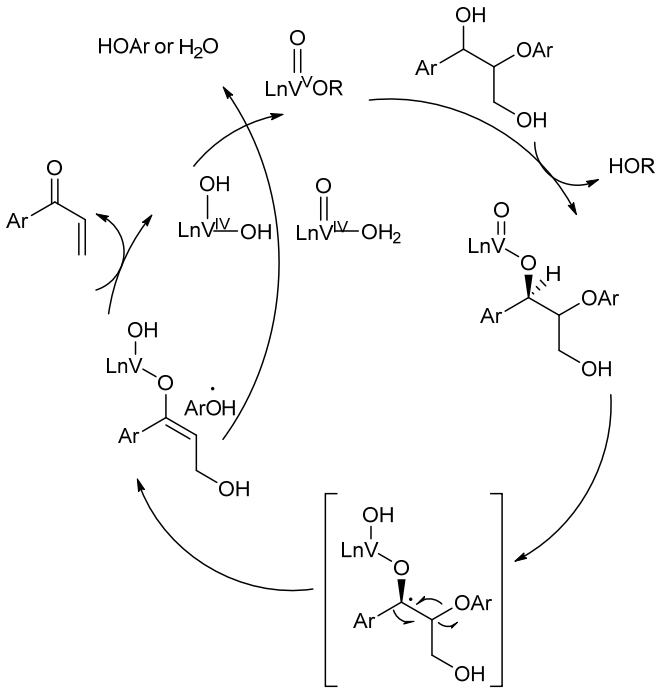

Scheme 2. Proposed mechanism for vanadium-catalyzed non-oxidative cleavage reported by Toste.[5]

The first step involves the exchange of the alcholate ligand on the vanadium(V) complex **1** with the benzylic hydroxyl group, followed by the abstraction of the hydrogen to form a ketyl radical which subsequently eliminates the aryloxyradical. The reaction proceeds with the elimination of the hydroxyl group from the resulting enolate yielding an enone product and the reduced species of vanadium (IV) which can be re-oxidized into vanadium (V) species by the aryloxyradical. These latter results are supported by thermodynamic studies of hydrogen atom transfer reaction between phenol derivatives and vanadium–oxo species.[17] The same authors inspired by these promising results obtained with vanadium(V) catalyst **1**, proceeded toward the extension of this catalytic system into lignin derived from *Miscanthusgiganteus*. The reactions were followed by GPC and it was found that V(V) catalyst **1** remained active and can efficiently perform the cleavage of the β-O-4 linkage yielding valuable aromatic compounds.

More recently, Hanson *et al.* reported other vanadium complexes as catalysts for oxidative C-C bond cleavage of a phenolic lignin compound.[18] These studies had the aim to identify catalysts able to control the selectivity toward C-C or C-O bond cleavage of lignin in aerobic oxidation. Both in catalytic aerobic oxidation conditions and the cleavage of specific linkages represent a challenge in homogeneous catalysis, as this strategy would provide the production of fine chemicals without the use of stoichiometric reagents. As previously mentioned, lignin is composed by irregular

[17] C. R. Waid- Mann, X. Zhou, E. A. Tsai, W. Kaminsky, D. A. Hrovat, W. T. Borden, J. M. Mayer, *J. Am. Chem. Soc*. **2009**, 131, 4729.
[18] a) Hanson, S. K.; Wu, R.; Silks, L. A. *Angew. Chem. Int. Ed*. **2012**, 51, 3410. b) Sedai, B.; Diaz-Urrutia, C.; Baker, R. T.; Wu, R.; Silks, L. A.; Hanson, S. K. *ACS Catal.* **2011**, 1, 794.

phenolic subunits, each containing 1,2-hydroxy ether substituents. In these studies the reactivity of 8-quinolinate vanadium(V) complex **6** was investigated with the phenolic lignin model compound **7** (Scheme 3). In previous work, it was found that complex **6** is able to catalyze the aerobic oxidation of benzylic and allylic alcohols when an additive, generally a base, is used.[19] The reaction was carried out using 10 mol% of catalyst **6** in the presence of triethylamine and the results are presented in Scheme 3.

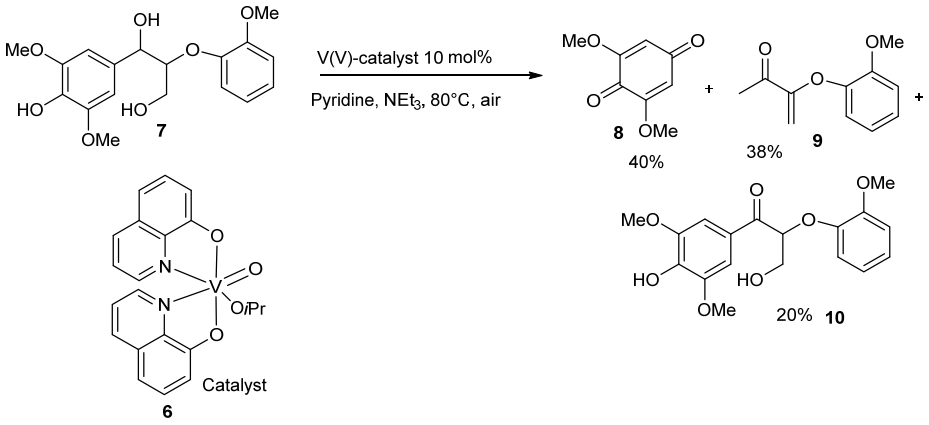

Scheme 3.

Under these conditions the reactions affords the products derived from cleavage of the C-C bond: compound **8** (2,6-dimethoxybenzoquinone 40%), an acrolein derivative **9** (38%), and the corresponding oxidized ketone **10** (38%) (Scheme 3). According to the authors, the formation of the acrolein product **9** was unexpected as the cleavage of C-C bond between alkyl and phenyl moieties is a rare reaction. The cleavage observed with the formation of the acrolein product, which differs from the non-oxidative C-O cleavage reported by Toste, indicates that the reaction selectivity depends upon the catalyst used. When the same lignin model was tested with Toste's catalyst the products derived from C-O bond cleavage were observed. This confirms that selectivity in cleavage sites can be achieved using different catalysts. The role played by the phenoxy group in the lignin model compound in selectivity was highlighted when the experiment was carried out using a non-phenolic lignin model compound. In this case, products derived from the C-C bond cleavage were not detected.

[19] S. K. Hanson, R. Wu, L. A. Silks, *Org. Lett.* **2011**, 13, 1908.

According to the authors, the mechanism of the oxidative C-C bond cleavage may involve the formation of a phenoxy radical intermediate. This pathway has been also proposed for metal complexes based on cobalt.[20]

More recently, the same group reported a vanadium complexes based on bis-(phenolate) ligands (Scheme 4). These complexes were employed as catalysts in the aerobic oxidation of lignin model compounds and in the oxidation of 1,2-diols and benzyl alcohol.[21] In this case, for lignin transformation, vanadium complexes have shown different selectivity toward the cleavage of C-O and C-H bond and lower reactivity in comparison with the V(V) 8-quinolinate **6** previously discussed. For example, it was found that complex **10**, employing phenolic lignin model compound **7**, gave only 20% of conversion, whereas for **11**, a non-phenolic lignin model, 84% of conversion was obtained with a mixture of C-O and C-H bond cleavage products, as reported in Scheme 4.

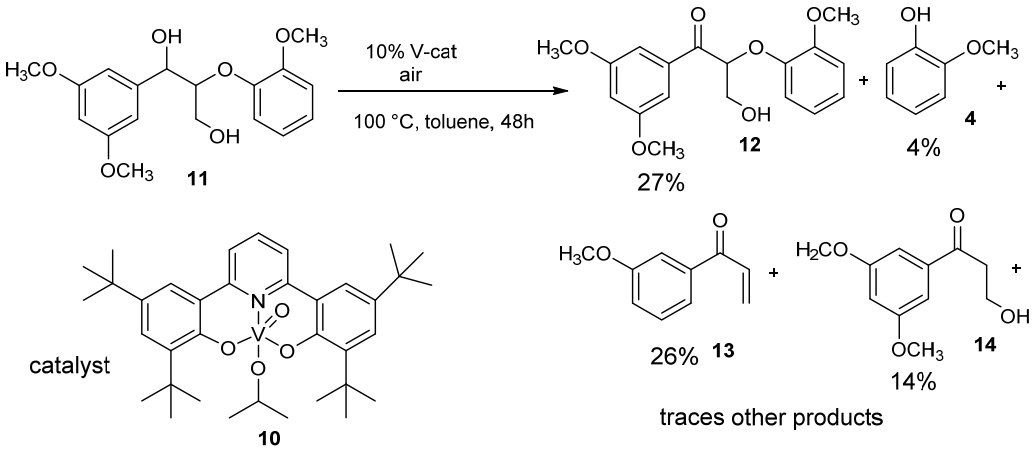

Scheme 4. Lignin model **11** degradationcatalyzed by **10**. [21]

In view of the latest studies obtained with V(V) complexes and in the light of the promising results achieved previously with V(V) amino triphenolate catalysts in oxidation reactions,[22] we tested the potential reactivity of V(V) amino triphenolate complexes in the oxidative carbon-carbon bond cleavage in aerobic conditions of diols and β-hydroxy ether compounds.

The work here presented will be focused on the reactivity of a vanadium (V) amino triphenolate complex in the oxidative C-C bond cleavage under aerobic conditions of both 1,2-diols and one ethereal derivative.

[20] a) C. Canevali, M. Orlandi, L. Pardi, B. Rindone, R. Scotti, J. Sipila, F. Morazzoni, *J. Chem. Soc. Dalton Trans.* **2002**, 3007. b) E. Bolzacchini, C. Canevali, F. Morazzoni, M. Orlandi, B. Rindone, R. Scotti*, J. Chem. Soc. Dalton Trans.* **1997**, 4695. c) E. Bolzacchini, L. B. Chiavetto, C. Canevali, F. Morazzoni, M. Orlandi, B. Rindone, *J. Mol. Catal. A.* **1996**, 112, 347.
[21] G. Zhang, B. Scott, W. Ruilian, L. A. Silks, S. Hanson. *Inorg. Chem.* **2012**, 51, 7354.
[22] M.; Mba, M. Pontini, S. Lovat, C. Zonta, G. Bernardinelli, E. P. Kundig, G. Licini. *Inorg. Chem.* **2008**, 47, 8616.

3.2 V(V) Amino Triphenolate Complex

The V(V) amino triphenolate complex used in this study was synthesized as depicted in Scheme 5 and characterized as reported previously. [22]

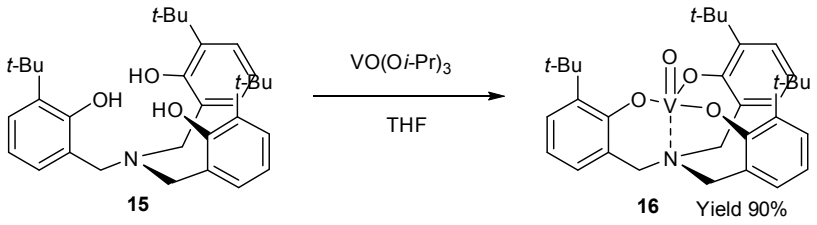

Scheme 5. Synthesis of V(V) complex **16**.

Equimolar amounts of the ligand **15** with the precursor VO(O*i*-Pr) in dry THF in inert atmosphere afforded complex **16** in high yield (90%).

3.2.1 Electrochemical and UV-Vis Studies

To evaluate the potential of V(V) amino triphenolate to be employed as oxidant, cyclic voltammetry experiments were performed in dichloromethane for the complex **16** which exhibits quasi-reversible waves at -625 mV (*vs* Ag/AgCl) corresponding to a vanadium (IV) species and at -1.024 mV (*vs* Ag/AgCl) corresponding to a vanadium (III) species, as reported in Figure 2.

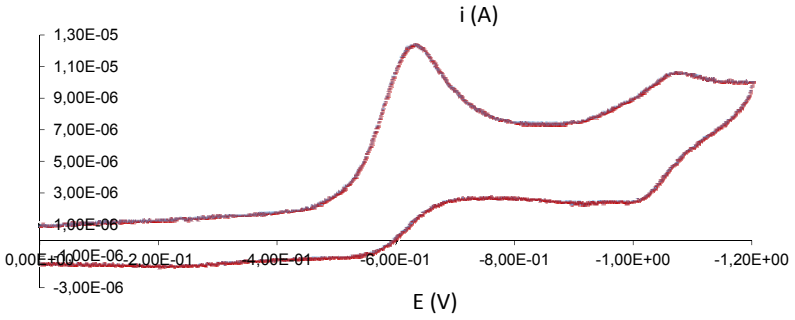

Figure 2. Cyclic voltammograms of V(V) complex **16** ($5 \cdot 10^{-4}$ M) in CH_2Cl_2 at 298 K (scan rate = 100 mV s^{-1}) using 0.1 M NBu_4PF_6 as supporting electrolyte, glassy carbon working electrode, platinum wire auxiliary electrode, and Ag/AgCl/NaCl (sat) reference electrode.

In order to further characterize the vanadium species at different oxidation states, the UV-vis spectra of the three different oxidation states corresponding to V(V), V(IV) and V(III) of **16** were recorded in CH_2Cl_2. This was performed by measurement of UV-Vis spectrum during electrochemical reduction of the V(V) complex **16 (**Figure 3).

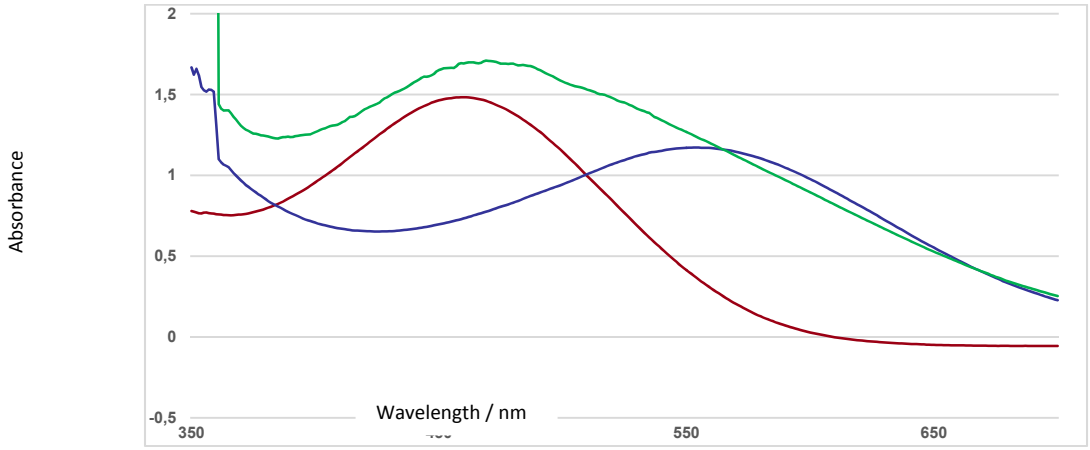

Figure 3. UV-Vis spectra of V(V) complex **16** ($5 \cdot 10^{-4}$ M) in CH_2Cl_2 at 298 K. Red Curve V(V) species at equilibrium potential, green curve at -625 mV potential and blue curve at -1025 mV potential.

The red curve, corresponding to the V(V) species **16** has a maximum at 460 nm, was recorded at initial time at equilibrium potential. After the application of a -700 mV (*vs* Ag/AgCl) potential, the UV-vis spectrum of a different species was recorded, with a maximum of adsorbtion at 470 nm. This spectrum can be assigned can assigned to the corresponding V(IV) species (green curve, Figure 3). Finally, applying a potential of-1025 mV (*vs* Ag/AgCl), a third spectrum was obtained, with a maximum of absorption at 567 nm, that we could assign to the V(III) species (blue curve).

3.3 Catalytic reactivity of vanadium (V) catalyst: Pinacol aerobic oxidation

Investigations to assess the potential of the V(V) amino triphenolate complex **16** to catalyze an oxidative C-C bond cleavage reaction were performed. The reactions were carried out using pinacol as substrate in different solvents and were monitored in order to detect the consumption of the pinacol and formation of the products. The results obtained are summarized in Table 1.

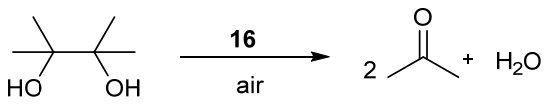

Table 1. Aerobic oxidation of pinacol catalyzed by **16** (10%).

Entry	Solvent	Time (h)	Conversion [b] %
1	DCE	8	>98
2	Toluene	4	>98
3	Pyridine	2	>98
4	NMP	2	>98

5	Toluene[c]	24	>98

[a] *Reaction conditions*: 10% of catalyst **16**, $[substrate]_0$= 0.05M, at 80 ºC, performed in air. [b] Conversions were determined by ^{1}H-NMR (%) analysis on the crude of the reaction mixture after complete consumption of substrate using dimethylsulfone as internal standard. [c] The reaction was performed in the presence of triethylamine 2 mol%.

It was found that complete consumption of pinacol after 2 h in >98% ^{1}H-NMR yield was observed using pyridine and NMP as solvent. Toluene and DCE afforded reaction slightly slower (4 and 8 h respectively to go to completion). Having established that pyridine has a positive effect on the rate of the reaction, we also investigated the effect of another base such as triethylamine (20%). In the presence of triethylamine, it was possible to observe a significant decrease of the rate of the reaction resulting in longer reaction time (24 h Table 1 entry 5). Due to the less problematic handling of toluene, in respect to pyridine and NMP, it was chosen as optimal solvent for the further studies and the reactions were carried out without the presence of any additives.

The catalyticity of the system was tested as well by decreasing the catalyst loading down to 0.2 %. The results are reported in Table 2.

Table 2. Aerobic oxidation of pinacol catalysed by **16**: catalyticity.

#	**16 (%)**	Solvent	Time (h)	T (°C)	Conversion %
1	2	Toluene	4	80	>98
2	1	Toluene	8	80	>98
3	0.2	Toluene	48	80	>98
4	0.2	Neat	24	80	>98

Reaction conditions: 2-0.2% of catalyst **16**, $[substrate]_0$= 0.05M, at 80 ºC, performed in air. Yield determined by ^{1}H-NMR (%) analysis of the crude reaction mixture after complete consumption of substrate using dimethylsulfone as internal standard.

Even using a lower catalyst loading (2 mol%) we obtained a complete conversion of the reagent into product in 4 only hours, indicating that the system is able to performed 100 TON. When the reaction was performed using 1 mol% and 0.2 mol% of catalyst in toluene complete consumption of pinacol was obtained after 8 h and 48 h respectively (entry 2, 3 Table 2). The reaction was also carried out in neat conditions and after 24 h using 0.2 mol% of catalyst complete conversion of pinacol was obtained.

To further investigate the scope of the reaction, two different substrates were studied: 1,1-2,2–tetraphenylethandiol and 1,2-diphenyl-1,2-ethandiol. The results are summarized in Table 3.

Table 3. Oxidative cleavage of 1,2 diols under aerobic condition.

Entry	Substrate	Product	**16** (mol%)	Time (h)	Conversion (%)
1	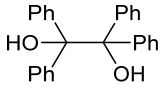	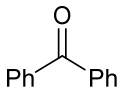	1 0.2	8 24	>98 >98
2	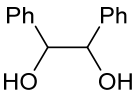	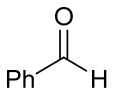	1 0.2	4 24	>98 >98

Reaction conditions: 1-0.2 % of catalyst **16**, $[substrate]_0$= 0.05M, at 80 ºC, performed in air. Yield determined by ^{1}H-NMR (%) analysis on the crude reaction mixture after complete consumption of substrate using hexamethyl benzene or 1,3,5-tri-*tert*-butyl benzene as internal standard.

When the reactions were performed using 1 mol% of catalyst **16**, complete consumption of the starting material was observed after 8 h and 4 h, respectively. Complete conversion into the corresponding carbonyl derivatives was obtained also working at lower catalyst loading (0.2%) after 24 h. It is worth of mention that for 1,2-diphenly-1,2-ethandiol in both cases the only product obtained was benzaldeyde (Table 3 entry 2 and 4) without any farter oxidation to the corresponding benzoic acid.

3.5 Aerobic C-C bond cleavage of 1,2-hydroxyethers.

The catalytic activity of complex **16** has been preliminary tested with an 1,2-hydroxyether compound, 1,2-diphenyl- 2-methoxyethanol, a compound that contains a β-hydroxy linkage.

The aerobic oxidation of 1,2-diphenyl- 2-methoxyethanol in the presence of complex **16** (10%) was tested both in toluene and DCE, in presence or absence of a base. The results obtained are reported in Table 4.

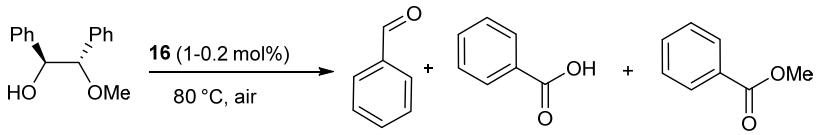

Table 4. Aerobic oxidation of 1,2-diphenyl-2-methoxyethanol catalysed by **16** (10%).

Entry	mol% **16**	Solvent	Additive	Time (h)	Conversion %
1	0.2	DCE	Et_3N	48	20
2	0.2	Toluene	Et_3N	4 days	20
3	0.2	DCE	__	48	>98
4	0.2	Toluene	__	3 days	>98
5	1	DCE	__	36	>98
6	--	DCE	__	48	--

Reaction conditions: 1-0.2 mol% of catalyst **16**, $[substrate]_0$= 0.05M at 80 ºC, performed in air. Yield determined by ^{1}H-NMR (%) analysis of the crude reaction mixture after complete consumption of substrate using 1,3,5-tri-*tert*-butyl benzene as internal standard

From the data reported in the Table 4, it is possible to observe that also in this case catalyst **16** is able to perform the oxidative C-C cleavage in both toluene and DCE under aerobic conditions. The products obtained by substrate cleavage are mainly benzaldehyde (up to 77%), benzoic acid (7%) and benzoin methyl ether (16%) determined via ^{1}H-NMR (internal standard, 1,3,5-tri-*tert*-butyl benzene) (Table 4 entry 5).

Also in this case, the presence of the base inhibits the reactions (Table 4 entry 1 and 2). Reactions are faster in DCE and the complete consumption of the starting material was obtained after 36 h (1% catalyst loading entry 5) or 48 h (0.2% catalyst loading entry 6).

In order to determine if the oxidation occurs via oxidation to the corresponding ketone and subsequent C-C bond cleavage, as suggested in some recent work reported by Hanson *et al.*,[24] we attempt the oxidation of (2-methoxy-2-phenylacetophenone) (Scheme 6). Even after 48 h no products originating from C-C bond cleavage could be detected (benzaldehyde or benzoic acid/ester). The reaction has been monitored via ^{1}H-NMR and ^{51}V-NMR spectroscopy and no changes on the NMR signals of the substrate/catalyst were registered.

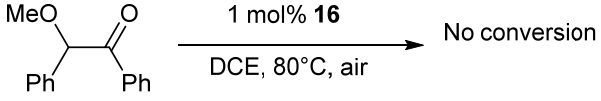

Scheme 6. Oxidation of 2-methoxy-2-phenylacetophenone under aerobic conditions

This result, even if very preliminary, indicate that V(V) catalyst **16** operates with a different mechanism in respect to the ones studies by Hanson *et al*. Further investigation on different substrates and reaction conditions will be performed in the future, in order to elucidate the reaction mechanism and apply the method to lignin itself.

3.5 Conclusions

V(V)/TPA complex **16** has been found to be a very effective catalyst for the aerobic oxidative C-C cleavage of tertiary and secondary vicinal diols. The mild reaction conditions and high yields achieved for 1,2-diols and an ethereal derivative make this catalyst not only competitive to those previously reported but also good candidate for lignin model compounds transformation.

3.6 Experimental part

General methods: All chemicals and solvents were purchased from commercial suppliers and used as supplied. Triphenolamine[23] and its corresponding V(V) complex were synthetized as previously reported.[22] ^{1}H-NMR spectra were recorded on Bruker Avance DRX 300 (300.13 MHz) spectrometer, using partially deuterated solvent, $CHCl_3$ = 7.26 ppm. ^{51}V NMR spectra have been recorded at 301 K with 10000 scans at 78.28 MHz with a broadband probe. V(V) complex **16**, once prepared in Glove-Box under inert atmosphere, can be handled in open air.

UV-Vis measurements were carried out on a Shimadzu UV-1700PC spectrophotometer equipped with a photomultiplier detector, double beam optics, and D2 and W light source.
All oxygen or moisture sensitive compounds have been handled under controlled atmosphere in a glove-box Mbraun MB 200MOD, equipped with a MB 150 G-I recycling system. UV-Vis spectra was recorded using a quarz cell with a 1 cm of path length, of a solution of **16** ($5X10^{-4}$ M) in CH_2Cl_2 at 298 K.

Cyclic voltammetry experiments were performed using a BAS EC-epsilon potentiostat. A standard three-electrode electrochemical cell was used. Glassy carbon electrode from BAS and a Pt wire

[23] L. J. Prins, M. Mba Blázquez, A. Kolarović, G. Licini. *Tetrahedron Lett.* **2006**, 47, 2735.

were used respectively as working and auxiliary electrode. Potentials were refered to an Ag/AgCl/3 M NaCl reference electrode.

The experimental data were obtained under N_2 atmosphere using V(V) complex **16** ($5 \cdot 10^{-4}$ M) in CH_2Cl_2 at 298 K (scan rate = 100 mV s^{-1}) and 0.1 M NBu_4PF_6 as supporting electrolyte

Catalytic Experiments

In a typical experiment, the substrate (0.1 mmol of 1,2 diol or β-hydroxy compound), complex **16** (0.01 mmol) and the internal standard (0.5 mmol of 1,3,5-tri-*tert*-butylbenzene, dimethysulfone or hexamethylbenzene) were dissolved in 2 mL of toluene or DCE (1,2- dichloroethane). The reactions were performed in a 5 mL glass vessel equipped with a Teflon stopcock and stirred under air. An initial ^{1}H-NMR spectra was recorded and afterward the vessel was closed and heated at 80° C under magnetical stirring. The reactions were monitored periodically, recording ^{1}H-NMR spectra by transferring an aliquot of the mixture in NMR tube after concentrating with reduced pressure. After the consumption of the starting materials, product yields were determined by integration against the internal standard.

Compounds Determination

Aerobic Pinacol oxidation. (Table 1 and 2)

In a 5 mL glass vessel, the substrate 0.1 mmol and 0.01-0.002 mmol of complex **16** were dissolved in toluene under aerobic condition. To the mixture (red colour) was added 0.05 mmol of internal standard (dimetilsulfone). An initial ^{1}H-NMR was detected and the mixure was left stirring at 80° C. During the course of the reaction, it was possible to observe a change of colour in the solution at the end of the reaction, from deep red to slightly green and purple. After cooling and exposure of the mixture to air the reddish colour was again observed.

The consumption of pinacol was revealed and quantified after recording periodically ^{1}H-NMR spectra.

Aerobic oxidation of 1,1-2,2–tetraphenylethandiol (Table 3, entry 1).

Same procedure followed for pinacol. In this case, to a 2 mL of toluene solution containing the substrate 0.1 mmol and the catalyst **16** 1-0.2 mmol, was added 0.05 mmol of hexamethylbenzene as internal standard and the product detected was benzophenone ($C_{13}H_{10}O$).

^{1} H NMR (300 MHz, CDCl3) δ 7.82 – 7.79 (m, 4H), 7.76-7.45 (m, 6H), 1.26 (s, 3H).

MS m/z (M^+, 182).

Aerobic oxidation of 1,2-diphenyl-1,2-ethandiol (Table 3, entry 2)

Same procedure followed for pinacol. In this case, to a 2 mL solution of toluene, containing 0.1 mmol of substrate and 1-0.2 mmol of catalyst **16**, was added 0.05 mmol of 1,3,5-tri-*tert*-butylbenzene as internal standard and the product detected was benzaldehyde.

^{1}H NMR (300 MHz, CDCl3) δ 10.03 (s, 1H), 7.87-7.84 (d, 2H), 7.63-7.48 (m, 3H), 1.34 (s, 9H). MS m/z (M^+ H^+, 108)

1,2-diphenyl-2-methoxyethanol. (Table 4)

Same procedure followed for pinacol. In this case, to a 2 mL solution of DCE or toluene, containing 0.1 mmol of substrate and 1-0.2 mmol of catalyst **16**, was added 0.05 mmol of 1,3,5-tri-*tert*-butylbenzene as internal standard and the product detected was benzaldehyde, benzoic acid and methyl benzoate. The data were compared with original spectra recorded for each sample.

Benzaldehyde: ^{1}H NMR (300 MHz, CDCl3) δ 9.97 (s, 1H), 7.87-7.84 (m, 2H), 7.63-7.48 (m, 3H), 1.34(s, 9H).

Benzoic Acid: ^{1}H NMR (300 MHz, CDCl3) δ 8.13-8.11 (d, 2H), 7.64-7.59 (t, 1H), 7.50-7.45 (t, 2H), 1.34 (s, 9H).

Methyl Benzoate: ^{1}H NMR (300 MHz, CDCl3) δ 8.04-8.01 (m, 2H), 7.54-7.52 (t, 1H), 7.50-7.4 (m, 2H), 1.34 (s, 9H).

Chapter 4

Fe(III) Amino Triphenolates as Catalysts for CO_2 Activation

Abstract

This chapter describes the synthesis and characterization of new Fe(III) amino triphenolate complexes and their use as catalysts in carbon dioxide activation, in particular the cycloaddition to epoxides and oxetanes to yield cyclic carbonates. Fe(III) amino triphenolates allows CO_2 activation under mild conditions (low temperature and CO_2 pressure) with a series of epoxides and oxetanes. Different activities have been observed depending on the substituents on the phenyl ring and the nuclearity of the complexes. The catalytic reactivity of their analogues, V(V) and Mo(VI) complexes has been also investigated.

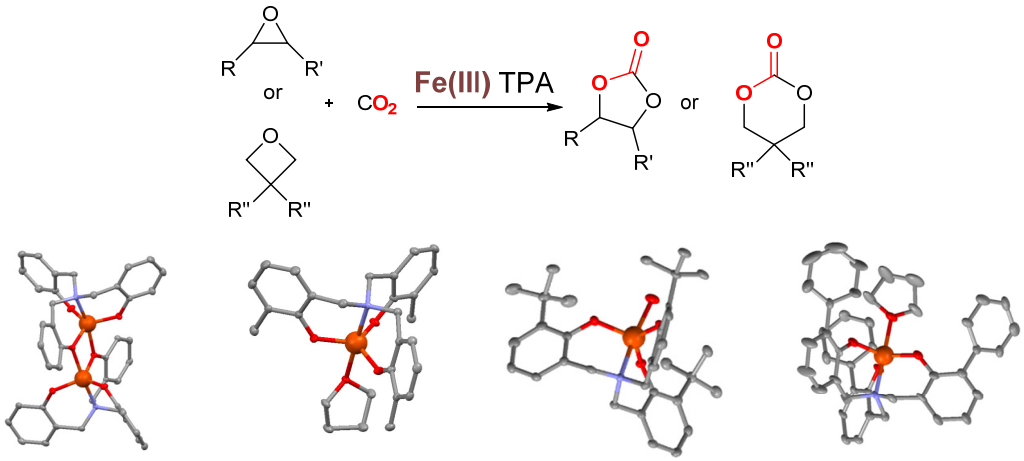

Part of the work reported in the Chapter has been published: [1]

4.1 Introduction

In recent years, the transformation of carbon dioxide into useful chemicals has been of great interest to the scientific community because CO_2 can be considered a renewable carbon source (C_1), abundant, cheap and non-toxic.[2] [3] Since fossil fuels (coal, oil) are limited, carbon dioxide can be considered as an alternative chemical feedstock for the production of high-value products. Despite this desire, very few industrial processes utilize carbon dioxide as sustainable carbon resource and this is mainly due to the low reactivity of CO_2. However, the annual consumption of CO_2 per year

[1] C. J. Whiteoak, B. Gjoka, E. Martin, M. Martinez Belmonte, G. Licini, A. W. Kleij, *Inorg. Chem*. **2012**, 51, 10639.
[2] *Carbon Dioxide as Chemical Feedstock* (Ed.: M. Aresta), Wiley-VCH, Weinheim, **2010**.
[3] T. Sakakura, J. Choi and H. Yasuda, *Chem. Rev*., **2007**, 107, 236.

as a synthetic building block is 110 Mtonnes. [2 4] Industrial processes in which carbon dioxide is used [5] include the synthesis of urea from CO_2 and ammonia, [6] the synthesis of salicylic acid from phenol and CO_2 (the Kolbe-Schmitt reaction) [7] and the synthesis of cyclic carbonates and polypropylene carbonate from CO_2 and epoxides. [4 8 9]

The production of urea is the largest scale chemical process currently in operation (100 Mtonnes/year). [10] This is also an excellent example of the use of the waste CO_2 obtained as by-product in the synthesis of hydrogen from methane.

The synthesis of salicylic acid has been already developed on an industrial scale since the 1890.[11] The process used today is based on the reaction of sodium phenolate with CO_2 at a pressure of 0.5 mPa at 0° C. After absorption of approximately one mole of CO_2 the temperature is risen to 50°C for several hours until the reaction is completed (Scheme 1).

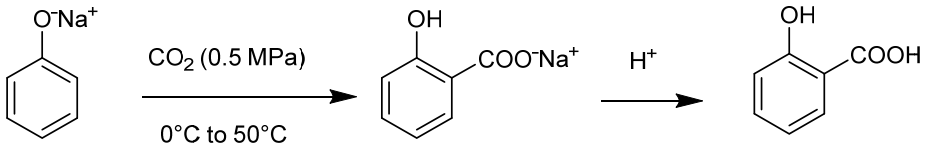

Scheme 1. Industrial synthesis of salicylic acid.

The transformation of carbon dioxide and epoxides/ oxetanes into cyclic organic carbonates is a rather important reaction (equation 1).

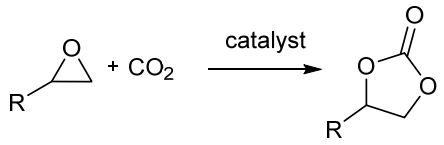

(1)

Catalysts employed for industrial scale synthesis: KI or TBAB (tetrabutylammonium bromide)

[4] a) H. Arakawa, M. Aresta, J. N. Armor, M. A. Barteau, E. J. Beckman, A. Bell, J. E.Bercaw, C. Creutz, E. Dinjus, D. A. Dixon, K. Domen, D. L. DuBois, J. Eckert, E. Fujita, D. H. Gibson, W. A. Goddard, D. W. Goodman, J. Keller, G. J. Kubas, H. H. Kung, J. E. Lyons, L. E. Manzer, T. J. Marks, K. Morokuma, K. M. Nicholas, R. Periana, L. Que, J. Rostrup-Nielson, W. M. H. Sachtler, L. D. Schmidt, A. Sen, G. A. Somorjai, P. C. Stair, B. R. Stults and W. Tumas, *Chem. Rev*., **2001**, 101, 953. b) M. North.; R. Pasquale.; C. Young. *Green Chem.,* **2010**, 12, 1514.

[5] I. Omae, *Catal. Today*, **2006**, 115, 33. M. Aresta and A. Dibenedetto, *Dalton Trans*., **2007**, 2975.

[6] a) F. Shi, Y. Q. Deng, T. L. Si-Ma, J. J. Peng, Y. L. Gu, B. T. Qiao, *Angew. Chem., Int. Ed.* **2003**, 42, 3257. b) C. C. Tai, M. J. Huck, E. P. Mc Koon, T. Woo, G. J. Jessop, *Org. Chem*. **2002**, 67, 9070. c) R. Nomura, Y. Hasegawa, M. Ishimoto, T. Toyosaki, H. Matsuda. *J. Org. Chem.* **1992**, 57, 7339.

[7] a) H. Kolbe, E. Lautemann. *Annalen* **1869**, 113, 125. b) R. Schmitt, E. Burkard, Ber. Dtsch. Chem. Ges. **1877**, 20, 2699. c) Y. Kosugi, Y. Imaoka, F. Gotoh, M. A.; Rahim, Y. Matsui, K. Sakanishi. *Org. Biomol. Chem*. **2003**, 1, 817. d) A. Sclafani, L. Palmisano, G. Farneti. *Chem. Commun*. **1997**, 52.

[8] a) M. Yoshida, M. Ihara, *Chem.–Eur. J*., **2004**, 10, 2886; b) J. Sun, S.-I. Fujita and M. Arai, *J. Organomet. Chem*., **2005**, 690, 3490; c) W.-L. Dai, S.-L. Luo, S.-F. Yin and C.-T. Au, *Appl. Catal., A*, **2009**, 366, 2.

[9] T. Sakakura, K. Kohno. *Chem. Commun.,* **2009**, 1312. A. Decortes, A. M. Castilla, A. W. Kleij*, Angew. Chem., Int. Ed*., **2010**, 49, 9822.

[10] F. Barzagli, F. Mani, M. Peruzzini, *Green Chem.,* **2012**, 13, 1267.

[11] M. Aresta, A. Dibenedetto, *Catal. Today*, **2004**, 98, 455.

These class of compounds are of interest for a wide variety of applications, including the production of aprotic polar solvents, fine chemical intermediates, starting materials for the synthesis of polymers, engineering plastics, biomedical materials and electrolytes in lithium ion batteries.[12] The current production of cyclic carbonates is around 100 ktonnes/year. [8] Traditionally the synthesis of these compounds was carried out using phosgene as reagent (equation 2), which is highly toxic and in addition, this methodology affords two equivalents of corrosive hydrochloric acid.

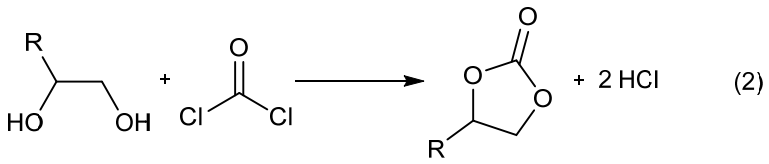

(2)

The necessity to replace this conventional route with greener and safer process motivated intense research to find new effective systems for producing cyclic carbonates by using CO_2.

4.1.1 Cyclic carbonate synthesis from epoxides and CO_2 catalyzed by metal based complex

As previously mentioned, the addition of CO_2 to epoxides cleanly generates cyclic carbonates, [3b 7 8] which are the thermodynamically favored products or, under different reaction conditions, polycarbonates. [13 14]

The synthetic routes developed for the preparation of cyclic carbonates from carbon dioxide and epoxides (equation 1) are all catalytic processes. Catalysts that have been used are amines or phosphines, [15] ammonium [16 17] or metal halides[18 19] and metal complexes. The catalysts currently

[12] a) J. H. Clements, Ind. Eng. *Chem. Res.,* **2003**, 42, 663.; B. Schaffner, F. Schaffner, S. P. Verevkin, A. Borner, *Chem. Rev.,* **2010**, 110, 4554. b) M. North, F. Pizzato, P. Villuendas, *ChemSusChem*, **2009**, 2, 862. c) M. North, M. Omedes-Pujol, *Tetrahedron Lett*. **2009**, 50, 4452. d) W. Clegg, R. W. Harrington, M. North, F. Pizzato, P. Villuendas, *Tetrahedron: Asymmetry,* **2010**, 21, 1262. e) M. North and P. Villuendas, *Org. Lett*., **2010**, 12, 2378; M. North and M. Omedes-Pujol, Beilstein *J. Org. Chem*., **2010**, 6, 1043. f) C. Beattie, M. North and P. Villuendas, *Molecules*, **2011**, 16, 3420. g) M. Morcillo, M. North and P. Villuendas, *Synthesis*, **2011**, 1918; P. Lenden, P. M. Ylioja, C. Gonzalez-Rodriguez, D. A. Entwistle, M. C. Willis, *Green Chem*., **2011**, 13, 1980.

[13] X-Bing. Lu, D. J. Darensbourg, *Chem. Soc. Rev.*, **2012**, *41*, 1462.

[14] a) H. Sugimoto and S. Inoue, J. Polym. Sci., *Part A: Polym. Chem.,* **2004**, 42, 5561. b) D. J. Darensbourg, R. M. Mackiewicz, A. L. Phelps, D. R. Billodeaux, *Acc. Chem. Res.,* **2004**, 37, 8. c) G. W. Coates and D. R. Moore, *Angew. Chem., Int. Ed*., **2004**, 43, 6618. d) D. J. Darensbourg, *Inorg. Chem*., **2010**, 49, 1076. e) M. R. Kember, A. Buchard, C. K. Williams, *Chem. Commun.* **2011**, 47, 141.

[15] a) Y. M. Shen, M. Shi. *Adv. Synth. Catal*. **2003**, 345, 337. b) H. Kawanami, Y. Ikushimaab. *Chem. Commun.* **2000**, 21, 2089. c) L. N. He, H. Yasuda, T. Sakakura. *Green Chem*. **2003**, 5, 92. d) J. W. Huang, M. Shi. *J. Org. Chem*. **2003**, 68, 6705. e) J. L. Song, Z. F. Zhang, S. Q. Hu, T. B. Wu, T. Jiang, B. X. Han. *Green Chem.* **2009**, 11, 1031. f) Y. B. Xiong, H. Wang, R. M. Wang, Y. F. Yan, B. Zheng, Y. P. Wang. *Chem. Commun.* **2010,** 46, 3399. g) Y. Tsutsumi, K. Yamakawa, M. Yoshida, T. Ema, T. Sakai. *Org. Lett*. **2010**, 12, 5728.

[16] D. J. Darensbourg, M.W. Holtcamp *Coord. Chem.* **1996**, 153, 155.

[17] A. Sibaouih, T. Repo. *Appl. Catal. A*, **2009**, 365, 194.

[18] N. Kihara, N. Hara, T. Endo. *J. Org. Chem*. **193**, 58, 6198.

[19] V. Calo, A. Nacci, A. Monopoli, A. Fanizzi. *Org. Lett.* **2002**, 4, 2561.

employed for industrial production of cyclic carbonates (equation 1) are metals and ammonium halides such as KI or tetrabutylammonium bromide (TBAB).

These salts are suitable for large scale synthesis because they are stable, soluble in the reaction products (cyclic carbonate), and they do not solidify when the reaction mixture is concentrated during the purification step. In Scheme 2 a possible reaction mechanism for the synthesis of cyclic carbonates starting from epoxides and CO_2 catalyzed by tetrabutylammonium bromide (TBAB) is reported. [18] This reaction proceeds through the ring opening of the epoxide by nucleophilic attack of the halide ion (Br^-), which leads to an oxy anion species that is transformed into the corresponding cyclic carbonate after reaction with CO_2.

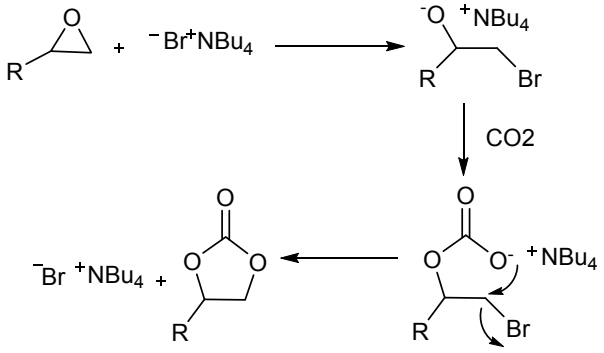

Scheme 2 General mechanism of cyclic carbonates synthesis catalysed by TBAB. [18]

These catalytic systems require high temperatures (100-150°C) and pressures (up to 20 bar) and the catalysts are difficult to recover and reuse. [20] Furthermore they are active only with terminal epoxides.

Metal complexes have been found to be much more active catalysts in order to operate under milder conditions (lower temperature and CO_2 pressure) and with less reactive epoxides. Metal-based complexes usually are used in the presence of a co-catalyst, a quaternary ammonium halide, [6 21] (tetra-butyl ammonium chloride, bromide or iodide) or phosphonium halide. Examples of co-catalysts anchored on the ligand backbone, arising a bifunctional systems, have been also reported. [22 23 24] Generally, in the catalytic cycle, the metal complex acts as Lewis acid, activating the epoxide toward nucleophilic attack by the halide co-catalyst. Then the insertion of CO_2 and ring closure yields the cyclic carbonate (Scheme 3).

[20] M. Aresta, A. Dibenedetto, A. Angelini. *Chem. Molec. Sciences, and Chem. Ing.* **2013**, 563.
[21] S. Fukuoka, M. Kawamura, K. Komiya, M. Tojo, H. Hachiya, K. Hasegawa, M. Aminaka, H. Okamoto, I. Fukawa, S. Konno. *Green Chem.* **2003**, 5, 497.
[22] S. Klaus, M.W. Lehenmeier, C. E. Anderson, B. Rieger, *Coord. Chem. Rev.* **2011**, 255, 1460.
[23] J. Mel_ndez, M. North, P. Villuendas, C. Young, *Dalton Trans.* **2011**, 40, 3885.
[24] T. Ema, Y. Miyazaki, S. Koyama, Y. Yano, T. Sakai, *Chem. Commun*. **2012**, 48, 4489.

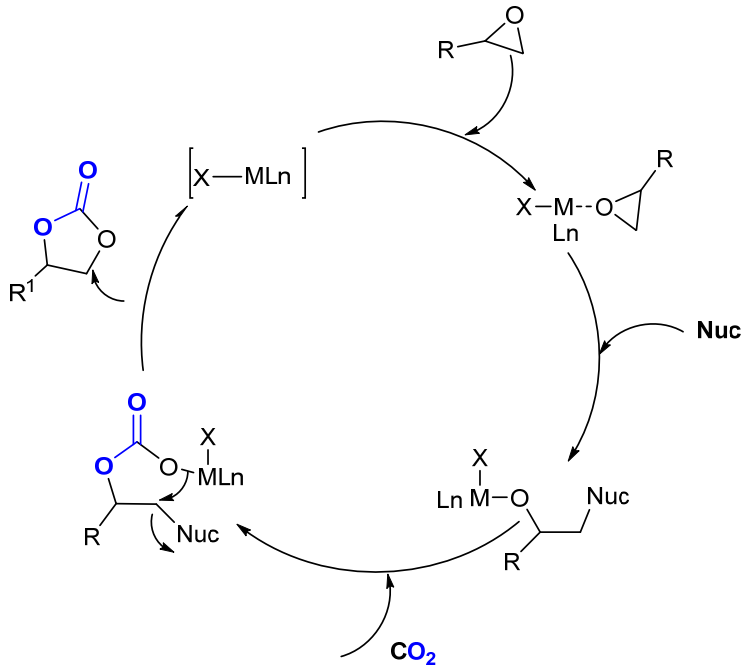

Scheme 3 General reaction mechanism for metal catalysed cyclic carbonate synthesis.

In the recent years effective catalysts for the synthesis of cyclic carbonates from epoxides have been reported. It is worth mentioning that Al, Co, Cr salen (**1-3**), [25] Zn(salophen) (**4**), [26, 27] Zn(metalloporphyrin) (**5**)[23] phatocyanine (**6**) and Fe (**7**) and Al (**8**) amino triphenolate complexes[28] [29] are the most successful catalysts reported in literature Figure 1.

[25] a) A. Decortes, A. M. Castilla, A. W. Kleij, *Angew. Chem*. **2010**, 122, 10016. b) L.-N. He, J.-Q. Wang, J.-L. Wang, *Pure Appl. Chem.* **2009**, 81, 2069. c) X.-B. Lu, X.-J. Feng, R. He, *Appl. Catal. A*. **2002**, 234, 25. d) X.-B. Lu, B. Liang, Y.-J. Zhang, Y.-Z. Tian, Y.-M. Wang, C.-X. Bai, H. Wang, R. Zhang, *J. Am. Chem. Soc*. **2004**, 126, 3732.
[26] A. Decortes, M. Martinez Belmonte, J. Benet-Buchholz, A. W. Kleij, *Chem. Commun*. **2010**, 46, 4580. b) A. Decortes, A. W. Kleij, *Chem. Cat.Chem*. **201**1, 3, 831.
[27] D. Ji, X. Lu, R. He, *Appl. Catal. A*. **2000**, 203, 329.
[28] C. J. Whiteoak, E. Martin, M. Martínez Belmonte, J. Benet-Buchholz, A. W. Kleij, *Adv. Synth. Catal*., **2012**, *354*, 469.
[29] C. J. Whiteoak, N. Kielland, V. Laserna, E. C. Escudero-Adán, E. Martin, A. W. Kleij, *J. Am. Chem. Soc*. **2013**, 135, 1228.

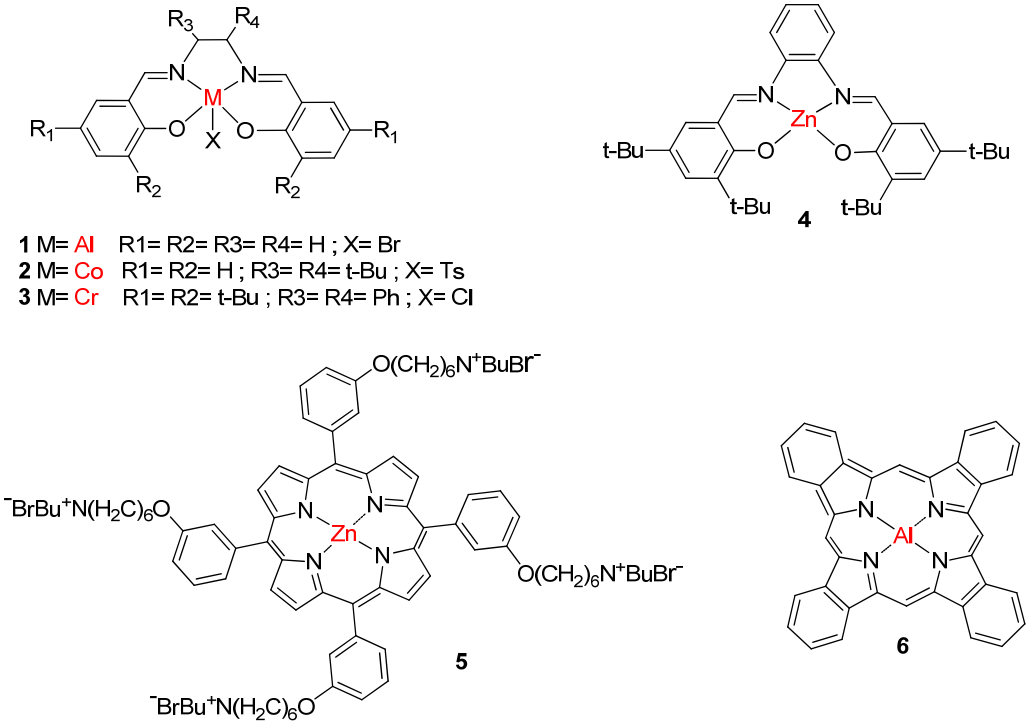

Figure 1

In Table 1 are reported the results obtained using the different catalytic systems in the reaction with propylene (**9**) or 1-hexene oxide (**10**).

Table 1. Effect of different metal catalysts (**1-8**) on the reaction of terminal epoxides (propylene oxide (**9**) or 1-hexene oxide (**10**) with CO_2.

#	Sub	Cat (%)	co-cat.	P_{CO2}(bar)	T(°C)	TOF (h^{-1})	solvent	Time (h)
1	**9**	**1** (0.125)	nBu_4NI	6	35	63.0	neat	8
2	**9**	**2** (0.1)	nBu_4NBr	35	45	316	neat	16
3	**9**	**3** (0.075)	DMAP	7	100	916	CH_2Cl_2	1
4	**9**	**4** (0.5)	nBu_4NI	10	85	n.d.	MEK	18
5	**10**	**5** (0.03)	nBu_4NBr	17	120	12.000	neat	10

6	**9**	**6** (0.18)	nBu_3N	50	140	801	neat	1.2
7	**9**	**7** (1)	Bu_4NI	10	25	n.d.	MEK	18
8	**10**	**8** (0.5)	nBu_4NI	10	30	901	neat	2

In most of the cases the reactions can be carried out at relatively low CO_2 pressures (6-10 bar) and catalyst loadings. In the case of the reaction with porphyrine **5** as catalyst the presence of the co-catalyst in the ligand allowed to very high reactivity (TOF's up to12.000 h^{-1}).

More recently, effective catalytic systems based on Fe(III) and Al(III) amino triphenolate complexes have been reported. [26] [27] Either the dinuclear Fe(III) and Al(III) amino triphenolate complexes **7** and **8** have shown excellent reactivity with a broad substrate scope and low catalyst loadings.

In the present work the reactivity of amino triphenolate complexes as catalysts for cyclic carbonate formation has been explored more in detail. In particular the effect of the nature of the ligand on the reactivity of Fe(III) amino triphenolate complexes, and the resulting nuclearity, has been investigated together with the performance of the corresponding analogous V(V) and Mo(VI) complexes.

4.2 Synthesis and Characterization of Iron(III) *ortho*-substituted Amino Triphenolate Complexes

4.2.1 Synthesis

All the ligands used in this study have been synthesized by a three-fold reductive amination. [30] Fe(III) complexes were obtained by the reaction of the triphenolamines $\mathbf{L_{1\text{-}4}H_3}$, **11**, where R = H, methyl, *tert*-butyl, or phenyl with 3 equiv. of sodium hydride in tetrahydrofuran and subsequent addition of 1 equiv. of $FeCl_3$, after filtration to remove the sodium salt, analytically pure mono- or di-iron(III)complexes were obtained. Scheme 4.

[30] L. J. Prins, M. Mba Blázquez, A. Kolarović, G. Licini. *Tetrahedron Lett.* **2006**, 47, 2735.

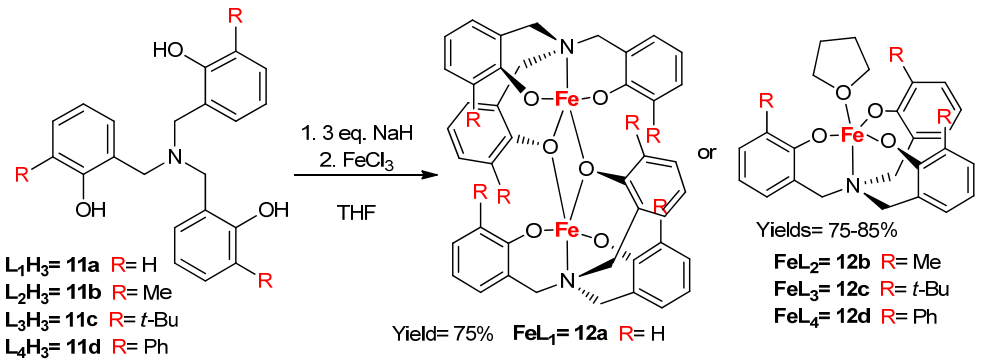

Scheme 4. Synthesis of Fe(III) complexes **12a-d**

All complexes **12a-d** have been characterized by Maldi-TOF-MS and elemental analysis. Crystals suitable for X-ray analysis have been obtained for all the compounds, confirming the mono and dinuclear nature of the complexes.

4.2.2 *X*-Ray Diffractometric Studies

Crystals for *X*-ray diffractometric studies were obtained by slow evaporation of tetrahydrofuran solutions of the complexes, except for **12a** where crystals were grown from a concentrated toluene solution. The solid state structures of iron(III) amino triphenolate complexes are shown in Figure 2, with selected bond lengths and angles reported in Tables 2 and 3.

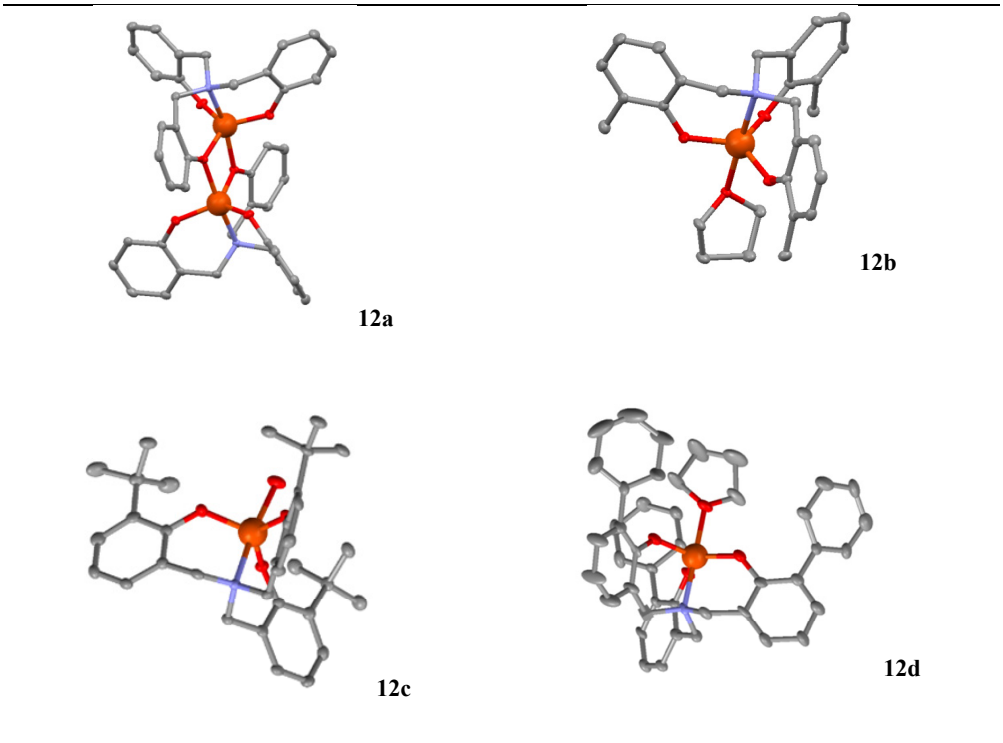

Figure 2. Solid state structures of **12a** (top left), **12b** (top right), **12c** (bottom left), and **12d** (bottom right). H-atoms, co-crystallized solvent and disorder have been omitted for clarity, and only a partial numbering scheme is provided.

The molecular structure of the complex **12a** consists of two iron(III) amino triphenolate complexes forming a dinuclear assembly, with one phenoxide O-atom from each individual complex acting as a bridging ligand, resulting in the formation of a central Fe_2O_2 motif. The solid state structures of the complexes **12b**, **12c** and **12d** are mononuclear containing an apical ligand originating from the solvent media. The molecular structure **12c** contains a water ligand in place of the expected tetrahydrofuran ligand, which is likely to be a consequence of ligand exchange with the water present in the solvent used during crystallization. The molecular structure of complex **12b**, as has been mentioned, shows the mononuclear form of the complex, but further investigations (vide infra) indicate that a dinuclear structure may be easily formed as in the case of complex **12a**. No evidence of dinuclear complexes in the cases of **12c** or **12d** have been found. The solid state structure of **12b** displays idealized C_3 symmetry, with the corresponding angle between the amine and the oxygen atom of the tetrahydrofuran ligand (178.24(4)°) close to the ideal value of 180° expected in a perfectly C_3 symmetrical molecule. The structure also displays similar bond length values for all the Fe−O bonds with the ligand and an elongated Fe−O bond length for the bond between the tetrahydrofuran and metal. The addition of *tert*-butyl groups, impacts severely on the C_3 symmetry of the complex in **12c** compared with **12b**. It appears that the *tert*-butyl groups have a significant steric effect on the structure. The angles between of O(1)−Fe(1)−O(2), O(1)−Fe(1)−O(3), and O(1)−Fe(1)− O(3) are significantly different from those expected in a perfect C_3 symmetrical molecule and have values of 113.79(17)°, 115.77(17)°, and 130.41(17)°, respectively. These distortions are similar in value to those observed by Safaei and co-workers for a similar complex containing a methanol ligand in the apical position. [31] A further difference in this molecule compared to **12b** is that not all the Fe−O bond lengths between the metal and the ligand have the same length, with one of them being clearly elongated. The observation of these differences in structure adds weight to the proposal that the original tetrahydrofuran ligand has exchanged with the water ligand during crystallization to form a more stable complex. Similar but less significant distortions from perfect C_3 symmetry are also observed in the case of **12d** compared with **12c** indicating that the phenyl groups contribute less to the steric constraints immediately around the Fe(III) center.

[31] E. Safaei, H. Sheykhi, T. Weyhermüller, B. Eckhard. *Inorg. Chim. Acta.* **2012**, 384, 69.

Table 2. Selected bond lengths (A) of iron (III) complexes.

Bond Lengths (A)				
	12a	12b	12c	12d
Fe(1)-O(1)	1.9713(18)	1.8643(12)	1.885(4)	1.856(3)
Fe(1)-O(2)	1.8611(18)	1.8555(12)	1.853(4)	1.859(3)
Fe(1)-O(3)	1.8519(19)	1.8685(11)	1.861(4)	1.878(3)
Fe(1)-O(4)	2.0642(17)	2.1063(11)	2.097(4)	2.055(5)
Fe(1)-N(1)	2.1440(20)	2.1795(13)	2.178(4)	2.163(4)

The resulting angles being 116.22(14)°, 121.82(14)°,and 121.94(14)° for O(1)−Fe(1)−O(2), O(1)−Fe(1)−O(3),and O(1)−Fe(1)−O(3), respectively. The dinuclear complex **12a** displays two Fe−O bonds with lengths of 1.8611(18) Å and 1.8519(19) Å corresponding to the non-bridging phenoxide moieties and two longer Fe−O bonds with lengths of 1.9713(18) Å and 2.0642(17) Å for the bonds involving the bridging phenoxide moieties. These bond lengths are similar to those previously reported for a similar dinuclear structure. [32]

Table 3. Selected **angles** (deg) of iron (III) complexes

Bond Angles (deg)				
	12a	12b	12c	12d
O(1)-Fe(1)-O(2)	120.76(8)	121.15(5)	113.79(17)	116.22(14)
O(1)-Fe(1)-O(3)	116.00(8)	119.08(6)	130.41(17)	121.94 (14)
O(2)-Fe(1)-O(3)	123.14(9)	119.58(5)	115.77(17)	121.82(14)
O(1)-Fe(1)-O(4)	77.44(7)	89.28(5)	92.16(16)	93.41(18)
O(1)-Fe(1)-N(1)	91.15(8)	91.71(5)	89.75(16)	90.11(13)
N(1)-Fe(1)-O(4)	168.33(8)	178.24(4)	172.98(17)	173.95(19)

4.2.3 UV−VIS Studies.

The electronic spectra of all complexes **12a-d** are very similar to one another. A metal-to-ligand charge transfer band (MLCT) is observed in all the complexes around 400−450 nm. A second MLCT band is detected for all complexes around 310−360 nm and in addition, **12a** displays a third MLCT band in this region as a shoulder at 358 nm which is most likely as a result of the bridging phenoxide moieties.

[32] A. J. Chmura, M. G. Davidson, C. J. Frankis, M. D. Jones, M. D. Lunn. *Chem. Commun.* **2008**, 1293.

In order to investigate the behaviour of the Fe(III) complexes in solution, titration studies were performed. In this regard, it has been reported that complex **7**, similar to **12b,** can be disrupted by titration with propylene oxide. [26] From the UV-Vis spectra of **12b** a slight change in the absorption curve was observed after addition of the titrant (Figure 3, bottom), whereas titration of the remaining complexes (**12a**, **12c** and **12d**) with propylene oxide did not give rise to any significant changes in the spectra. These data suggested that the complex **12a** due to its strong tendency to form dinuclear species did not show any changes in the UV-Vis spectra. On the contrary, **12c** and **12d** complexes because of their mononuclear nature, did not give any change upon addition of propylene oxide (Figure 4 top and bottom).

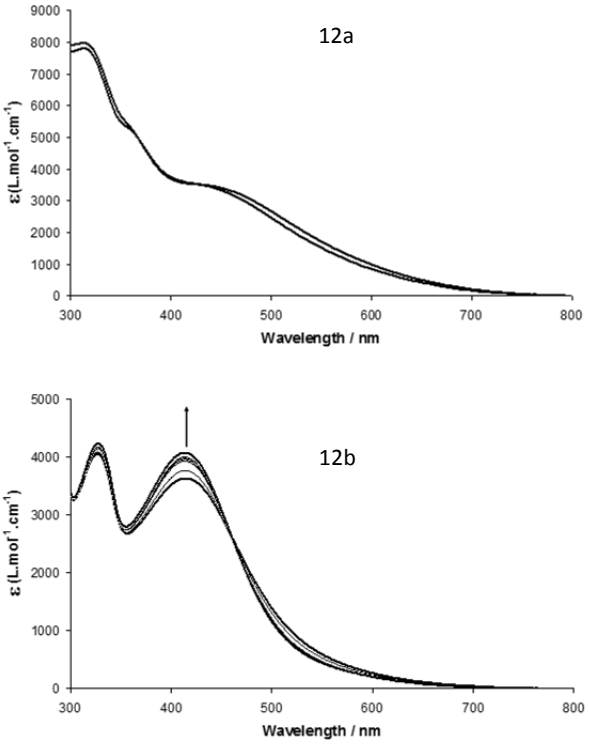

Figure 3. UV-Vis spectra of **12a** (top) and **12b** (bottom) (1.0 x10^{-4}M) titrated with propylene oxide (0 to 1000 equiv.) in toluene.

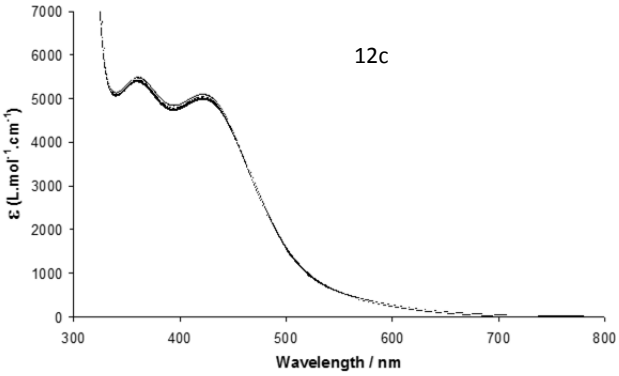

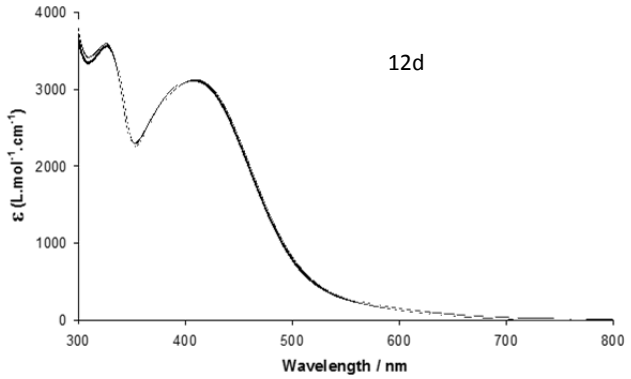

Figure 4. UV-Vis spectra of **12c** (top) and **12d** (bottom) ($1.0x10^{-4}$M) titrated with propylene oxide (0 to 1000 equiv.) in toluene.

However, when the dinuclear complex **12a** is titrated with pyridine (a much more basic ligand), a significant change in spectra is observed (Figure 5). For comparison the same experiment performed with the mononuclear complex **12d** is reported, where the addition of an excess of pyridine causes only minor modification of the UV-Vis spectrum (Figure 5 right). These results suggest that **12a** is a stable dinuclear complex also in solution and only in the presence of highly basic ligands it can form the corresponding mononuclear species.

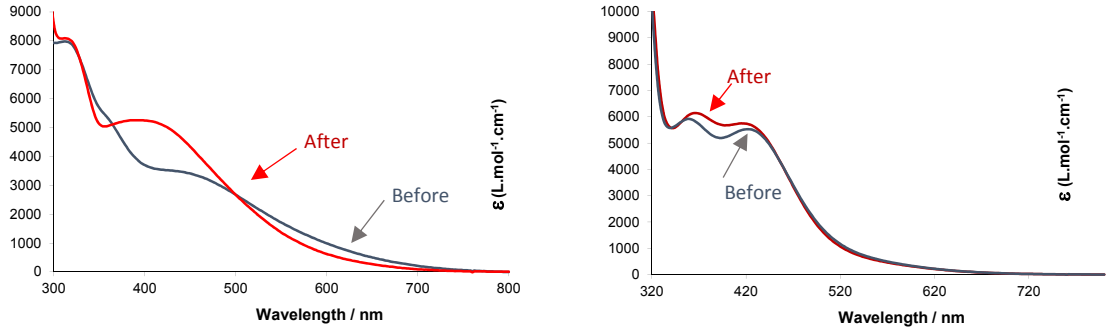

Figure 5. UV−vis spectra in toluene of **12a** (left), **12d** (right) $1x10^{-4}$M before and after addition of pyridine (0-1000 eq).

4.2.4 ^{1}H NMR Characterization.

Paramagnetic complexes generally exhibit broad resonances with large chemical shifts. The ^{1}H NMR spectra of all the complexes were recorded in $CDCl_3$ at 298 K and are shown in Figure 6, with the region between 15 and −5 ppm omitted for clarity (this region principally displays resonances for the protio-impurities of the deuterated solvents, a broad resonance for the alkyl protons of the ligand and in the case of **12c**, a broad resonance for the protons of the *tert*-butyl

group). Additionally, the ^{1}H NMR spectra of all complexes were obtained in a $CDCl_3$:d_5-Pyridine (90:10 v/v) mixture to allow for comparison with the species obtained in the solution magnetic susceptibility measurements. The paramagnetically shifted resonances have been assigned tentativelly, as efforts to acquire 2D NMR spectra were unsuccessful.

In the ^{1}H NMR spectra of both **12a** and **12b**, there are no observable strongly shifted resonances to indicate the presence of a paramagnetic species. Most likely, in the case of **12a,** as a result of strong antiferromagnetic coupling between the two iron(III) centers, very broad signals were observed. Upon addition of pyridine to both of these complexes it is possible to observe the appearance of new resonances in the 90 to −80 ppm range, indicating the formation of paramagnetic species. In the case of **12a**/pyridine, we propose that the observed resonances, shown in Figure 6, are those of the aromatic protons of the ligand.

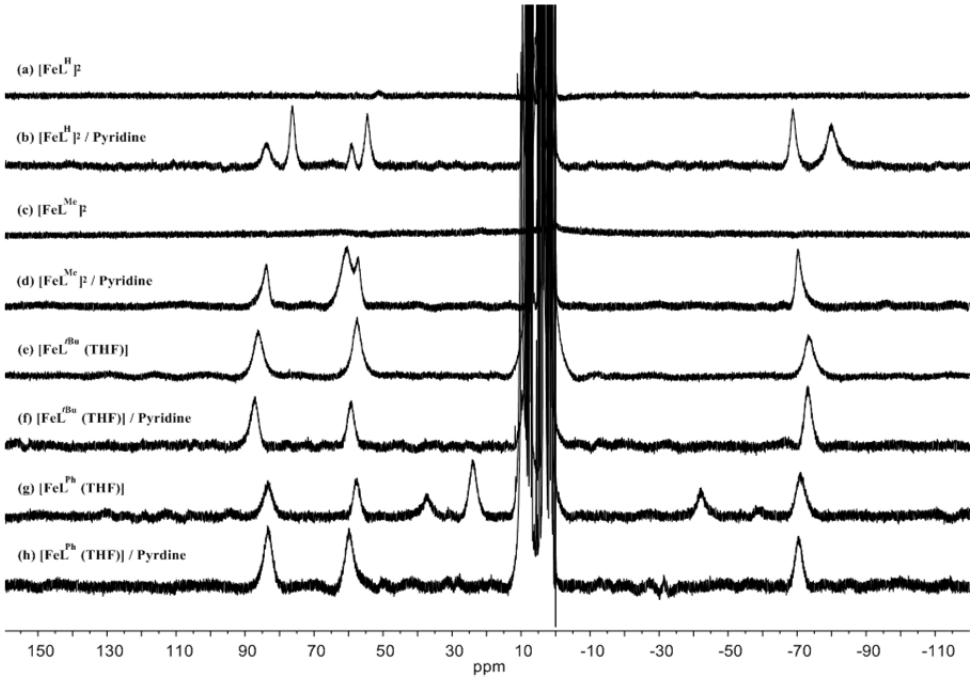

Figure 6. ^{1}H NMR spectra (500 MHz, CDCl3, 298 K) of **12a**, **12b**, **12c**, and **12d**; with/without the addition of d_5- Pyridine. For clarity 15 to −5 ppm region has been omitted

Three of the aromatic protons appear as a pair of resonances (Ha′ =Ha″, Hb′ = Hb″, and Hc′ = Hc″), with the resonance corresponding to the remaining *ortho*-proton of the aromatic moiety being likely present in the 0−12 ppm range. We propose that a pair of resonances is observed for each proton because of the possibility of either one or two pyridine ligands coordinating to the iron(III) center, and this is further confirmed by the presence of only a single set of resonances when the experiment is run in neat d_5-pyridine. In the case of a single coordinated pyridine, the complex would display trigonal bipyramidal geometry, whereas upon coordination of a second pyridine ligand the complex becomes octahedral in geometry, resulting in different

orbital overlap and therefore displaying slightly different chemical shifts. The proposed ability of **12a** to bind two external ligands and form an octahedral complex is a result of lower steric constraints imposed by this ligand compared with the other ligand structures and this complex would also be similar in structure to the first iron(III) amino triphenolate complex reported by Koch and co-workers, 12a (dipyridine), containing two pyridine molecules as apical ligand Scheme 5. [33]

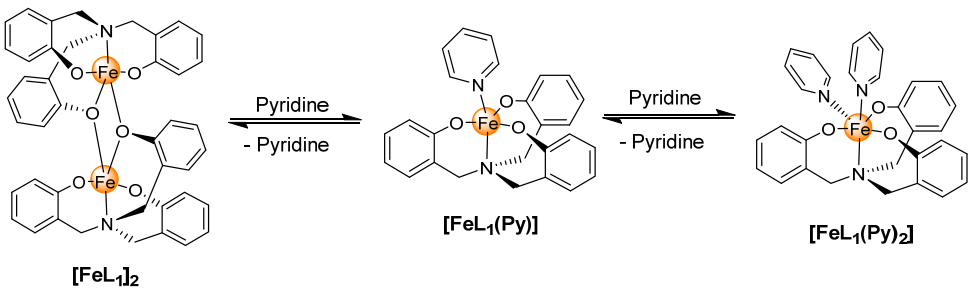

Scheme 5. Schematic Representation of the Proposed Reaction of Pyridine with **12a**

In the case of **12b**, the steric constraints imparted by the methyl groups of the ligand prevent the coordination of a second pyridine ligand, and hence only a single set of resonances (Ha, Hb, and Hc) are observed for each proton. The protons from the methyl group of **12b** are observed as the second resonance (CH_3) at around 60 ppm. Both the spectra of **12c** and **12d** display the paramagnetically shifted resonances for the aromatic protons (Ha, Hb, and Hc) in the absence of pyridine, further adding to the evidence that these two complexes exist in their mononuclear form. Upon addition of pyridine to **12c** there is no change in the spectrum, as the pyridine is only substituting the tetrahydrofuran ligand to yield **12c** (Py) in situ.

The same behaviour is not true for **12d** as after addition of pyridine the resonances which we propose are assigned to the protons of the *ortho*-phenyl group disappear (Hd, He, and Hf). The X-ray structure of **12d** (Py) has been resolved and indicates that pyridine can coordinate and act as a ligand though resulting in a reduced rotational freedom of the Ph groups of the triphenolamine ligand Figure 7 and Table 4.

[33] J. W. Hwang, K. Govindaswamy, S. A. Koch. *Chem. Commun*. **1998**, 1667.

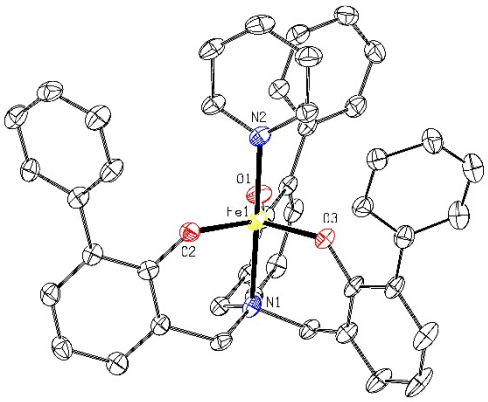

Figure 7. Solid state structure of 12d (Py). H-atoms and co-crystallized solvent molecules, and rotational disorder are omitted for clarity. A partial numbering scheme (around the Fe center) is provided.

Table 4. Selected bond lengths (Å) and angles (deg) in 12d (Py).

Bond Lengths (Å)		**Bond Angles (°)**	
Fe(1)-O(1)	1.856(3)	O(1)-Fe(1)-O(2)	123.40(14)
Fe(1)-O(2)	1.870(3)	O(1)-Fe(1)-O(3)	117.45(13)
Fe(1)-O(3)	1.860(3)	O(1)-Fe(1)-N(1)	88.43(13)
Fe(1)-N(1)	2.182(4)	O(1)-Fe(1)-N(2)	89.76(13)
Fe(1)-N(2)	2.135(4)	N(1)-Fe(1)-N(2)	177.99(13)

4.2.5 Electrochemical Studies

Cylic voltammetry experiments have been performed in dichloromethane for all the complexes Figure 8. The complexes **12c** and **12d** exhibit respectively quasi-reversible waves at -0.825 and -1.008 V. Complexes **12a** and **12b** have a more complex electrochemical behavior. In the case of the dinuclear species **12a**, a single quasi reversible wave at -0.288 V was obtained. This value is remarkably lower than for the mononuclear species, most likely because there is an easier reduction of the metal center due to the delocalized electron density between the two iron centers. The data observed and the cyclic voltamograms are reported in Table 5 and Figure 8.

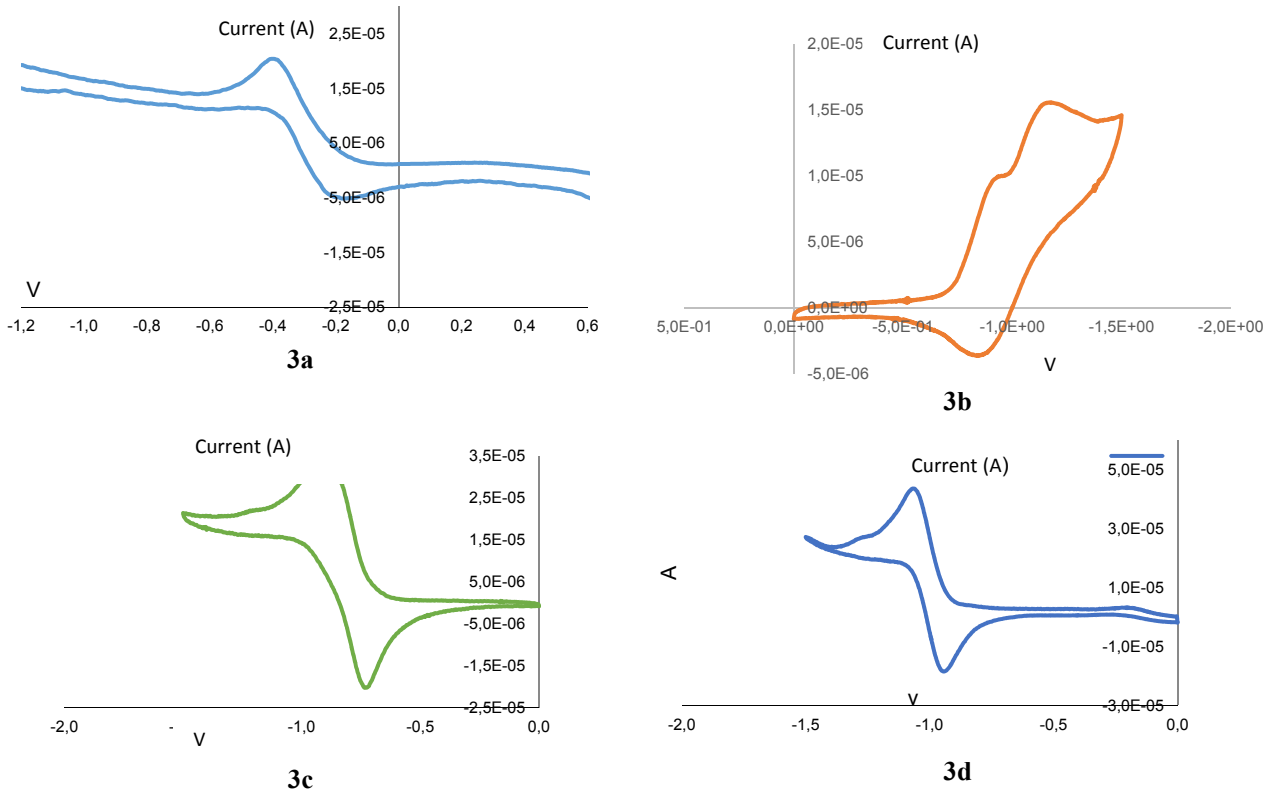

Figure 8. Cyclic voltammograms at 298 K in CH_2Cl_2 (scan rate = 100 mV s−1) using 0.1 M NBu_4PF_6 as supporting electrolyte at a glassy carbon working electrode, platinum wire auxiliary electrode, and Ag-AgCl (sat. NaCl) reference electrode of **12a**, **12b, 12c**, and **12d**.

Table 5. Electrochemical data for **12a**, **12b**, **12c** and **12d**. [a]

	$E_{1/2}$**{Complex}**	
Complex	$E_{1/2}$**(1)**	$E_{1/2}$**(2)**
12a	-0.288	-
12b	-1.013	-0.930[b]
12c	-1.008	-
12d	-0.825	-

[a] In CH_2Cl_2 at 298 K (scan rate = 100 mV s^{-1}) using 0.1 M NBu_4PF_6 as supporting electrolyte at a glassy carbon working electrode, platinum wire auxiliary electrode and Ag-AgCl (sat. NaCl) reference electrode. [b] Potential for irreversible reduction

4.3 Iron (III) complexes: Catalytic activity

The reactivity of complexes **12a-d** has been explored in the cycloaddition of CO_2 to epoxides. As mentioned before, recently the dinuclear iron (III) amino triphenolate complex **7** was found to be an excellent catalyst for the conversion of CO_2 and epoxides into cyclic carbonates using an alkylammonium bromide or iodide as co-catalyst. [26] In order to investigate the reactivity of the new complexes and compare their performance, experiments were carried out by using similar reaction conditions previously applied to **7**.

The results obtained from the cycloaddition of carbon dioxide (CO_2) to propylene oxide are reported in Table 6.

Table 6. Yields (%) [a]of cyclic carbonate from propylene oxide obtained using Fe(III) complexes **7** and **12a-d** as catalysts and TBAB as co-catalyst.

Substrate	Solvent	7	12a	12b	12c	12d
	DCM	n.d.	16	13	82	78
	MEK	65	56	72	85	88

[a]Yields (%) calculated via ^{1}-H NMR with mesitylene as internal standard. Conditions: 2.0 mmol epoxide, 0.01 mmol **12a** or **7**, 0.02 mmol **12b-d**, 0,1 mmol nBu$_4$NBr, 2,0 mmol mesitylene, 5mL of solvent, 1.0 Mpa CO_2, (0.2 MPa in the reaction catalysed by **7**), 25°C, 18h. MEK = methylethylketone, DCM= dichloromethane.

The reactions were performed in a 25 mL autoclave, charged with methylethyl ketone (MEK) and dichloromethane (DCM) solutions containing the catalyst and co-catalyst, substrate and mesitylene as internal standard. From the data reported in Table 6 it is evident that the mononuclear catalysts **12b-d** afford better results than the dinuclear ones. Catalytic performances are better when the reactions are carried out using a coordinating solvent such as MEK. This is particularly true in the case of catalyst **12b** (13 vs 72% yields) probably due to the preferential mononuclear nature of the catalyst under these reaction conditions.

In order to investigate the scope of the reaction, the catalytic systems were tested with a series of different substrates, including the less reactive oxetanes Table 7.

Table 7. Cycloaddition of CO_2 to differently epoxides and oxetanes using catalysts **12a-d**.

	Substrate	Product	12a (%)[a]	12b (%)[a]	12c (%)[a]	12d (%)[a]
1	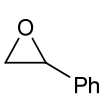	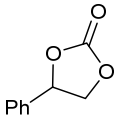	12	10	90	67

2		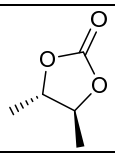	83	75	82	50
3	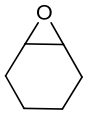	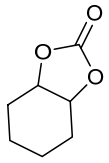	42	62	38 (75)[b]	45 (67)[b]
4		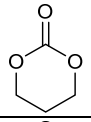	10	94	90	50
5	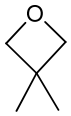	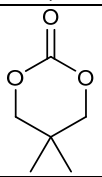	4	8	8	10

[a] Yields (%) calculated *via* ^{1}-H NMR, mesitylene as internal standard. Conditions: 2.0 mmol epoxide, 0.01 mmol **12a** or 0.02 mmol **12b-d**, 0,1 mmol nBu$_4$NBr, 2,0 mmol mesitylene, 5mL of solvent, 1.0 Mpa CO_2, 85°C, 18h. [b] yields after 36h.

With styrene oxide (entry 1) the mononuclear complexes are more effective catalysts, especially **12c**. With *trans*-2,3-epoxy butane (entry 2) all catalysts were found to convert stereospecifically the internal epoxide into the corresponding *trans* cyclic carbonate in very good reactivity and selectivity.

Cyclohexene oxide (entry 3), a very interesting substrate for the production of polycarbonates, afforded the bicyclic carbonate in yields up to 75%.

The reaction with oxetanes, which are particularly challenging substrates due to their low reactivity [34 35] were quite successful. In particular with a simple oxetane (entry 4) a six-membered cyclic carbonate was obtained with yields up to 94% (with catalyst **12b**). Some reactivity could be also observed with the 3,3-dimethyl oxetane (up to 10%).

Very interestingly, in the case of **12c** it was possible to obtain the solid state structure of the complex whereby the tetrahydrofuran ligand is replaced by a *trans*-2,3-epoxybutane ligand Figure 9, indicating that the substrate is indeed able to bind to the iron(III) center. Thus, it seems that the catalytic activity of these complexes is controlled by their tendency to form dimeric structures, the solvent medium, the reaction temperature and the steric impediment upon coordination of the substrate to the Fe(III) center. In Table 8 are reported selected angles and bonds

[34] D. J. Darensbourg, A. Horn Jr, A. I. Moncada, *Green Chem*. **2010**, 12, 1376.
[35] D. J. Darensbourg, P. Ganguly, W. Choi, *Inorg. Chem*. **2006**, 45, 3831.

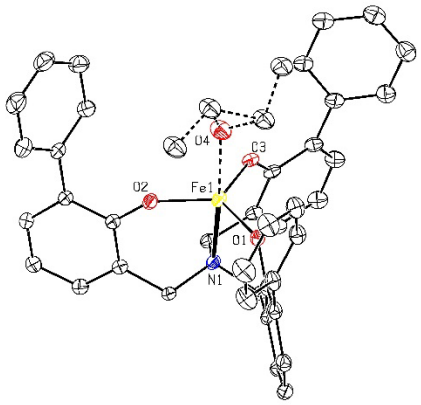

Figure 9. X-ray Crystal Structure of **12d** (*trans*-2,3-epoxybutane). H-atoms, co-crystallized solvent molecules and the disorder in the position of the epoxide ligand and the Ph groups of the ligand L_4 are omitted for clarity. Only a partial numbering scheme is provided.

Table 8. Selected **Bond Lengths** (Å) and **Angles** (deg) in 12d (*trans*-2,3-epoxybutane).

Bond Lengths (Å)		Bond Angles (º)	
Fe(1)-O(1)	1.860(2)	O(1)-Fe(1)-O(2)	116.23(10)
Fe(1)-O(2)	1.860(2)	O(1)-Fe(1)-O(3)	119.79(10)
Fe(1)-O(3)	1.880(2)	O(1)-Fe(1)-N(1)	90.66(9)
Fe(1)-O(4)	2.145(10)	O(1)-Fe(1)-O(4)	98.00(30)
Fe(1)-N(2)	2.174(2)	O(4)-Fe(1)-N(1)	171.10(30)

4.4 V(V) and Mo(VI) Amino Triphenolate Complexes as catalysts for CO_2 fixation.

4.4.1 Mo(VI) Amino Triphenolate: Catalytic Activity

The reactivity of other amino triphenolate complexes, in particular Mo(VI)/TPA **13** and V(V)/TPA **14**, was also investigated.

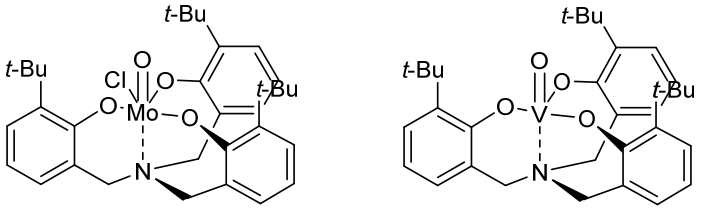

13 **14**

Beside the finding of new catalysts active in the CO_2 cycloaddition to epoxides, the possibility that complexes such as **13** act as catalysts in the CO_2 addition to epoxides could allow the direct synthesis of cyclic carbonates from olefins *via* a two consecutive steps: epoxidation and subsequent CO_2 cycloaddition (Scheme 6). Mo(VI) complex **13** , in fact, is an active catalyst for the activation of *tert*-butylhydroperoxide in the epoxidation of olefins. [36] (Scheme 6).

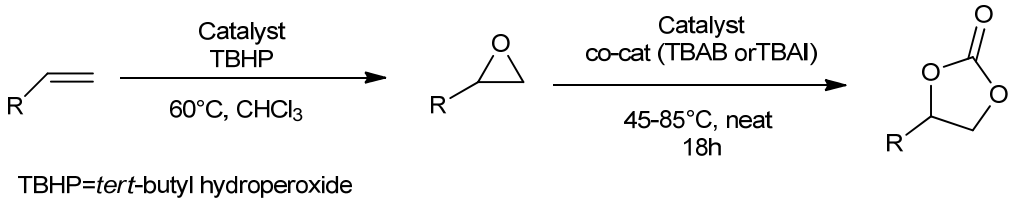

Scheme 6. Two step catalytic synthesis of cyclic carbonates via epoxidation and CO_2/epoxide cycloaddition.

Mo(VI) complex **13** has been tested as a catalyst in the CO_2 cycloaddition with a series of terminal and internal epoxides. The experiments were performed under the best conditions obtained for the Fe(III)/TPA catalysts. The reactions were carried out under neat conditions
(for liquid epoxides) or using a minimal amount of MEK (for the solid ones). With terminal aliphatic epoxides TBAI was used as co-catalyst while with more hindered substrates (styrene and *trans*-2,3-epoxybutane) TBAB was employed. [26] The results obtained are reported in Table 9.

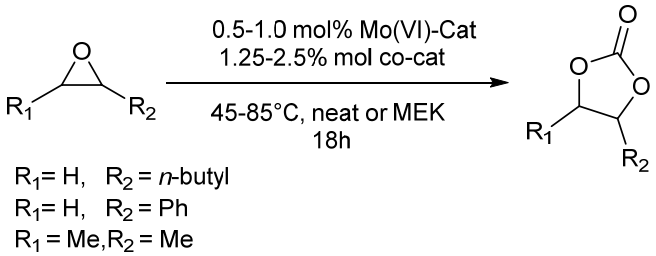

Table 9. CO_2 cycloadditions with different epoxides in the presence of Mo(VI) **13** as catalyst.

Entry	Substrate	13 (mol%)	Co-catalyst (mol%)	T (°C)	Yield ^{1}H-NMR (%)[a]

[36] F. Romano, A. Linden, M. Mba, C. Zonta, G. Licini. *Adv. Synth. Catal.* **2010**, *352*, 2937.

1	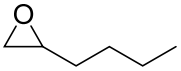	0.5	TBAI (2.5)	45	70
2		1.0	TBAI (2.5)	45	77
3		1.0	--	45	n.r.
4		1.0	--	85	13
5		1.0	--	100	5
6	 + 0.5 ml MEK	--	TBAI (2.5)	45	58
7		1.0	TBAB (2.5)	45	20
8		--	TBAB (2.5)	45	16
9		1.0	TBAB (2.5)	45	16
10		--	TBAB (2.5)	45	10
11		1.0	TBAB (2.5)	85	40
12		--	TBAB (2.5)	85	10

Conditions: substrates (1.0 g), catalyst= (0.5 mol%), (1mol%), TBAB = *tert*-butylammonium bromide, TBAI = *tert*-butylammonium iodide, 45-85°C, 10 bar initial CO_2 pressure in a 30 mL autoclave. [a] Yields determined by ^{1}H-NMR from the crude reaction mixture.

The results obtained show that Mo(VI) complex **13** is a less effective catalyst than the corresponding Fe(III) and Al(III) complexes. However, in the case of 1,2-epoxyhexane, a terminal epoxide and using TBAI as co-catalyst, reasonably high conversions were obtained (77% yield). This result is quite promising for the future design of a two-step procedure (epoxidation/CO2 cycloaddition) on terminal olefins.

4.4.2 V(V) Amino Triphenolate: Catalytic Activity

The reactivity of the V(V) complex **14** has also been investigated. V(V) salophen complexes have been reported to be able to catalyze carbon dioxide addition to epoxides, although the catalytically active species in the process are indeed *in-situ* formed polyoxometalate species. [37]

Initially, reactions were performed with 1,2-epoxyhexane and styrene oxide in order to compare these results with the ones obtained with Mo(VI) **13**. (Table 10). In this case much better results have been obtained, with yields up to 99%, even upon decreasing the catalyst/co-catalyst loading. In order to investigate the scope of the catalytic system, a variety of differently substituted epoxides were tested. In all cases substrates were transformed into the corresponding carbonates in excellent yields using catalyst loadings as low as 0.5 mol % and TBAI/TBAB as co-catalysts (1.25 mol %) at 45°C under neat conditions.

[37] A. Coletti.; C. J. Whiteoak., V. Conte.; A. W. Kleij. *ChemCatChem*. **2012**, 4, 1190.

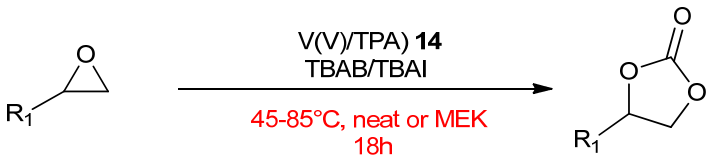

Table 10: CO_2 cycloaddition with a series of terminal epoxides with V(V)/TPA **14** as catalyst.

Entry	R	14 (%)	Co-catalyst (%)	Solvent	Temperature (°C)	Conversion ^{1}H-NMR (%)[a]
1	n-Bu	1.0	TBAI (2.5)	-		>99
2		0.5	TBAI (1.25)	-		>99
3	Ph	1.0	TBAB (2.5)	MEK		>99
4		0.5	TBAB (1.25)	MEK		>99
5	CH_2Cl	0.5	TBAI (1.25)	-		>99
6	CH_2OH	0.5	TBAI (1.25)	-		>99
7	CH_2OMe	0.5	TBAI (1.25)	-		>99
8	CH_2OEt	0.5	TBAI (1.25)	-		>99

Conditions: substrates (1.0 g), catalyst= (0.5 mol %), (1 mol%), TBAB= *tert*-butylammonium bromide, TBAI= *tert*-butylammonium iodide, 45-85°C, 10 bar initial CO_2 pressure in a 30 mL autoclave. [a] Conversion determined by ^{1}H- NMR from the crude reaction mixture.

The catalytic performance of catalyst **14** has also been tested with internal epoxides, in particular *trans*-butene and trans-β-methyl styrene oxide. Due to the decreased reactivity reactions were carried out at 85°C with a CO_2 pressure of 10 bar. The results obtained are reported in Table 11.

Table 11: CO_2 cycloadditions to *trans*-butene and trans-β-methyl styrene oxide catalyzed by V(V)/TPA.

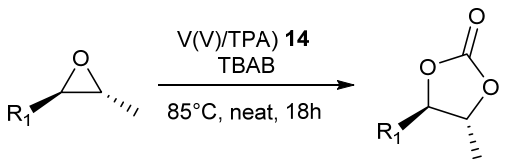

R	14 (%)	TBAB (%)	Conversions ^{1}H-NMR (%)[a]	Yields, % [a]
Ph	0.5	1.25	98	60
Ph	0.5	5.0	98	98
Ph	--	5.0	15	15

Me	0.5	1.25	79	79

Conditions: substrates (1.0 g), catalyst= (0.5 mol %), TBAB= *tert*-butyl ammonium bromide, 85°C, 10 bar initial CO_2 pressure in a 30 mL autoclave. [a] Conversions and yields determined by ^{1}H-NMR from the crude reaction mixture.

Also in this case the catalyst was found to be quite reactive with both substrates. In particular with *β*-methylstyrene oxide (Table 11, entry 1-2) high conversions and yields were obtained using 0.5 mol% of catalyst and 5 mol% of the co-catalyst. In the presence of less amounts of co-catalyst (Table 11, entry 1) some decomposition of the reagent/product was observed, while the absence of catalyst gave poor conversions and chemical yields (15%, Table 11, entry 3).

However, the results obtained with both Mo(VI) an V(V) amino triphenolate complexes are very promising in order to further investigate the possibility to form cyclic carbonates from olefins in a one-pot synthesis.

4.5. Conclusions

In summary, four new Fe(III) amino triphenolate complexes have been synthesized and fully characterized. These complexes have been found to be dinuclear (in the case of **12a**) or mononuclear (in the case of **12b**, **12c**, **12d**). The potential to form a dinuclear structure is dependent upon the substituent in the ortho-position of the phenolate moiety. Catalytic testing of the complexes for the cycloaddition of carbon dioxide to oxiranes has shown that the mononuclear form of these iron complexes is significantly more active than the dinuclear species. It has also been shown that by changing the reaction conditions (higher temperatures, using a solvent with coordinating potential and better CO_2-dissolution potential) the dinuclear structure can be disrupted and a more active form of the complex can be obtained. Future prospects include the implementation of these iron complexes in other types of catalytic processes.

Also Mo(VI)/TPA **13** and V(V)/TPA **14** have been found to be active catalysts in the same reaction. In particular the vanadium catalyst **14** was found to be active with terminal and internal epoxides, affording the corresponding cyclic carbonates in high yield under mild reaction conditions.

4.6 Experimental Part

General Remarks

All manipulations of moisture and/or air sensitive compounds were carried out under an atmosphere of nitrogen using standard Schlenk and cannula techniques. Conventional nitrogen atmosphere glove boxes were used for the preparation of analytical and spectroscopic samples as well as for the weighing and storage of air sensitive compounds. The ligands were prepared by a known literature procedure. [28] All Fe(III) amino triphenolate complexes once prepared, were no longer considered as air /moisture sensitive and were stored on the bench. Tetrahydrofuran and other dry solvents used during the synthesis of the complexes were dried using a Solvent Purification System (SPS), and all other solvent were reagent grade and used without any further purification. All other reagent or starting material and carbon dioxide gas phase (purchased from PRAXAIR) were used as received without any purification.

The NMR spectra have been recorded on Bruker AV 400 (^{1}H: 300.13 MHz; ^{13}C: 75.5 MHz) spectrometer. Chemical shift (δ) have been reported in parts per million (ppm) relative to the residual undeuterated solvent as an internal reference ($CDCl_3$; 7.26 ppm for ^{1}H NMR and 77.0 ppm for ^{13}C NMR; CD_3OD: 4.84 ppm for ^{1}H NMR and 49.05 ppm for ^{13}C NMR). The following abbreviations have been used to describe the multiplicities of the NMR signals: s (singlet), d (doublet), t (triplet), dd (double doublet), dt (double triplet), br (broad) and m (multiplet). The ^{13}C NMR spectra were all proton decoupled.

X-Ray Crystallography

The measured crystals were stable under atmospheric conditions; nevertheless they were treated under inert conditions immersed in perfluoropoly ether as protecting oil for manipulation. Data collection measurements were made on a Bruker-Nonius diffractometer equipped with an APPEX 2 4 K CCD area detector, an FR591rotating anode with MoKα radiation, Montel mirrors, and a Kryoflex low temperature device (T = −173 °C). Full-sphere data collection was used with ω and ϕ scans. Programs used: data collection Apex2V2011.3 (Bruker-Nonius 2008), data reduction Saint+ Version 7.60 A (Bruker AXS 2008) and absorption correction SADABS V. 2008-1 (2008). For structure solution SHELXTLVersion 6.10 (Sheldrick, 2000)36 was used (Table 12). Structure refinement: SHELXTL-97-UNIX version.

Table 12: X-ray structure data collection and refinement parameters for all reported structures **12a, 12b, 12c and 12d**.

	12a	12b	12c	12d
Formula	$C_{105}H_{96}Fe_4N_4O_2$	$C_{28}H_{32}FeNO_4$	$C_{33}H_{46}FeNO_5$	$C_{43}H_{34}FeNO_4$
*F*w (g·mol^{-1})	1829.26	502.40	592.56	684.56
T (K)	100(2)	100(2)	100(2)	100(2)
λ (Å)	0.71073	0.71073	0.71073	0.71073
Crystal system	Triclinic	Triclinic	Monoclinic	Monoclinic
Space group	*P*-1	*P*-1	*C*2/*c*	$P2_1/c$
a (Å)	13.5240(13)	10.4445(6)	25.102(2)	16.0348(19)
b (Å)	17.1679(17)	10.9051(6)	10.9015(11)	16.1658(18)
c (Å)	19.236(2)	11.2722(6)	25.252(3)	13.0742(14)
□ (º)	77.392(3)	73.886(2)	90.00	90.00
□ (º)	79.290(3)	75.873(2)	112.938(3)	92.126(4)
□ (º)	78.116(4)	79.199(2)	90.00	90.00
Volume (Å^3), *Z*	4218.4(7), 2	1186.23(11), 2	6363.8(11), 8	3386.7(7), 4
ρ(calcd) (mg·m^{-3})	1.440	1.407	1.237	1.343
μ (mm^{-1})	0.744	0.671	0.513	0.491
Absorption correction	Empirical	Empirical	Empirical	Empirical
Refinement method	Full-matrix least-squares on F^2	Full-matrix least-squares on F^2	Full-matrix least-squares on F^2	Full-matrix least-squares on F^2
Data/ restraints/ parameters	26557/ 0/ 1129	6294/ 0/ 311	5817/ 4/ 382	8248/ 641/ 586
GoF on F^2	1.043	1.041	1.161	1.066
Final *R* indices [I > 2□(*I*)]	R_1 = 0.0546, wR_2 = 0.1238	R_1 = 0.0359, wR_2 = 0.0944	R_1 = 0.0833, wR_2 = 0.2054	R_1 = 0.0979, wR_2 = 0.2416
R indices (all data)	R_1 = 0.1003, wR_2 = 0.1438	R_1 = 0.0402, wR_2 = 0.0970	R_1 = 0.1002, wR_2 = 0.2144	R_1 = 0.1453, wR_2 = 0.2524
Largest diff. peak and hole (e.Å^{-3})	0.833 and -0.889	0.822 and -0.257	1.267 and -0.671	1.161 and -1.170

Table 12 X-ray structure data collection and refinement parameters for all reported structures

	12d (Py)	12d (*trans*-2,3-epoxybutane
:Formula	$C_{44}H_{35}FeN_2O_3$	$C_{43}H_{38}FeNO_4$
*F*w (g·mol^{-1})	695.59	688.59
T (K)	100(2)	100(2)
λ (Å)	0.71073	0.71073
Crystal system	Monoclinic	Monoclinic
Space group	$P2_1/c$	$P2_1/c$

a (Å)	16.140(2)	16.0716(16)
b (Å)	16.580(2)	16.2018(17)
c (Å)	12.8255(16)	13.2037(12)
□ (º)	90.00	90.00
□ (º)	91.774(4)	94.218(3)
□ (º)	90.00	90.00
Volume (Å^3), *Z*	3430.3(8), 4	3428.8(6), 4
ρ(calcd) (mg·m^{-3})	1.347	1.334
μ (mm^{-1})	0.484	0.485
Absorption correction	Empirical	Empirical
Refinement method	Full-matrix least-squares on F^2	Full-matrix least-squares on F^2
Data/ restraints/ parameters	8392/ 204/ 496	8457/ 2746/ 953
GoF on F^2	1.050	1.056
Final *R* indices [I > 2□(*I*)]	R_1 = 0.0770, wR_2 = 0.1640	R_1 = 0.0678, wR_2 = 0.1624
R indices (all data)	R_1 = 0.1346, wR_2 = 0.1824	R_1 = 0.0944, wR_2 = 0.1769
Largest diff. peak and hole (e.Å^{-3})	0.426 and -1.032	0.798 and -0.972

Cyclic Voltammetry

Cyclic voltammetric measurements were carried out with a Princeton Applied Research PARSTAT 2273 electrochemical analyzer. A three electrode assembly, comprising a glassy carbon working electrode, a platinum wire auxiliary electrode, and Ag/AgCl (sat. NaCl) reference electrode was used. The experimental data were obtained under an argon atmosphere in dichloromethane solvent using NBu_4PF_6 as supporting electrolyte.

FT-IR measurements were carried out on a Bruker Optics FTIR Alpha spectrometer equipped with a DTGS detector, KBr beamsplitter at 4 cm^{-1}.

UV-vis measurements were carried out on a Shimadzu UV-1800 spectrophotometer.

UV-Vis Titration Procedure with propylene oxide: A 1.0x10^{-4}M toluene solutions of **12a**, 1**2b**, **12c** and **12d** were prepared and the UV-Vis spectrum recorded using a quartz cell with a 1 cm path length. An 0.40 M solution of propylene oxide containing the Fe complex (at 1.0x10^{-4}M) was prepared and added in 50 mL aliquots to 2.0 mL of the solution of the Fe complex, with spectra being recorded after each addition.

UV-Vis Titration Procedure with pyridine. A 1.0 x10^{-4}M toluene solutions of **12a** and **12d** were prepared and the UV-Vis spectrum recorded using a quartz cell with a 1 cm path length. An 0.40 M solution of pyridine containing the Fe complex (**12a** or **12d**) (at 1.0 x10^{-4}M) was prepared and added in 50 mL aliquots to 2.0 mL of the solution of the Fe complex, with spectra being recorded after each addition.

Synthesis Fe(III) amino triphenolate complexes 12a-d.

General synthetic procedure for all complexes **12a-d** is the following. To a suspension of sodium hydride (75.2 mg, 3.13 mmol) in tetrahydrofuran (10 mL) was slowly added a solution of **11a** (350 mg, 1.04 mmol) in tetrahydrofuran (10 mL). The mixture was stirred for 18 h and after this time it was added to a solution of anhydrous iron(III) chloride (167.7 mg, 1.04 mmol) in tetrahydrofuran (10 mL). The mixture was stirred for a further 4 h and then filtered through a path of Celite, followed by removal of the solvent to yield a brown residue, which was subsequently dissolved in dichloromethane, filtered and the solvent then removed to yield a brown powder.

12a Yield: 397 mg (88%). Anal. Calcd for $C_{42}H_{36}Fe_2N_2O_6$: C, 64.97, H, 4.67; N, 3.61.Found: C, 64.92; H, 4.61; N, 3.38. MALDI (+)−MS (pyrene): for $C_{21}H_{18}FeNO_3$ m/z =388 $[M]^+$ (calcd. 388), for 777 $C_{42}H_{36}Fe_2N_2O_6$ $[2M^+H]^+$ (calcd 777). UV−vis (CH_2Cl_2, 0.1 mM, 25 °C, ε = L·mol^{-1}·cm^{-1}): 314 nm (ε = 7970), 358 nm (ε =5290, sh), 430 nm (ε = 3510). Magnetic moment (298 K) μeff = 4.14μB.

12b This compound was prepared in an analogous manner to that described above for **12a**. Yield: 231 mg (89%). Anal. Calcd for $C_{24}H_{24}FeNO_3$: C, 66.99; H, 5.62; N, 3.26. Found: C, 67.21; H, 5.82; N, 3.02. MALD I(+)−MS (pyrene): m/z = 430 $[M]^+$ (calcd. 430). UV−vis (CH_2Cl_2, 0.1 mM, 25 °C, ε = L·mol^{-1} cm^{-1}): 329 (ε = 4065), 416 (ε = 3625). Magnetic moment (298 K) μeff = 6.74 μB.

12c (THF) This compound was prepared in an analogous manner to that described above for **12a** Yield: 408 mg (90%). Anal. Calcd for $C_{37}H_{50}FeNO_4$: C, 70.69; H, 8.02; N, 2.23. Found: C, 70.60; H, 8.34; N, 2.12. MALDI(+)−MS (dithranol): m/z = 557 [M+H−THF]+ (calcd. 557).UV−vis (CH_2Cl_2, 0.2 mM, 25 °C, ε = L·mol−1·cm−1): 329 nm (ε = 3570), 410 nm (ε = 3135). Magnetic moment (298 K) μeff = 5.49 μB.

12d (THF) This compound was prepared in an analogous manner to that described above for **12a** Yield: 266 mg (61%). Anal. Calcd for $C_{43}H_{38}FeNO_4$: C, 75.00; H, 5.56; N, 2.03. Found: C, 74.75; H, 5.80; N, 2.12. MALDI (+)−MS (pyrene): m/z = 616 $[M^{-}THF]^{+}$ (calcd. 616). UV− vis (CH_2Cl_2, 0.2 mM, 25 °C, ε = $L \cdot mol^{-1}$ cm^{-1}): 357 nm (ε = 5460), 426 nm (ε = 5045). Magnetic moment (298 K) μeff = 5.53 μB.

X-Ray Crystallography.

Crystals suitable for single crystal X-ray analysis were obtained by slow evaporation of tetrahydrofuran solutions of **12b**, **12c**, and **12d** or in the case of **12a**, crystals were obtained from a concentrated toluene solution after three weeks. The structure obtained for **12c** contains a molecule of water instead of the expected molecule of tetrahydrofuran as the co-ligand and is denoted as 12c. The crystals of **12d** (Py) were grown by slow evaporation of a concentrated solution of the complex in tetrahydrofuran/pyridine (50:1).

Catalytic Experiments.

In a typical catalytic experiment the oxirane (2.0 mmol), tetra-butyl-ammonium bromide (TBAB) (32.6 mg, 0.1 mmol), the respective iron(III) amino triphenolate complex (0.01 mmol of complex **12a** or **12b**, and 0.02 mmol **12c** or **12d** and mesitylene (278 μL, 2.0 mmol) were dissolved in the respective solvent (5 mL). The reaction mixture was then transferred to a stainless steel autoclave and three cycles of pressurization and depressurization with carbon dioxide were applied (pCO_2 = 0.5 MPa). The final pressure was then adjusted to 1.0 MPa, and the reaction was left stirring at the required temperature for 18 h. After this time, the yield was calculated using the ^{1}H NMR spectrum (d_6-DMSO or $CDCl_3$) of an aliquot of the reaction mixture and mesitylene as the internal standard.

Product Characterization

All organic products from the catalysis experiments were characterized by ^{1}H-NMR and IR spectroscopy and the spectra were compared with the data reported in literature. For these see characterization. For each cyclic carbonate compounds references are provided.

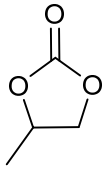

4-methyl-1,3-dioxolan-2-one (**Table 6, 4a**) [38]

Yield calculated by ^{1}HNMR using mesitylene as internal standard. (400 MHz, $CDCl_3$): δ m 4.94-4.86 (m, 1H), 4.58 (t, *J*=8.0 Hz, 1H), 4.01 (t, *J*=8.8 Hz, 1H), 1.45 (d, J= 6.0 Hz, 3H).

IR Neat: 1751cm^{-1}.

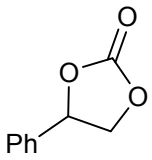

4-phenyl-1,3-dioxolan-2-one (**Table 7, Entry 1**) [39]

Yield calculated by ^{1}HNMR using mesitylene as internal standard are reported in Table 7 (400MHz, $CDCl_3$): δ

7.35–7.44 (m, 5H), 5.86 (t, *J*= 8.0 Hz, 1H), 4.80 (t, *J*= 8.4 Hz, 1H), 4.34 (t, *J*= 8.4 Hz, 1H).

IR Neat: 1788 cm^{-1}.

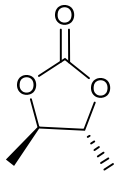

(*4R*, *5R*)-4,5-dimethyl-1,3-dioxolan-2-one (**Table 7, entry2**) [39]

Yields for each complex are reported in Table 7.

^{1}H NMR (300 MHz, $CDCl_3$) δ 4.39 – 4.27 (m, 2H), 1.45 (d, J = 5.9 Hz, 6H).

IR Neat: 1796 cm^{-1} (C=O).

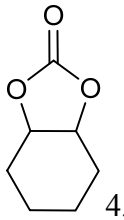

4, 5-tetramethylene-1, 3-dioxolan-2-one (**Table 7, Entry 3**) [40]

^{1}H NMR (300 MHz, $CDCl_3$) δ 4.78 – 4.59 (m, 2H), 2.02 – 1.79 (m, 4H), 1.69 – 1.52 (m, 2H), 1.51 – 1.24 (m, 2H). IR Neat: 776 cm^{-1} (C=O).

[38] J. Sun, L. Han, W. Cheng, J. Wang, X. Zhang, S. Zhang, *ChemSusChem,* **2011**, 4, 502.
[39] K. Matsumoto, Y. Sato, M. Shimojo, M. Hatanaka, *Tett. Assymmetry*, **2000**, 11, 1965.
[40] A. Buchard, M. R. Kember, K. G. Sandeman, C. K. Williams, *Chem. Commun*., **2011**, 47, 212.

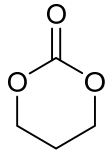

1,3-dioxan-2-one (**Table 7, Entry 4**). [41] Yield for each complex are given in table 3. ^{1}H NMR (400 MHz, CDCl3) δ 4.53 – 4.35 (m, 4H), 2.27 – 2.08 (m, 2H). IR Neat: 1728 cm-1 (C=O)

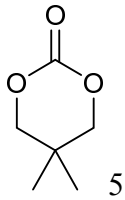

5,5-dimethyl-1,3-dioxan-2-one (**Table 7, Entry 5**). [42] Yield for each complex are given in table 3. ^{1}H NMR (300 MHz, $CDCl_3$) δ 4.06 (s, 4H), 1.10 (s, 6H). IR Neat: 1736 cm-1 (C=O).

The synthesis of tiphenolamine ligands **11c** is reported in literature. [29] The synthesis of Mo(VI) amino triphenolate complex **13c** and **14d** is reported in literature and fully characterized. [35 42]
The general procedure for **13c** is the following. Milled MoO_2Cl_2 (200 mg, 1 mmol) and the ligand precursor 2d (503 mg, 1 mmol) were mixed with toluene (50 mL) and the stirred suspension was heated to reflux for 18 h. The resulting intense purple solution was filtered through a short pad of silica and evaporated to afford complex 3-Cl as a violet solid; yield: 500 mg (80%).
^{1}H NMR (300 MHz, $CDCl_3$): d=7.40 (dd, J=7.8, 1H, and 1.4 Hz, ArH), 7.34 (dd J=7.8, 2H, and 1.8 Hz, ArH), 7.15 (dd, J=9.2, 3H, and 1.4 Hz, ArH), 6.98 (m, 3H, ArH), 3.99 (d, 2H, J=11.5, NCH_2), 3.6 (d, J=21.1 Hz, 2H, NCH_2), 3.49 (s, 2H, NCH_2),1.59 (s, 9 H), 1.47 (s, 18H); ESI-MS: m/z=672.2 (M^+Na^+), 650.2 (M^+ H^+), 614.3 (M-Cl).

General procedure for the synthesis of cyclic carbonate reported in Table 9, 10 and 11.

In a typical CO_2 cycloaddition reaction, a 30 mL autoclave was charged with the epoxide, Mo(VI) amino triphenolate complex 13c and co-catalyst TBAB or TBAI (and if necessary 0.5 mL of methyl ethyl ketone (MEK) in the cases where the substrate/cyclic carbonate product is a solid). The reaction was stirred for 18 h at the required temperature, after which time the reaction was cooled and an aliquot of the reaction mixture analyzed by ^{1}H NMR spectroscopy in order to calculate the conversion and compared with those reported in literature.
Same procedure was followed for cyclic organic carbonate reported in Table 11 catalyzed by 14c.

[41] B. A. Sweileh, Y. M. A.Hiari, K. M. Aiedeh, J. *Applied Poly. Sci.,* **2008**, 110, 2278.
[42] M. Mba, M. Pontini, S. Lovat, C. Zonta; G. Bernardinelli, E. P. Kundig, G. Licini. *Inorg. Chem.***2008**, 47, 8616.

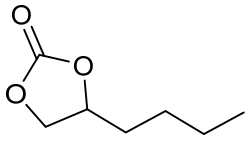 4-butyl-1,3-dioxolan-2-one (**Table 9, Entry 1**). [43] Conversion into the corresponding cyclic carbonate are reported in table 6.

^{1}H NMR (300 MHz, CDCl3) δ 4.79 – 4.62 (m, 1H), 4.52 (dd, J= 8.1 and 8.1 Hz, 1H), 4.06 (dd, J = 8.1, 7.3 Hz, 1H), 1.90 – 1.58 (m, 2H), 1.53– 1.25 (m, 4H), 0.92 (t, J =7.0 Hz, 3H).

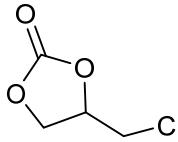 4-(chloromethyl)-1,3-dioxolan-2-one (**Table 10, Entry 5**) [43]

^{1}H NMR (300 MHz, $CDCl_3$) δ 5.09 – 4.81 (m, 1H), 4.59 (dd, *J* = 8.5 and 8.5 Hz, 1H), 4.41 (dd, *J* = 8.5, 5.8 Hz, 1H), 3.91 – 3.53 (m, 2H). IR Neat: 1778 cm-1 (C=O).

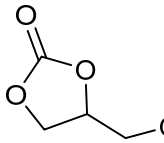 4-(hydroxymethyl)-1,3-dioxolan-2-one (**Table 10, Entry 6**) [44]

^{1}H NMR (500 MHz, $CDCl_3$) δ 4.87 – 4.78 (m, 1H), 4.55 (dd, *J* = 8.4 and 8.4 Hz, 1H), 4.48 (dd, *J* = 8.4 and 6.6 Hz, 1H), 4.01 (dd, *J* = 12.8, *J* = 3.0 Hz, 1H), 3.73 (dd, *J* = 12.8, *J* = 3.5 Hz, 1H), 2.86 (br s, 1H). IR Neat: 1788 cm^{-1} (C=O).

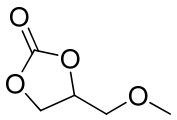 4-(methoxymethyl)-1,3-dioxolan-2-one (**Table 10 Entry 7**) [26 28 38]

^{1}H NMR (500 MHz, $CDCl_3$) δ 4.88 – 4.77 (m, 1H), 4.51 (dd, *J* = 8.3 and 8.3 Hz, 1H), 4.38 (dd, *J* = 8.3 and 5.9 Hz, 1H), 3.66 (dd, *J* = 11.0, *J* = 3.9 Hz, 1H), 3.58 (dd, *J* = 11.0, *J*= 3.8 Hz, 1H), 3.44 (s, 3H).

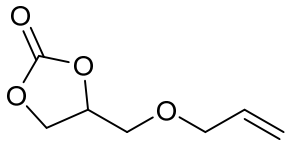 Allylglycidil ether 1,3-dioxolan-2one (**Table 10 Entry 8**) [28]

[43] J. Sun, L. Han, W. Cheng, J. Wang, X. Zhang, S. Zhang, *ChemSusChem*, **2011**, 4, 502.
[44] Y. Patel, J. George, S. M. Pillai, P. Munshi, *Green Chem.,* **2009**, 11, 1056.

^{1}H NMR (, $CDCl_3$) δ 5.88 – 4.76 (m, 1H), 5.27-5.14 (m, 2H), 4.84-4.77 (m, 1H), 4.50 (t, *J* = 3Hz, 1H), 3,36 (dd, *J* = 3.0, *J*= 3.0 Hz, 1H),4.01 (d, *J* = 3.01, 2H), 3.68-3.64 (d.d, *J*= 1Hz and 3Hz, 1H), 3.58-3.53 (d.d, *J*= 1Hz and 3Hz, 1H),

(Table 11). Conversion into the corresponding cyclic carbonate are reported in Table 11.

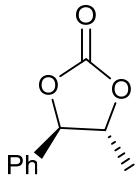

(4*R*,5*R*)-4-methyl-5-phenyl-1,3-dioxolan-2-one (**Table 11, Entry 1**). [28]

^{1}H NMR (400 MHz, $CDCl_3$) δ 7.52 – 7.42 (m, 3H), 7.41 – 7.33 (m, 2H), 5.16 (d, *J* = 8.0 Hz, 1H), 4.75 – 4.53 (m, 1H), 1.58 (d, 3*J* HH = 6.2 Hz, 3H). IR Neat:1797 cm^{-1} (C=O). HR MS (ESI+): calcd. *m/z* 179.0708 $[M^+ H]^+$; found: 179.0696.

Summary

This Ph.D thesis describes a novel synthesis of analogues of amino triphenolate ligands and the use of Fe(III) and V(V) amino triphenolate complexes as catalysts for renewable carbon feedstocks transformation into valuable compounds.

In general, in Chapter 1 an overview of synthetic approaches of triphenolamines are reported, followed by explanation of their coordination chemistry in particular with two metals, which are the subject of this thesis work, vanadium and iron. Finally the catalytic reactivity of both V(V) and Fe(III) complexes is reported. In particular the activity of V(V) amino triphenolate complexes is related to their capability to act as Lewis Acid, stabilizing the active species under turn-over conditions in oxygen transfer reaction such as sulfoxidation and halogenation of trimethoxybenzene in the presence of an oxidant. The reactivity of iron(III) amino triphenolate complexes as catalyst for the cycloaddition of carbon dioxide to epoxides for the synthesis of cyclic carbonate is reported.

Having established that amino triphenolate ligands and in particular the substituents in *ortho* positions to the phenoxy moieties play an important role in order to control the environment of the metal, modulate the electronic and steric properties around the metal centre and therefore control their catalytic properties, in Chapter 2, a novel synthetic methodologies for the synthesis of their analogues amino trithiophenolate ligands is reported. The synthetic methodology allows the synthesis of *ortho*-substituted trithiophenolamines with very satisfactory yields *via* a three step procedure starting form commercially available aldehydes. This approach led to the possibility, for the first time, to access this important class of ligands in a systematic way using either commercially or readily available building blocks.

In Chapter 3 a novel reactivity of V(V) amino triphenolate complex is described. More in detail, V(V)/TPA complex has been found to be a very effective catalyst for the aerobic oxidative C-C cleavage of tertiary and secondary vicinal diols. These studies were carried out in order to develop catalysts capable of controlled oxidative degradation of more challenging substrates, such as lignin models to demonstrate the feasibility of producing fine chemicals from a renewable carbon feedstock. The mild reaction conditions and high yields achieved for 1,2-diols and an ethereal derivative make this catalyst not only competitive to those previously reported but also good candidate for lignin model compounds transformation.

Finally, in Chapter 4 four new Fe(III) amino triphenolate complexes have been synthesized and fully characterized. These complexes have been found to be dinuclear or mononuclear. The potential to form a dinuclear structure is dependent upon the substituent in the *ortho*-position of the phenolate moiety. Catalytic testing of the complexes for the cycloaddition of carbon dioxide to oxiranes has shown that the mononuclear form of these iron complexes is significantly more active than the dinuclear species. It has also been shown that by changing the reaction conditions (higher temperatures, using a solvent with coordinating potential and better CO_2-dissolution potential) the dinuclear structure can be disrupted and a more active form of the complex can be obtained. Moreover, Mo(VI) and V(V) amino triphenolate have been found to be active catalysts in the same reaction. In particular the vanadium catalyst was found to be active with terminal and internal epoxides, affording the corresponding cyclic carbonates in high yield under mild reaction conditions.

In summary, this thesis work had the aim to identify new opportunities in homogeneous catalysis by using alternative carbon feedstocks for the production of small molecules.

Riassunto

Questa tesi di dottorato riporta una nuova sintesi degli analoghi dei leganti trifenolamminici e l'impiego dei complessi trifenolamminici di Fe(III) e V(V) come catalizzatori per la trasformazione di fonti di carbonio rinnovabili per la produzione di composti organici.

In generale nel Capitolo 1 vengono riportate le strategie sintetiche impiegate per l'ottenimento delle trifenolammine, seguita dalla spiegazione della loro chimica di coordinazione, in particolare con due metalli quali il ferro e il vanadio, oggetto di studio del lavoro di dottorato. Più in dettaglio vengono altresì riportate le reattività di questi complessi in catalisi. Per quanto riguarda il complesso di V(V), la sua reattività è legata alla sua capacità di fungere come Acido di Lewis, stabilizzando le specie attive in reazioni di ossidazione come per esempio nelle sulfossidazioni e alogenazioni in presenza di un opportuno ossidante.

Per quanto riguarda invece i complessi di Fe(III) con le trifenolammine viene riportata la loro reattività come catalizzatori nella addizione della CO_2 agli epossidi per la sintesi di carbonati ciclici. I leganti triphenolamminici e in particolare i sostituenti in *orto* al gruppo fenolico giocano un ruolo importante nel modulare le proprietà steriche ed elettroniche così come dell'intorno chimico del metallo a cui si vanno a complessare. Questo si traduce nella possibilità di modulare anche la loro attività catalitica. In virtù di quanto detto, nel secondo Capitolo 2 si è illustrato una nuova metodologia per la sintesi di leganti amino tritiofenolati, analoghi delle triphenolamine. La sintesi di questi leganti avviene solo in tre passaggi sintetici, partendo da substrati come i derivativi del aldeide salicilica, passando poi per la protezione del gruppo ossidrilico con un tiocarbammato il quale permette poi il successivo riarrangiamento, chiamato di Myazaki-Newmann-Kwart, consentendo così di avere la funzionalità tiofenolica. La sintesi procede con la successiva amminazione riduttiva per avere lo scheletro triamminico, seguita dal passaggio finale della deprotezione del gruppo carbammico ottenendo così il legante finale. Questo approccio di sintesi ha consentito per la prima volta ad avere leganti *orto* sostituiti, amino tritiofenolici in buone rese partendo da prodotti commercialmente disponibili.

Nel Capitolo 3 invece il lavoro è proseguito nello studio di una nuova reattività data da complessi amino trifenolati di V(V). In dettaglio in questa parte ha riguardato la loro attività come catalizzatori nelle reazioni di scissione di legami carbonio-carbonio di dioli e preliminarmente nella scissione di composti β-idrossi eteri. Il complesso di V(V) sì e rivelato essere moto attivo e in condizioni di reazioni blande. Questi studi sono stati effettuati al fine di poter sviluppare catalizzatori capaci di degradare, in condizioni controllate di ossidazione, substrati come la lignina

la quale è considerata essere, insieme alla cellulosa, una fonte di carbonio rinnovabile, difficile però da poter utilizzarla come tale.

Nella parte finale di questo lavoro viene riportato lo studio, sintesi, caratterizzazione e reattività di quattro complessi amino trifenolici di Fe(III). Questi complessi allo stato solido, a seconda del sostituente in *orto* al gruppo fenolico, hanno dimostrato essere mononucleari o binucleari. La loro attività poi è stata testata nella cicloaddizione della CO_2 a differenti epossidi e ossirani per la sintesi di carbonati ciclici. Test catalitici hanno dimostrato come la forma mononucleare del complesso è molto più reattiva di quella dinucleare. Inoltre è stato dimostrato come cambiando le condizioni di reazione, temperature alte o usando solventi con potenzialità coordinative e di dissoluzione per la CO_2, la forma dinucleare può essere aperta, permettendo in questo modo al substrato di coordinarsi e di avere una buona reattività. Nella seconda parte del Capitolo 4 sì è riportato l'attività di altri due complessi trifenolamminici rispettivamente di Mo(VI) e V(V) i quali sono stati testati come catalizzatori per la stessa reattività. Entrambi i catalizzatori hanno dimostrato avere buona reattività nell'attivazione dell'anidride carbonica. In particolare il complesso di V(V) ha dimostrato avere ottima reattività, ottenendo carbonati ciclici a cinque termini, sia partendo da epossidi terminali o interni.

In sintesi, questa tesi di dottorato ha avuto come obiettivo l'identificazione di nuove opportunità in catalisi omogenea sfruttando fonti di carbonio rinnovabili ed alternative per la produzione di piccole molecole organiche.